

2013

Semi-Interpenetrating Network Gelatin Fiber Scaffold for Oral Mucosal Delivery of Insulin

Leyuan Xu

Virginia Commonwealth University

Follow this and additional works at: <http://scholarscompass.vcu.edu/etd>

 Part of the [Biomedical Engineering and Bioengineering Commons](#)

© The Author

Downloaded from

<http://scholarscompass.vcu.edu/etd/3191>

This Thesis is brought to you for free and open access by the Graduate School at VCU Scholars Compass. It has been accepted for inclusion in Theses and Dissertations by an authorized administrator of VCU Scholars Compass. For more information, please contact libcompass@vcu.edu.

Copyright

by

Leyuan Xu

2013

Semi-Interpenetrating Network Gelatin Fiber Scaffold for Oral Mucosal Delivery of Insulin

by

Leyuan Xu

Thesis submitted to the Faculty of the
Virginia Commonwealth University
in partial fulfillment of the requirements for the degree of

Master of Science

in

Biomedical Engineering

Hu Yang, Chair
Gary L. Bowlin
W. Andrew Yeudall

August 2013
Richmond, Virginia

Keywords: Drug delivery, insulin, photoinitiator, scaffold

Copyright by Leyuan Xu, 2013

Acknowledgments

I would like to express my deep gratitude to my academic advisor, Dr. Hu Yang, for his extraordinary patience, mentoring, support and encouragement. I would also like to thank Dr. Andrew Yeudall and Dr. Gary Bowlin for allowing me to use the instruments, providing numerous advice, and serving as committee members.

I would like to thank all of my colleagues, current and past for making the lab a home away from home. I would like to particularly thank Dr. Olga Zolotarskaya and Dr. Quan Yuan as well as my student colleagues, Donald Aduba, Jingfei Tian, Christopher Holden, Gunjan Saxena and Natasha Sheybani for their help.

I would also like to acknowledge my former research advisors, Dr. Shunlin Ren, Dr. William Pandak, Dr. Daniel Rodriguez-Agudo, Dr. Phillip Hylemon and Dr. Huiping Zhou for their training, support and guidance at Hunter Holmes McGuire VA Medical Center, as well as my former research colleagues, Dr. Qianming Bai, Dr. Xin Zhang, Dr. Genta Kakiyama, Kaye Redford, Dalila Marques and Jin Koung Kim for their previous excellent technical support.

Lastly but not the least, I would like to thank my friends and family for supporting me throughout this journey. Specially, I want to thank my wonderful girlfriend, Hao, for your sharing, caring and support. To my dear mom and dad, thank you for your unconditional love, care, and prayers. You have made every possible opportunity to my life and I love you mom and dad. I will keep making you all proud.

LEYUAN XU

Virginia Commonwealth University

August 2013

Contents

Acknowledgments	iv
List of Tables	viii
List of Figures	ix
Abbreviations	xi
Abstract	xiii
1 Introduction	1
1.1 Background	1
1.2 Hypothesis and research goals	6
1.3 Thesis structure	7
2 Correlating intracellular AKT signaling transduction to cyto- compatibility of photoinitiators	9
2.1 Introduction	9
2.2 Materials and Methods	12
2.2.1 Materials	12
2.2.2 Photoinitiator preparation	12
2.2.3 Cell culture	13
2.2.4 Comparison of photoinitiators	13
2.2.5 Comparison of photoinitiators after UV irradiation	13
2.2.6 Cytotoxicity and cellular response of free radicals	14

2.2.7	Cellular proliferation rate	14
2.2.8	Western blot analysis	14
2.2.9	Statistical analysis	15
2.3	Results and discussion	15
2.3.1	The effect of photoinitiators on HN4 cell viability	15
2.3.2	The effects of photoinitiators on intracellular AKT signaling transduction in HN4 cells	19
2.3.3	The effect of UV-exposed photoinitiators on viability and in- tracellular AKT signaling transduction in HN4 cells	23
2.3.4	The evaluation of free radicals stability on viability and intra- cellular AKT signaling transduction in HN4 cells	29
2.4	Conclusions	32
3	Fabrication of semi-interpenetrating network scaffolds for transbuc- cal mucosal delivery of insulin	34
3.1	Introduction	34
3.2	Materials and Methods	38
3.2.1	Materials	38
3.2.2	Cell culture	39
3.2.3	Scaffold preparation	39
3.2.4	Preparation of GF and GIF	39
3.2.5	Preparation of crosslinked GF and GIF	40
3.2.6	Cytocompatibility assay	41
3.2.7	In vitro degradation studies	41
3.2.8	Uniaxial tensile testing	41
3.2.9	Scanning electron microscopy (SEM)	42
3.2.10	Insulin release studies	42
3.2.11	Western blot analysis	42
3.2.12	Oil red O staining	43
3.2.13	In vitro permeation studies	43

3.2.14	Statistical analysis	44
3.3	Results and discussion	45
3.3.1	Optimization of sINP GF scaffold	45
3.3.2	Mechanical properties of sINP GF scaffold	49
3.3.3	Morphology and fiber diameter of sIPN GF	50
3.3.4	Structure stability of sIPN GF	50
3.3.5	Insulin release kinetics of sIPN GIF	54
3.3.6	Bioactivity of the insulin released from sIPN GIF	56
3.3.7	Diffusion rate of insulin from sIPN GIF across porcine buccal mucosa	61
3.4	Conclusions	65
4	General conclusions and future directions	66
4.1	General conclusions	66
4.2	Future directions	68
4.2.1	Evaluation of sIPN GIF in in vivo model	68
4.2.2	Potential application of sIPN GF for wound healing	69
	Bibliography	71
	A Statistical analysis of the experimental data	84

List of Tables

1.1	Summary of in vivo bioavailability of insulin-loaded nanoparticles on oral administration [17, 12].	7
-----	---	---

List of Figures

1.1	Structures of proinsulin and insulin [74].	3
1.2	A schematic diagram of insulin signaling transduction pathway [78].	5
2.1	The effect of eosin Y on HN4 cell viability.	16
2.2	The effect of Irgacure 2959 on HN4 cell viability.	17
2.3	The effect of DMPA on HN4 cell viability.	18
2.4	The effect of eosin Y on intracellular AKT activity in HN4 cells.	20
2.5	The effect of Irgacure 2959 on intracellular AKT activity in HN4 cells.	21
2.6	The effect of DMPA on intracellular AKT activity in HN4 cells.	22
2.7	A schematic diagram of photoinitiator decomposition to free radicals [1, 52, 59].	24
2.8	The effect of UV-exposed eosin Y on HN4 cell viability.	25
2.9	The effect of UV-exposed Irgacure 2959 on HN4 cell viability.	26
2.10	The effect of UV-exposed DMPA on HN4 cell viability.	27
2.11	The effect of UV-exposed photoinitiators on intracellular AKT activity in HN4 cells.	28
2.12	The effect of the free radicals stability on HN4 cell viability.	30
2.13	The effect of the free radicals stability on intracellular AKT activity in HN4 cells.	31
3.1	Experimental setup to schematically illustrate the conventional electrospinning.	40
3.2	Effects of PEG and PEG-DA on cell viability.	46

3.3	Effects of different formulations of GF scaffolds on cell viability. . . .	48
3.4	In vitro degradation of different fabricated GF scaffolds in the cell culture media.	49
3.5	Mechanical properties of GF and sIPN GF.	51
3.6	Morphology of GF and sIPN GF.	52
3.7	Fiber diameter of GF and sIPN GF.	52
3.8	Morphology of sIPN GF after degradation.	53
3.9	In vitro insulin release kinetics.	55
3.10	In vitro insulin release kinetics of sIPN GIF.	56
3.11	Western blot analysis of intracellular AKT activity in responding to the fabricated GF scaffolds.	58
3.12	Western blot analysis of intracellular AKT activity in responding to sIPN GIF.	59
3.13	Oil red O staining of 3T3-L1 preadipocytes in responding to sIPN GIF.	60
3.14	In vitro degradation of sIPN GF in SSF.	62
3.15	Transport of insulin or benzylamine across porcine buccal mucosa.	63
3.16	Transport of insulin across porcine buccal mucosa.	64

Abbreviations

AKT	Protein kinase B
ANOVA	Analysis of variance
DMEM	Dulbecco's Modification of Eagle's Medium
DMPA	Dimethoxyphenyl acetophenone
DMSO	Dimethyl sulfoxide
ELISA	Enzyme-linked immunosorbent assay
ER	Endoplasmic reticulum
FBS	Fetal bovine serum
GF	Gelatin fiber scaffold
GIF	Gelatin-co-insulin fiber scaffold
GK	Glucokinase
GSK	Glycogen synthase kinase
HFP	1,1,1,3,3,3-Hexafluoro-2-propanol
Irgacure 2959	2-hydroxy-1-[4-(hydroxyethoxy)phenyl]-2methyl-1-propanone
IRS-1	Insulin receptor substrate-1
NA	No addition
NVP	1-vinyl-2 pyrrolidinone
p-AKT	Phosphorylated AKT
PBS	Phosphate buffer solution
PCL	Poly(ϵ -caprolactone)
PEG-DA	Polyethylene glycol diacrylate
PI3K	Phosphoinositide 3-kinase

PLA	Poly(lactide)
PLGA	Poly(lactide-co-glycolide)
PVDF	Polyvinylidene difluoride
ROS	Reactive oxygen species
SD	Standard deviation
sIPN	Semi-interpenetrating network
sIPN GF	Semi-interpenetrating network gelatin fiber scaffold
sIPN GIF	Semi-interpenetrating network gelatin-co-insulin fiber scaffold
T1DM	Type 1 diabetes mellitus
T2DM	Type 2 diabetes mellitus
TBS	Tris-buffered saline
TEOA	Triethanolamine

Semi-Interpenetrating Network Gelatin Fiber Scaffold for Oral Mucosal Delivery of Insulin

Leyuan Xu

Virginia Commonwealth University, 2013

Advisor: Hu Yang

ABSTRACT

Common therapy for diabetes mellitus is subcutaneous administration of insulin that is subject to serious disadvantages, such as patient noncompliance and occasional hypoglycemia. Hence, oral administration of insulin could be more convenient and serve as a desired route. However, oral administration of insulin is severely limited by the low bioavailability of insulin through the gastrointestinal tract. In this study, a semi-interpenetrating network gelatin fiber scaffold (sIPN GF) was fabricated for oral mucosal delivery of insulin as an alternative route. This sIPN GF was engineered from an electrospun gelatin fiber scaffold (GF), which was further crosslinked with polyethylene glycol diacrylate (PEG-DA) to enhance its stability. Within the crosslinking process, eosin Y served as a photoinitiator, and the ratio of PEG-DA to eosin Y was optimized with respect to cytocompatibility and degradation rate. The results showed that the fabricated scaffold morphology, mechanical properties, and degradation rate were significantly enhanced after the crosslinking process. This optimized formulation was used to fabricate sIPN gelatin-co-insulin fiber scaffold (sIPN GIF). Enzyme-linked immunosorbent assay (ELISA) was used to monitor the insulin releasing kinetics of sIPN GIF. Western blot analysis showed that sIPN GIF activated intracellular AKT phosphorylation in a releasing time-dependant manner. Oil red O staining confirmed the released insulin was able to induce 3T3-L1 preadipocyte differentiation. The permeability of insulin from sIPN GIF was determined on the

order of 10^{-7} cm/s using a vertical Franz diffusion cell system mounted with porcine buccal mucosa. These findings suggest that sIPN GIF holds a great potential for oral mucosal delivery of insulin.

Chapter 1

Introduction

1.1 Background

Diabetes mellitus, or simply diabetes, is defined as a group of metabolic diseases characterized by hyperglycemia that results from lack of insulin production or insulin response [28]. Diabetes is a major cause of heart disease and stroke, and it can also lead to vision loss, kidney failure, and amputations of legs and feet. It is reported as the seventh leading cause of death in the U.S. according to the National Diabetes Fact Sheet 2011 and Diabetes Report Card 2012 from the Centers for Disease Control and Prevention (CDC) (<http://www.cdc.gov/diabetes/pubs/reportcard.htm>). The reports show that about 8.3% of the U.S. population, including children and adults, has diabetes. The prevalence of diabetes is projected that one of three U.S. adults could have diabetes by 2050 if the current trend continues.

Generally, there are three common types of diabetes, referred to as type 1 diabetes mellitus (T1DM), type 2 diabetes mellitus (T2DM) and gestational diabetes. T1DM accounts for about 5% of all diagnosed cases of diabetes in the U.S., and it is commonly diagnosed in children and young adults. T1DM is characterized by the destruction of the pancreatic beta cells and insulin deficiency. The risk factors of T1DM can be autoimmune, genetic or environmental. To date, there is no therapy available to prevent T1DM. T1DM patients require daily insulin administration from an injection or a pump in order to survive. T2DM accounts for about 95% of all

diagnosed cases of diabetes in the U.S. T2DM is characterized by insulin resistance and impaired insulin secretion by the beta cells in the pancreas. As T2DM progresses, patients require more insulin, which leads to the pancreas eventually to lose its ability to produce insulin. Current reports indicate that healthy diet, regular exercise and prescribed medication can help to prevent, control health complications, and delay the onset of T2DM. Last, gestational diabetes is diagnosed as a result of pregnancy in 2-10% of pregnant women. Gestation diabetes can cause health problems for both mother and child. Women who have gestational diabetes may have a higher risk of developing T2DM in the future; while their children may have an increased risk of developing T2DM and obesity [28].

Insulin is a peptide hormone that is the key to regulate carbohydrate and fat metabolism in the body. Proinsulin is a prohormone and the precursor of insulin that is produced by beta cells of the islets of Langerhans. Proinsulin is synthesized and folded in the endoplasmic reticulum (ER) where its disulfide bonds are oxidized. After it is transported to the Golgi apparatus and packaged into secretory vesicles, it undergoes a series of digestion by proteases to form mature insulin. As an illustration shown in Figure 1.1, mature insulin (insulin) has 35 fewer amino acids, in which 4 amino acids are cleaved altogether and the remaining 31 amino acids form the C-peptide. After abstraction of C-peptide from the center of the proinsulin, insulin becomes a dimer of an A-chain (30 amino acids) and a B-chain (21 amino acids) connected by disulfide bonds.

Under physiological circumstances, when blood glucose concentration is below 90 mg/dl, it does not cause any insulin release. When carbohydrates are consumed, carbohydrates are digested and broken down to glucose molecules in the gut. These glucose molecules are subsequently absorbed into the bloodstream and elevate blood glucose concentration. The pancreas senses the rise of blood glucose concentration and in turn stimulates the secretion of insulin from the beta cells. Insulin is required for most cells to be able to uptake of glucose from the blood stream. The excess glucose can be stored in the liver in the form of glycogen for future use. The liver is

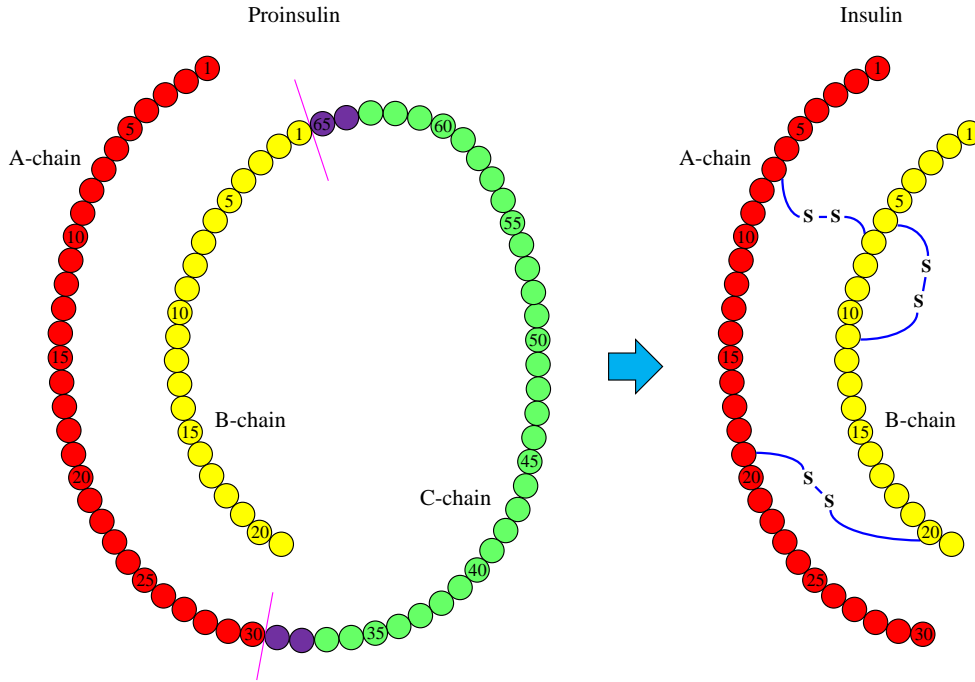


Figure 1.1: Structures of proinsulin and insulin [74].

able to convert glucose from fatty acids and amino acids to fat and protein respectively via gluconeogenesis. As a result, the increased secretion of insulin from the pancreas lowers blood glucose level, which in turn decreases insulin secretion.

Under pathophysiological circumstances, the insulin production and secretion are altered, which results the blood glucose uptake also changes. The limitation of the insulin production causes the decrease of glucose uptake by the cells, resulting in hyperglycemia. Because the pancreas cannot produce insulin in T1DM patients, glucose cannot enter cells, and it remains in the bloodstream. Subsequently, the fat is broken down to glycerol and free fatty acids via lipolysis in order to provide energy. Glycerol is converted to glucose as the energy source; while fatty acids are converted to ketone bodies. The elevated ketone bodies in body fluids cause a decrease of pH and loss of electrolytes, resulting diabetic ketoacidosis. The untreated diabetic ketoacidosis will cause coma or death. In T2DM, it is characterized by three disorders as peripheral insulin resistance, especially in muscle cells, increased glucose production from the liver, and eventually impaired insulin secretion pancreas.

The insulin signaling pathway plays an important role in homeostasis at the cellular level. This signaling pathway is regulated by feeding/fasting states, stress levels, and a variety of other hormones. Insulin does not directly enter the cell in its original form, but follows a sequential process as shown in Figure 1.2.

In detail, (1) Insulin binds to the extracellular portion of the α subunits of the insulin receptor. (2) It causes a conformational change in the insulin receptor that activates the kinase domain in the intracellular portion of the β subunits. (3) The activated kinase domain in turn autophosphorylates tyrosine residues on the C-terminus of the receptor and tyrosine residues in the insulin receptor substrate-1 (IRS-1) protein. (4) The phosphorylated IRS-1 binds and activates phosphoinositol 3 kinase (PI3K). (5) The activated PI3K catalyzes the reaction of $\text{PIP}_2 + \text{ATP} \rightarrow \text{PIP}_3 + \text{ADP}$. (6) PIP_3 phosphorylates and activates protein kinase B, also as known as AKT. (7) The phosphorylated AKT (p-AKT) further phosphorylates and inactivates glycogen synthase kinase (GSK). (8) The phosphorylated GSK in turn cannot phosphorylate glycogen synthase (GS). (9) The unphosphorylated GS becomes active form and produce glycogen. (10) The p-AKT can also facilitate glucose transporter type 4 into the plasma membrane.

Insulin serves as a common protein therapy to diabetes mellitus, and it is conventionally administered to patients via subcutaneous injection. Two common subcutaneous injection methods are recommended in order to mimic physiological release of insulin. One is multiple daily injections via a syringe or a pen; the other one is an external continuous subcutaneous insulin infusion via a pump [28, 17]. However, these subcutaneous injection methods have serious disadvantages, including patient noncompliance and occasional hypoglycemia. Thus, oral administration of insulin becomes a more convenient and desired route if available [17, 71]. Nonetheless, oral administration of insulin is severely limited by the low bioavailability of insulin, including inherent instability and low permeability across biological membranes through the gastrointestinal tract [71]. A variety of formulations for oral insulin delivery have been developed in the last decade. Nanoparticle-based insulin

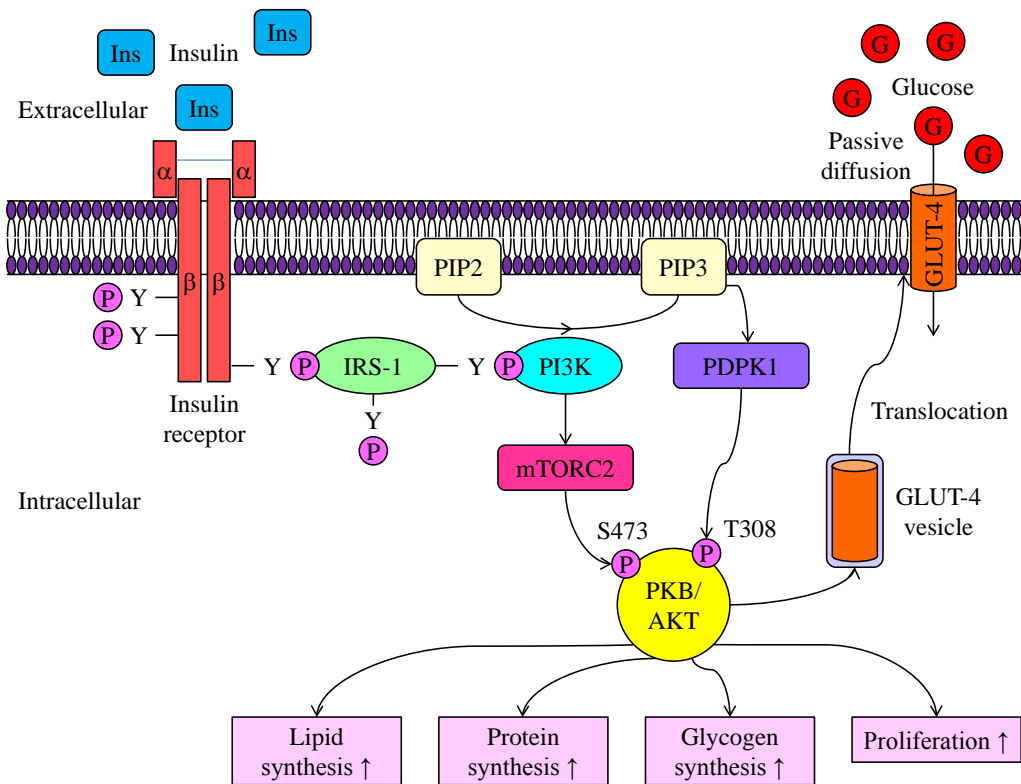


Figure 1.2: A schematic diagram of insulin signaling transduction pathway [78].

delivery systems were reported to be able to overcome these barriers, and these systems have been received considerable attention. The nanoparticles can be made from natural or synthetic polymers. Natural polymers are shown great interest due to their high biocompatibility and biodegradability. Chitosan and its derivatives, as one family of these natural polymers, have been widely explored for oral insulin delivery owing to their excellent mucoadhesive properties and permeability [54, 76, 39]. Synthetic polymers are attracting growing attention due to the high possibility of new dosage formulations and the potential applications in cell-specific drug targeting [3]. Poly(lactide-co-glycolide) (PLGA) [19, 20], poly(lactide) (PLA) [86], and poly(ϵ -caprolactone) (PCL) [21] have been used to fabricate nanoparticles for oral insulin delivery owing to their well-established safety records. As the summary shown in Table 1.1, the maximum bioavailability of insulin through oral administration is around 30% among these nanoparticle-based delivery systems. At this point, maximization of the absorptive cellular intestinal uptake and stabilization of insulin within the gastrointestinal tract remains as a challenge for nanoparticle oral delivery of insulin. Efficacy and economic reasons will impact a market launch for these nanoparticles as well.

1.2 Hypothesis and research goals

A gelatin-based electrospun fiber scaffold was developed to locally deliver nystatin for candidiasis [2]. Electrospun gelatin fiber scaffolds (GFs) possess high biocompatibility and mucoadhesive property that allow local sustained release of drug at the absorption site [2, 7]. GF can be stabilized using a crosslinker of photocurable polyethylene glycol diacrylate (PEG-DA) and form a semi-interpenetrating network fiber scaffold (sIPN). The fiber morphology, mechanical and physical properties as well as drug release kinetics can be controlled by modulating the concentration of crosslinker [2]. In this work, a semi-interpenetrating network gelatin-co-insulin fiber scaffold (sIPN GIF) was hypothesized for transbuccal mucosal delivery of insulin. The cytocompatibility

Table 1.1: Summary of in vivo bioavailability of insulin-loaded nanoparticles on oral administration [17, 12].

NP systems	BA	References
Chitosan NPs	14.9%	[57]
Chitosan-polyglutamic acid NPs	15.1%	[51]
Dextran sulfate-chitosan NPs	5.6%	[62]
VB12-dextran sulfate-chitosan NPs	26.5%	[14]
Alginate crosslinked dextran	13.0%	[83]
Aminoalkyl Vitamin B12 dextran sulfate chitosan	29.4%	[15]
Chitosan-TBA	1.7%	[38]
PLGA-Hp55 NPs	6.3%	[19]
Insulin-phospholipid complex loaded NPs	7.7%	[20]
Aspart-insulin loaded CS/ γ -PGA NPs	15.0%	[69]

Abbreviations: PLGA, poly(lactide-co-glycolide); Hp55, hypromellose phthalate, HPMCP-55; VB12, vitamin B12; SLNs, solid lipid nanoparticles; γ -PGA, poly(γ -glutamic acid); TBA, thiobutylamidine; NPs, nanoparticles; BA, relative bioavailability; Bioavailability of insulin systems was determined based on the serum insulin level relative to that achieved with subcutaneous insulin injection.

of each components of sIPN GF was evaluated, and the formulation of sIPN GF was optimized in respect to cytocompatibility and degradation rate. This optimized formulation was used to fabricate sIPN GIF. Enzyme-linked immunosorbent assay (ELISA) was used to monitor the insulin release kinetics of sIPN GIF. Western blot analysis and 3T3-L1 preadipocyte differentiation analysis were used to determine the bioactivity of insulin released from sIPN GIF. The permeability of the insulin released from sIPN GIF was evaluated through a porcine buccal mucosal membrane, which possesses analogous thickness, structure, morphology, and composition to normal human buccal epithelium [91].

1.3 Thesis structure

The goal of this work is to explore the potential of sIPN GF in transbuccal mucosal delivery of insulin. Photopolymerization was used to crosslink gelatin fiber in

order to modulate the scaffold stability and insulin release kinetics. Chapter 2 investigates the cytocompatibility of different photoinitiator systems, including eosin Y, dimethoxyphenyl acetophenone (DMPA) and 2-hydroxy-1-[4-(hydroxyethoxy)phenyl]-2-methyl-1-propanone (Irgacure 2959) systems. This chapter illustrates the correlation of intracellular AKT signaling transduction to cytocompatibility of photoinitiator systems and their free radicals on HN4 cells. Chapter 3 investigates sIPN GF as the primary material platform for transbuccal mucosal delivery of insulin. This chapter provides insights into: (1) the optimization of sIPN GF formulation in respect to cytocompatibility and degradation rate; (2) the structure stability and mechanical properties of sIPN GF; (3) the release kinetics and the bioactivity of insulin from sIPN GF; and (4) the permeability of insulin released from sIPN GF through a porcine buccal mucosal membrane. Chapter 4 summarizes the conclusions drawn from the presented investigations and proposes possible future research directions based on the results of this work.

Chapter 2

Correlating intracellular AKT signaling transduction to cytocompatibility of photoinitiators

2.1 Introduction

Photopolymerization has the ability to initiate rapid formation of a polymer network from a liquid monomer or macromer under physiological conditions [9]. It has been shown in great advantages of well spatial and temporal control of reaction kinetics, minimal heat production, ability to uniformly encapsulate cells, and significant adaptability for in situ polymerization by adapting light sources to fit biomedical applications [81]. Photopolymerizations have been used in a broad range of biological applications, such as dentistry [8], optical materials [72], encapsulating pancreatic islet cells [42], blood vessel adhesives [46], controlled release applications [13], drug delivery [29], and bone restorations [22]. For instance, a novel photopolymerized dendrimer hydrogel was reported for delivery of two antiglaucoma drugs, brimonidine and timolol maleate [29]. This dendrimer hydrogel was mucoadhesive to mucin par-

ticles and nontoxic to human corneal epithelial cells. Subsequently, this dendrimer hydrogel could increase the solubility of brimonidine and sustain the in vitro release of both drugs over 56-72 hours. This dendrimer hydrogel was also shown a significant increase of bovine corneal transport and human corneal epithelial cell uptake for both drugs compared to PBS-based eye drop formulations [29].

The mechanism for photopolymerization is to dissociate initiator molecules into radicals by exposure to specific wavelengths of light [9]. During irradiation, a photon from a light source excites and dissociates the photoinitiator molecule into a high-energy radical that can induce the polymerization of a macromer solution [81]. To date, a number of photoinitiators have been developed with their unique absorption spectrum. For instance, dimethoxyphenyl acetophenone (DMPA) has a peak maximum wavelength of 310 nm [44], eosin Y has a peak maximum wavelength of 510 nm [6], 1-Hydroxy-cyclohexyl-phenyl-ketone (Irgacure 184) has a peak maximum wavelength of 244 [48], 2-Methyl-1-[4-(methylthio)phenyl]-2-(4-morpholinyl)-1-propanone (Irgacure 907) has a peak maximum peak wavelength of 309 nm [48], and 2-Hydroxy-1-[4-(2-hydroxyethoxy)phenyl]-2-methyl-1-propanone Irgacure 2959 has a peak maximum wavelength of 276 nm [48]. Despite their unique absorption spectrums, these photoinitiators could be dissociated into free radicals at the wavelength of 365 nm and convert liquid monomers or macromers into hydrogels [9, 29].

The major limitation of photopolymerization techniques for tissue engineered scaffolds or hydrogels is that the high-energy free radicals can create the potential for oxidative damage to the photoencapsulated cell populations [9]. Unlike surgical adhesives and adhesion barriers, many photopolymerization applications involve cell encapsulation that leads direct contact between cells and free radicals. Free radicals can directly react with different cellular macromolecules (cell membranes, proteins and DNA) or indirectly induce formation of reactive oxygen species (ROS), thereby causing unwanted cellular damage [72]. Although the use of antioxidant reagents such as uric acid and melatonin could help prevent oxidative damage and quench intracellular ROS, exposure to ultraviolet A radiation can still induce ROS production, potentially leading to malignant transformation of photo-exposed cells [72]. Such

free radical-induced oxidative stress or UV-induced lesions may cause mutagenicity, but relatively few studies have investigated intracellular signaling transduction on photo-exposed cells.

Cells utilize numbers of signaling pathways to regulate their biological activities and transmit information from environment. AKT, also known as protein kinase B, is a serine/threonine-specific protein kinase that regulates cell proliferation, survival and oncogenesis [4]. It has been well documented that AKT plays a central role in promoting downstream of activated growth factor receptor signaling [47]. In cell survival signaling pathways, AKT enhances cell survival by blocking the function and processes of proapoptotic proteins. AKT suppresses the function and expression of several B-cell lymphoma 2 (Bcl-2) homology domains-only proteins, which binds and inactivates prosurvival Bcl-2 family members [47, 23]. AKT activates nuclear factor kappa-light-chain-enhancer of activated B cells (NF κ B) survival signaling or inhibits c-Jun N-terminal kinase/mitogen-activated protein kinase (JNK/p38) apoptotic signaling under certain circumstances [47, 37]. In cell growth signaling pathways, AKT promotes cell growth by activating mammalian target of rapamycin complex 1 (mTORC1) that is a critical regulator of translation initiation and ribosome biogenesis [47, 85]. In cell proliferation signaling pathways, AKT stimulates cell proliferation through multiple downstream targets regulating cell cycling such as glycogen synthase kinase 3 (GSK3), tuberous sclerosis 2 (TSC2) and proline-rich AKT substrate of 40 kDa (PRAS40) [47]. GSK3 plays central role in the G1 to S phase cell cycling transition [90]; while TSC2 and PRAS40 promotes cell growth by activating mTORC1 [66]. In angiogenesis signaling pathways, vascular endothelial growth factor (VEGF) robustly activates AKT in endothelial cells and subsequently promotes endothelial cell survival, growth, proliferation and migration [47, 56]. Understanding the fundamentals above, it is of interest to determine intracellular AKT signaling transduction in photo-exposed cells during photopolymerization process.

In this chapter, the intracellular AKT signaling and the cell viability were evaluated in response to the photoinitiators. HN4 cells were treated with DMPA, eosin Y and Irgacure 2959 in a broad range of concentrations with and without UV radiation.

The intracellular AKT activity were determined by Western blot analysis, and the cell viability was measured using WST-1 assay. The stability of free radicals induced by UV irradiation was also evaluated in HN4 cells in respect to the intracellular AKT activity and the cell viability.

2.2 Materials and Methods

2.2.1 Materials

1-vinyl-2 pyrrolidinone (NVP), dimethoxyphenyl acetophone (DMPA), dimethyl sulfoxide (DMSO), eosin Y, ethanol, phosphate buffer solution (PBS), and triethanolamine (TEOA) were purchased from Sigma-Aldrich (St. Louis, MO). Irgacure 2959 was provided by Ciba Corporation (Newport, DE). Cell proliferation reagent WST-1 was purchased from Roche Applied Science (Indianapolis, IN). Phospho-Akt (Ser473) (p-AKT) antibody was purchased from Cell Signaling Technology (Danvers, MA). AKT1 (559028) antibody was purchased from BD Biosciences Pharmingen (Mississauga, ON, Canada). β -actin (ACTBD11B7) antibody was purchased from Santa Cruz Biotechnology (Santa Cruz, CA). Goat anti-rabbit antibody conjugated to horseradish peroxidase and goat anti-mouse antibody conjugated to horseradish peroxidase were purchased from Bio-Rad (Hercules, CA).

2.2.2 Photoinitiator preparation

Three ultraviolet photoinitiating systems were examined in this work. The photoinitiator solutions were prepared based on weight per volume calculations per industry standard. Briefly, 0, 25, 50, 100 and 250 mg of DMPA was dissolved in 1 ml of ethanol, resulting 0, 25, 50, 100 and 250 mg/ml of DMPA stock solutions. 0, 50, 100, 250 and 500 mg of DMPA was dissolved in 1 ml of ethanol, resulting 0, 50, 100, 250 and 500 mg/ml of Irgacure 2959 stock solutions. Eosin Y photoinitiator stock solution was prepared by 0.1% eosin Y, 4% NVP, and 40% TEOA in PBS according to the previous reports [29, 24]. All resulting photoinitiator solutions were protected

from light and stored at room temperature until use.

2.2.3 Cell culture

HN4 cells were derived from a primary SCC of the head and neck. The cells were cultured in Dulbecco's Modification of Eagle's Medium (DMEM) (Life Technologies, Grand Island, NY) supplemented with high glucose, L-glutamine, 10% (v/v) fetal bovine serum (Fisher Scientific, Pittsburgh, PA), 100 units/ml of penicillin and 100 $\mu\text{g}/\text{ml}$ of streptomycin (Thermo Fisher Scientific, Ashville, NC) at 37°C in a humid environment with 5% CO₂ before any biocompatibility study was performed.

2.2.4 Comparison of photoinitiators

40 μl of each DMPA or Irgacure 2959 stock solution was added to 2 ml of fresh culture media to reach a final concentration of 0, 0.5, 1, 2 and 5 mg/ml of DMPA and 0, 1, 2, 5 and 10 mg/ml of Irgacure 2959. 0, 5, 10, 20 and 50 μl of eosin Y stock solution was added to 2 ml of fresh culture media to reach a final concentration of 0, 2.5, 5, 10 and 25 $\mu\text{l}/\text{ml}$ of eosin Y. For cell viability analysis, Pre-seeded HN4 cells on a 96-well plate were treated with above condition media for 1-4 days. The spent media were replaced by the same fresh condition media every day during the treatments in order to maintain a constant concentration of each photoinitiator. For protein expression analysis, Pre-seeded HN4 cells on a 6-well plate were treated with above condition media for 30 min, and total protein lysates were harvested by total cell lysate buffer with protease and phosphatase inhibitors (Roche Applied Science, Indianapolis, IN).

2.2.5 Comparison of photoinitiators after UV irradiation

The fresh cell culture media were mixed with different concentrations of each photoinitiator stock solution to reach a final concentration at 0, 0.5, 1 and 2 mg/ml of DMPA and 1, 2 and 5 mg/ml of Irgacure 2959 as well as 2.5, 5, 10 $\mu\text{l}/\text{ml}$ of eosin Y. These mixtures were equally exposed to UV radiation at 365 nm with an intensity of 100 watts for 30 min in order to decompose the photoinitiator into free radicals. Pre-

seeded HN4 cells were then subjected to the media right after UV irradiation. After 1 and 2 days treatments, the cellular proliferation rate was determined by WST-1 assay. After 30 min treatment, total cellular p-AKT and AKT1 expression was evaluated by Western blot analysis.

2.2.6 Cytotoxicity and cellular response of free radicals

The fresh cell culture media were mixed with the eosin Y stock solution to reach a final concentration at 20 $\mu\text{l}/\text{ml}$ of and then exposed to UV radiation at 365 nm with an intensity of 100 watts for 30 min to decompose into free radicals. Pre-seeded HN4 cells the conditioned media in 0, 6, 24, 48 hours after UV irradiation. After 2 days treatments, the cellular proliferation rate was determined by WST-1 assay. After 30 min treatment, total cellular p-AKT and AKT1 expression was evaluated by Western blot analysis.

2.2.7 Cellular proliferation rate

HN4 cells were seeded on a 96-well plate with a density of 10,000 cells/well and cultured for 2 days to allow the cells adhesion. At the end of each treatment, the cellular proliferation rate of surviving cells was determined by addition of 10% (v/v) of WST-1 reagent according to the manufacturers protocol. After 30 min incubation, the absorbance of the samples was measured at 450 nm, against a background control as a blank, and this value was then subtracted by the absorbance at 650 nm as a reference wavelength.

2.2.8 Western blot analysis

Western blot analysis of total cellular protein was carried out by standard procedures, as described previously [89, 88]. Briefly, total cell lysates (30 μg) were separated on a 10% SDS-PAGE gel and transferred onto a polyvinylidene difluoride (PVDF; Bio-Rad, Hercules, CA) membrane using Bio-Rad Mini-Blot transfer apparatus. The membrane was blocked for 2 hours in Tris-buffered solution (TBS) containing 5%

of non-fat dried milk. The specific proteins on the membrane were determined by incubating with the primary antibodies overnight at 4 °C with shaking. The membrane was washed three times and then incubated in a 1:3,000 dilution of a secondary antibody at room temperature for 1 hour in the washing buffer (Tris-buffered solution containing 0.5% Tween 20). The specific antigen-antibody interactions were detected using enhanced chemiluminescence (Pierce ECL Western Blotting Substrate; Thermo Scientific, Rockford, IL). The total cellular expression of β -actin was used as the loading control.

2.2.9 Statistical analysis

All the data were expressed as means \pm standard deviation (SD) and subjected to one way analysis of variance (ANOVA) followed by Holm-Sidak method for significance using SigmaPlot 12. A value of $p < 0.05$ was considered as statistically significant. Statistical analysis data is provided in Appendix A (p85-119).

2.3 Results and discussion

2.3.1 The effect of photoinitiators on HN4 cell viability

The effects of photoinitiators including eosin Y, Irgacure 2959 and DMPA on the viability of HN4 cells were first evaluated. As shown in Figures 2.1, 2.2 and 2.3, eosin Y exhibited less cytotoxicity than Irgacure 2959 and DMPA, as the evidence showed that HN4 cells were tolerant to a wider concentration range of eosin Y than Irgacure 2959 and DMPA. Up to 4-day treatment of 2.5 μ l/ml of eosin Y or 1 mg/ml Irgacure 2959, HN4 cells were able to maintain nearly 100% cell viability (Figures 2.1 and 2.2). Eosin Y reduced HN4 cell viability in a concentration-dependent manner at each time period treatment; whereas nearly no viable HN4 cell was observed after 1-day treatment of Irgacure 2959 at the concentration greater than 2 mg/ml. In contrast,

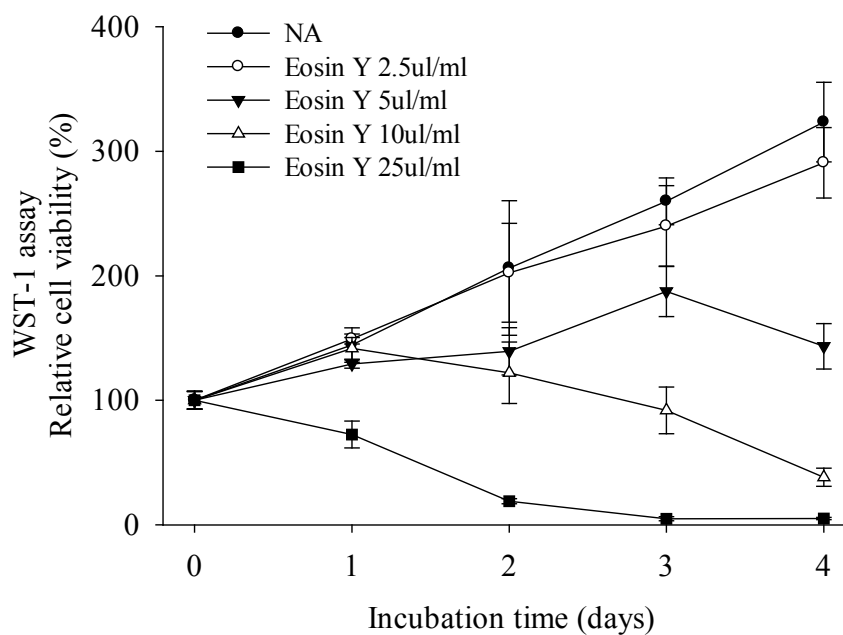


Figure 2.1: The effect of eosin Y on HN4 cell viability.

HN4 cells were plated at a density of 1×10^4 cells/well into 96-well plates and treated with different concentrations of eosin Y as indicated for 0, 1, 2, 3 and 4 days. The cell viabilities were measured by WST-1 assay at the end of the treatment. The bars are mean \pm standard deviation.

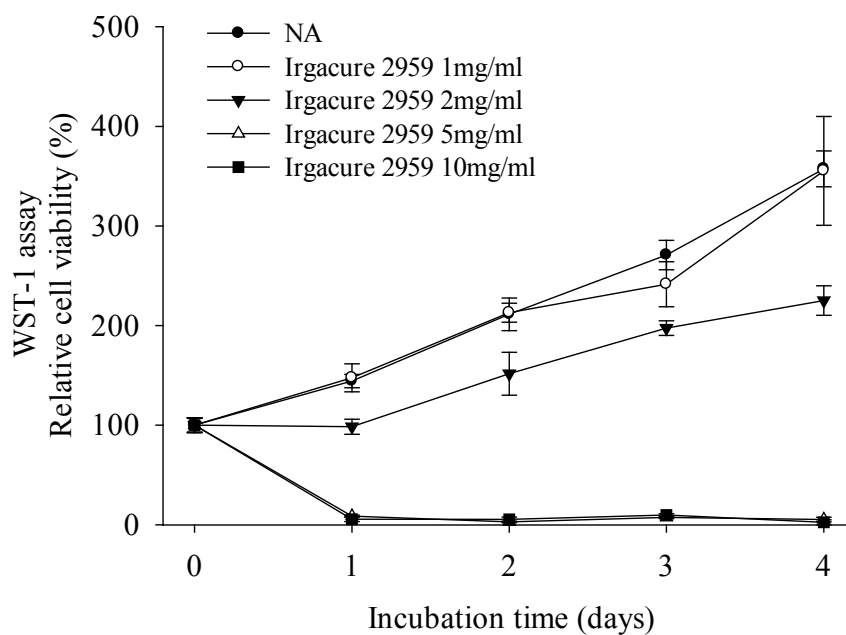


Figure 2.2: The effect of Irgacure 2959 on HN4 cell viability.

HN4 cells were plated at a density of 1×10^4 cells/well into 96-well plates and treated with different concentrations of Irgacure 2959 as indicated for 0, 1, 2, 3 and 4 days. The cell viabilities were measured by WST-1 assay at the end of the treatment. The bars are mean \pm standard deviation.

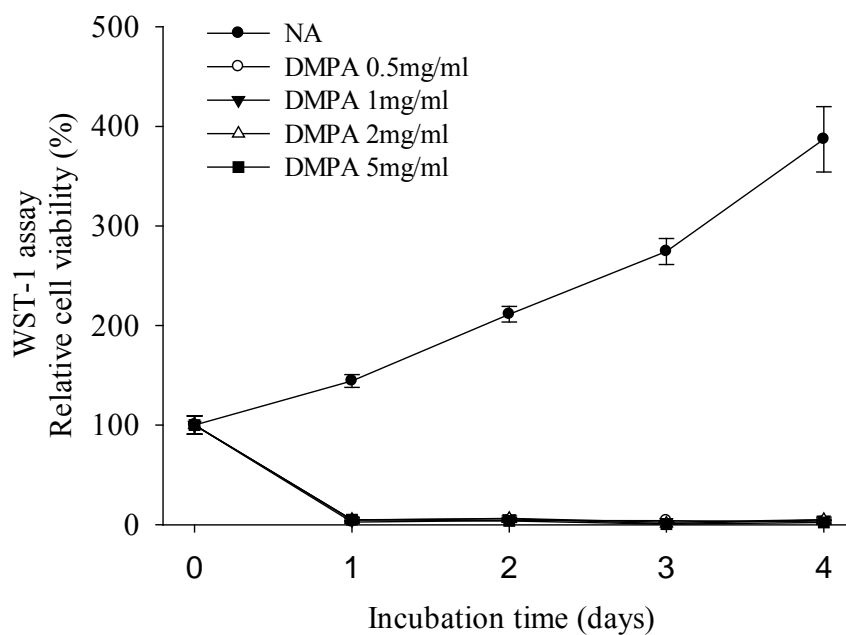


Figure 2.3: The effect of DMPA on HN4 cell viability.

HN4 cells were plated at a density of 1×10^4 cells/well into 96-well plates and treated with different concentrations of DMPA as indicated for 0, 1, 2, 3 and 4 days. The cell viabilities were measured by WST-1 assay at the end of the treatment. The bars are mean \pm standard deviation.

DMPA exhibited a significant cytotoxic effect to cells, as the evidence showed that no viable HN4 cell was observed at each concentration of DMPA in each time period treatment (Figure 2.3).

The cytotoxicity profile of Irgacure 2959 was consistent with the previous report, which showed there was nearly no cytotoxicity of Irgacure 2959 up to 1 mg/ml in both bovine chondrocytes and human fetal osteoblasts [9, 81]. Up to date, there is very few reports investigating a wide concentration range of photoinitiators on the cell viability. This is the first time to show that an approximate maximum concentration of eosin Y and Irgacure 2959 can be used in cell culture with a desirable cytotoxicity. However, in vivo circumstances are different as in vitro 2-dimensional cell culture. The use of photoinitiators in in vivo biomedical application needs to be further evaluated based on these in vitro cell culture results.

2.3.2 The effects of photoinitiators on intracellular AKT signaling transduction in HN4 cells

AKT is one of the key regulators in cell proliferation and survival that transmits information from environment and regulates cell viability. To further evaluate the effects of photoinitiators on cellular response, the intracellular signaling transduction was determined in response to eosin Y, Irgacure 2959 and DMPA. HN4 cells were used as our model cell line to determine the intracellular AKT activity in acute response to the three photoinitiators because HN4 cells keep a constitutive high AKT activation [79]. After 30 min treatment, eosin Y had no significant effect on the phosphorylation of AKT up to 25 μ l/ml in HN4 cells as shown in Figure 2.4. In contrast, both Irgacure 2959 and DMPA diminished the phosphorylation of AKT in a concentration-dependent manner as shown in Figure 2.5 and Figure 2.6, respectively.

These results suggest that the inhibition of AKT activation by Irgacure 2959 and DMPA could lead to several downstream effects, including reducing cell viability and motility, decreasing angiogenesis, and inducing apoptosis, which are consistent

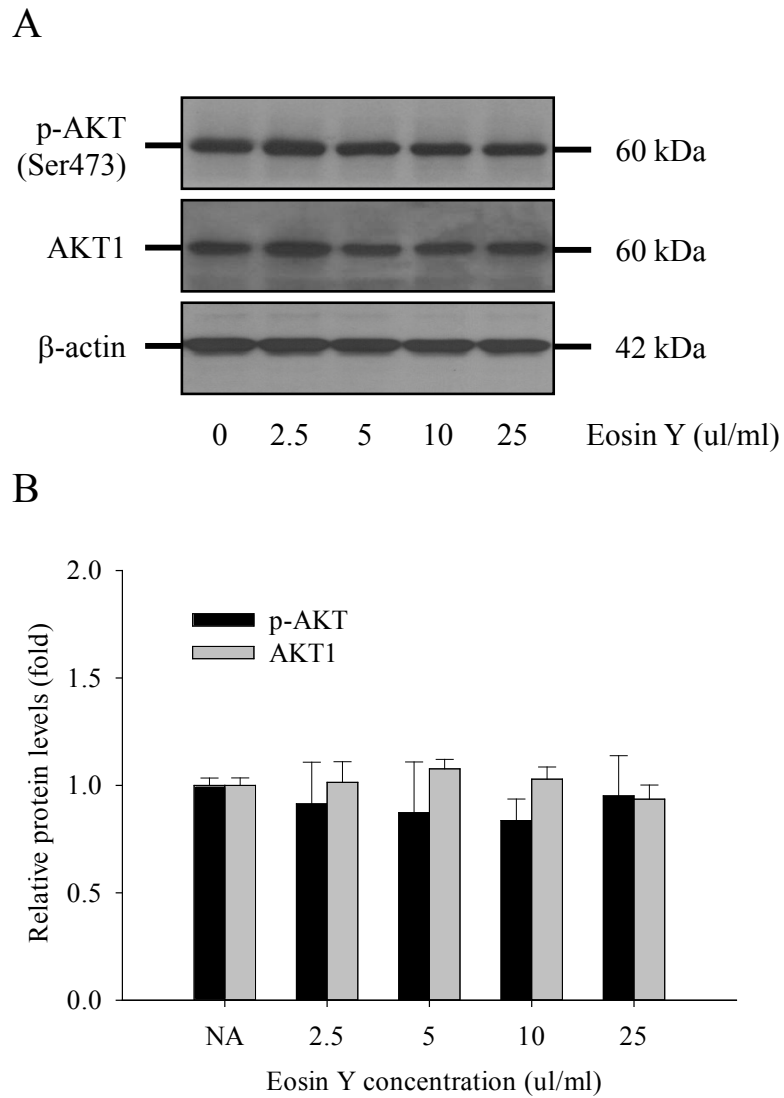


Figure 2.4: The effect of eosin Y on intracellular AKT activity in HN4 cells.

HN4 cells were plated at a density of 5×10^4 cells/well into 6-well plates and treated with different concentrations of eosin Y as indicated for 30 min. At the end of treatment, the total cell lysates were harvested and the intracellular phospho-AKT (p-AKT) and total AKT levels were analyzed by Western blot analysis (A). Each positive band was normalized to β -actin and was quantified by NIH ImageJ (B). The data represent typical one of three experiments. Each value represents mean \pm standard deviation.

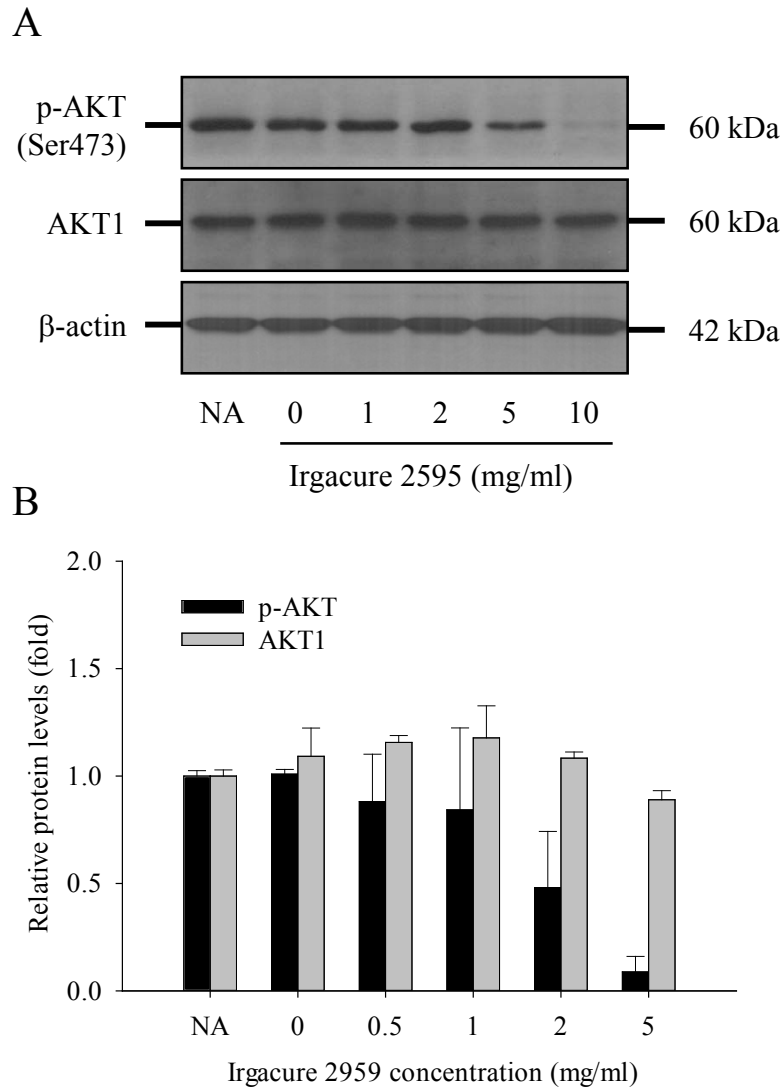


Figure 2.5: The effect of Irgacure 2959 on intracellular AKT activity in HN4 cells.

HN4 cells were plated at a density of 5×10^4 cells/well into 6-well plates and treated with different concentrations of eosin Y as indicated for 30 min. At the end of treatment, the total cell lysates were harvested and the intracellular phospho-AKT (p-AKT) and total AKT levels were analyzed by Western blot analysis (A). Each positive band was normalized to β -actin and was quantified by NIH ImageJ (B). The data represent typical one of three experiments. Each value represents mean \pm standard deviation.

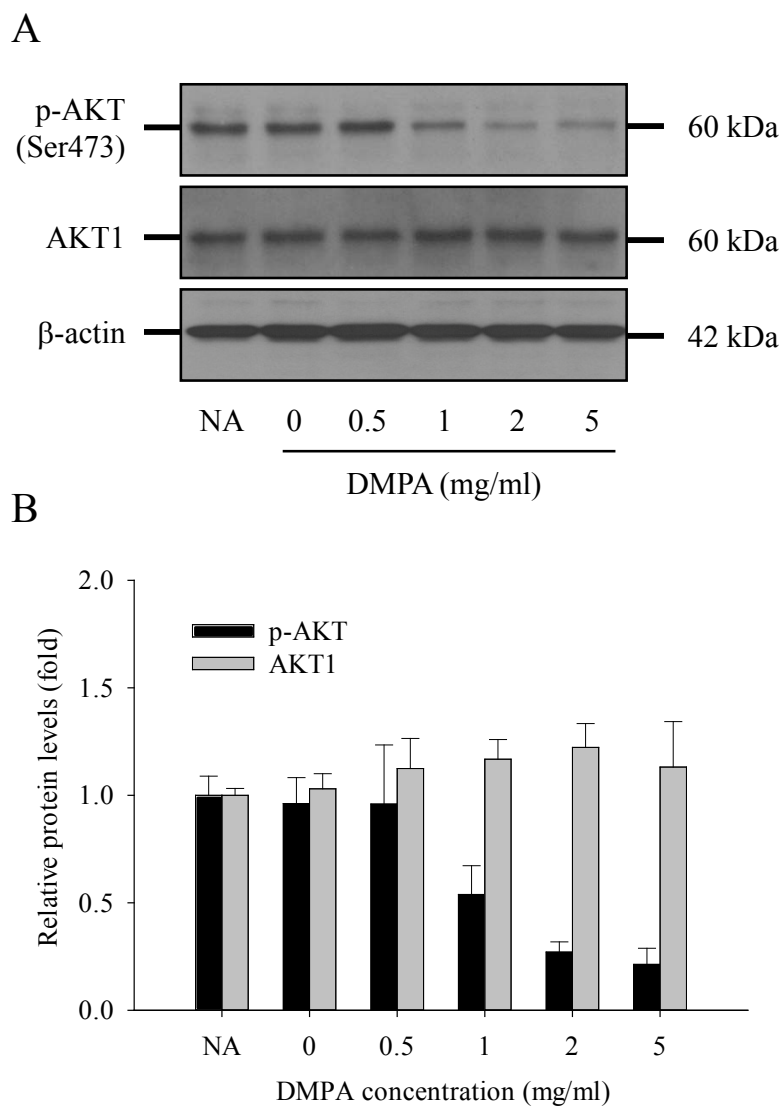


Figure 2.6: The effect of DMPA on intracellular AKT activity in HN4 cells.

HN4 cells were plated at a density of 5×10^4 cells/well into 6-well plates and treated with different concentrations of eosin Y as indicated for 30 min. At the end of treatment, the total cell lysates were harvested and the intracellular phospho-AKT (p-AKT) and total AKT levels were analyzed by Western blot analysis (A). Each positive band was normalized to β -actin and was quantified by NIH ImageJ (B). The data represent typical one of three experiments. Each value represents mean \pm standard deviation.

with the cell viabilities shown in Figures 2.1, 2.2 and 2.3. Cell invasion, migration and proliferation as well as angiogenesis are crucial for the success of photocrosslinking polymer scaffold in biomedical applications, especially tissue engineering. This is the first time to show the interaction of photoinitiators on the intracellular signaling pathway. The results suggest that eosin Y could be a much safer photoinitiator for photopolymerization in biomedical applications than Irgacure 2959 and DMPA.

2.3.3 The effect of UV-exposed photoinitiators on viability and intracellular AKT signaling transduction in HN4 cells

Besides the precursor of photoinitiators, the free radicals generated during the photocrosslinking process could be cytotoxic as well. As shown in Figure 2.7, eosin Y, Irgacure 2959 and DMPA can be decomposed into high-energy radicals. The cell viability and intracellular AKT activity were evaluated in HN4 cells in response to these free radicals. Eosin Y, Irgacure 2959 and DMPA were mixed with cell culture media first and subjected to UV irradiation for 30 min to allow free radical generation. HN4 cells were then immediately treated with these photoinitiator solutions for 1 and 2 days. HN4 cells failed to maintain 100% viability during the 2 days incubation with 2.5 $\mu\text{l/ml}$ of eosin Y and 0.5 mg/ml of Irgacure 2959 after UV irradiation (Figures 2.8 and 2.9), comparing to the non-UV irradiation treatment (Figures 2.1 and 2.2). After UV irradiation, 2.5 $\mu\text{l/ml}$ of eosin Y and 0.5 mg/ml of Irgacure 2959 reduced cell viability about 30% and 50%, respectively; while 10 $\mu\text{l/ml}$ of eosin Y and 2 mg/ml of Irgacure 2959 reduced cell viability about 70% and 95%, respectively. DMPA was consistently cytotoxic to HN4 cells as its precursor (Figures 2.3 and 2.10), and both precursor and free radicals could cause a significant cytotoxicity effect. These results suggest that eosin Y is more biocompatible than Irgacure 2959 and DMPA after UV irradiation, which is consistent with Figures 2.1, 2.2 and 2.3. It was noticed that the free radicals generated from UV irradiation were more cytotoxic to cells than their precursor. These results were further confirmed by intracellular AKT signaling

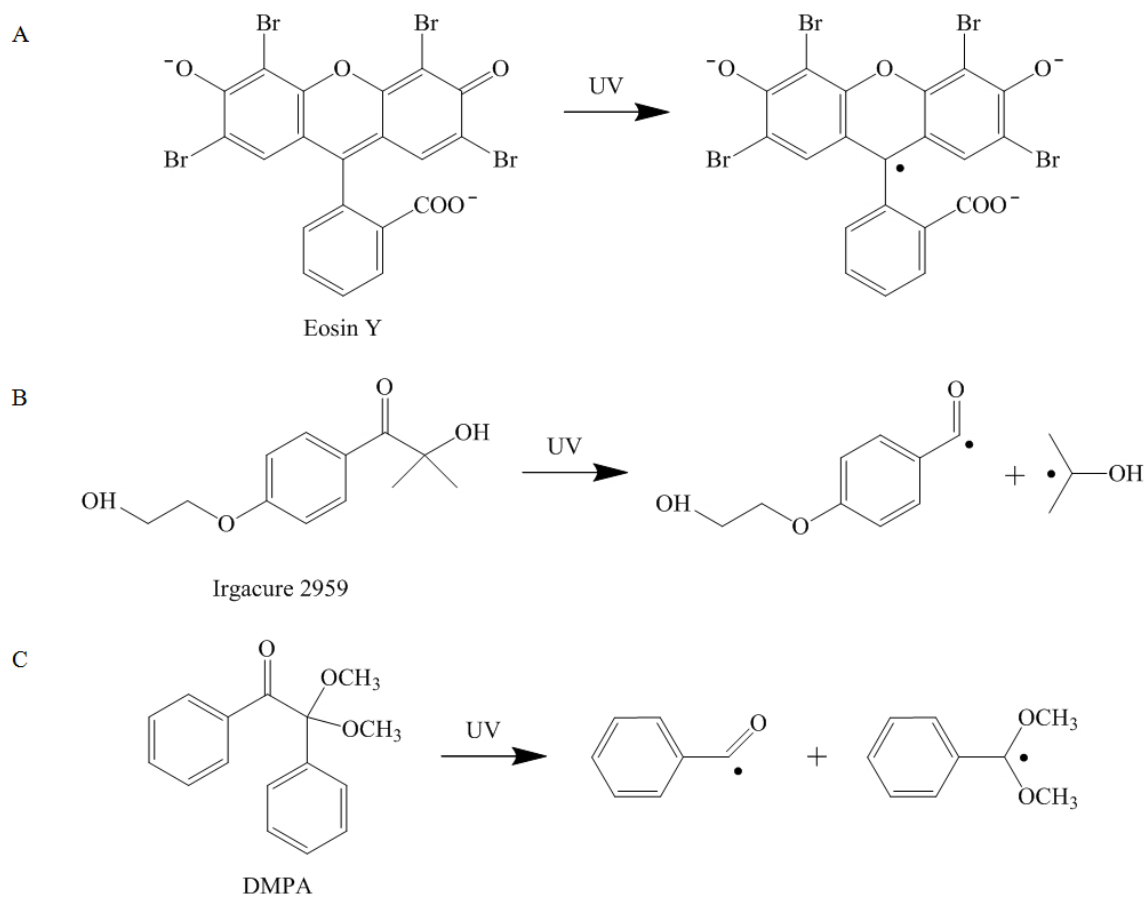


Figure 2.7: A schematic diagram of photoinitiator decomposition to free radicals [1, 52, 59].

A, eosin Y; B, Irgacure 2959; and C, DMPA.

transduction in HN4 cells in response to these free radicals. All three UV exposed photoinitiators diminished the phosphorylation of AKT in HN4 cells as shown in Figure 2.11.

These results only represent the worst case scenario, in which all the free radicals generated from photopolymerization process have the highest likelihood to interact with cells. However, these results indicate the way in which cells response to free radicals at the early stage. The free radicals induce fast AKT dephosphorylation, which in turn alters numerous intracellular signaling transductions, such as inhibiting

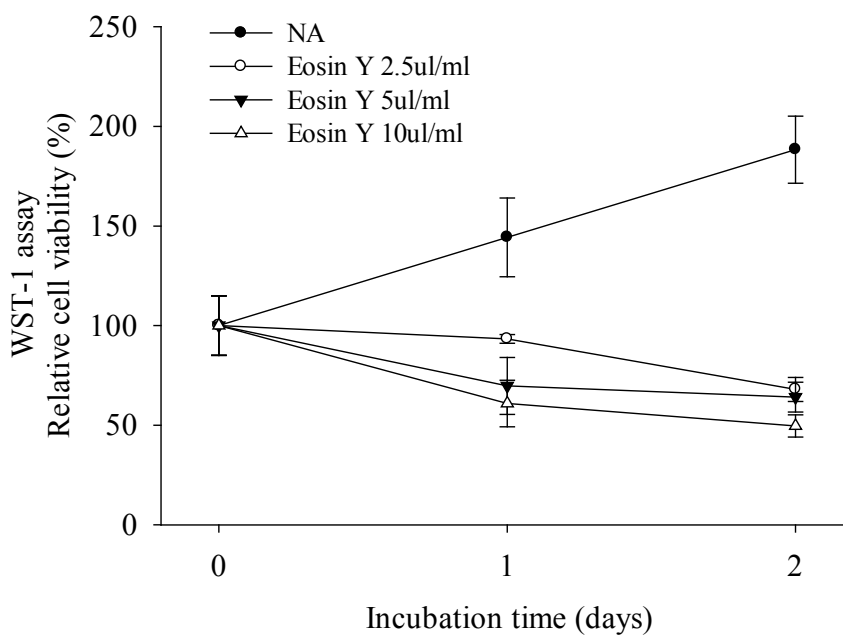


Figure 2.8: The effect of UV-exposed eosin Y on HN4 cell viability. The cell culture media were first mixed with different concentrations of eosin Y, and then the mixtures were exposed to the longwave UV at 365 nm with an intensity of 100 watts for 30 min. After the UV irradiation, the mixtures were immediately to treat HN4 cells for 0, 1 and 2 days. The cell viabilities were measured by WST-1 assay at the end of the treatment. The bars are mean \pm standard deviation.

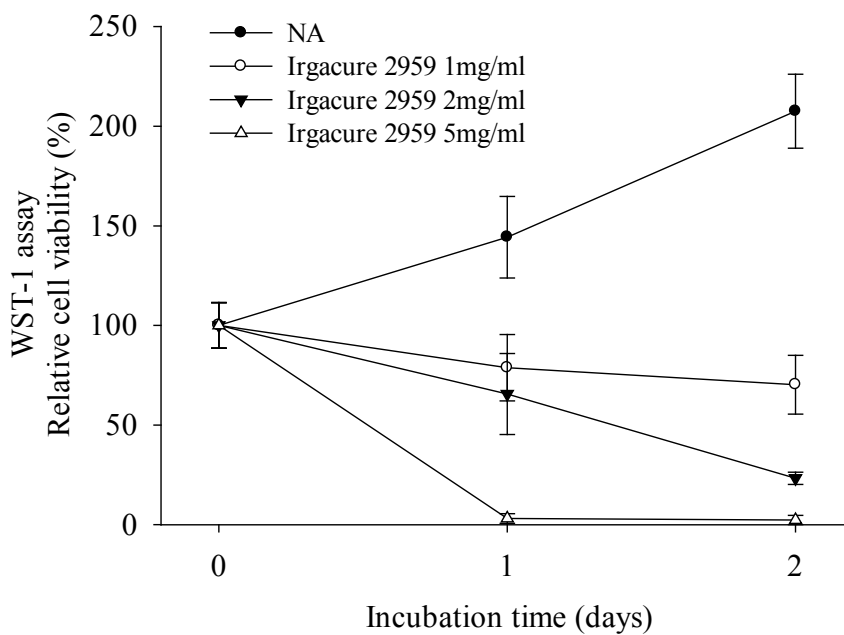


Figure 2.9: The effect of UV-exposed Irgacure 2959 on HN4 cell viability.

The cell culture media were first mixed with different concentrations of Irgacure 2959, and then the mixtures were exposed to the longwave UV at 365 nm with an intensity of 100 watts for 30 min. After the UV irradiation, the mixtures were immediately to treat HN4 cells for 0, 1 and 2 days. The cell viabilities were measured by WST-1 assay at the end of the treatment. The bars are mean \pm standard deviation.

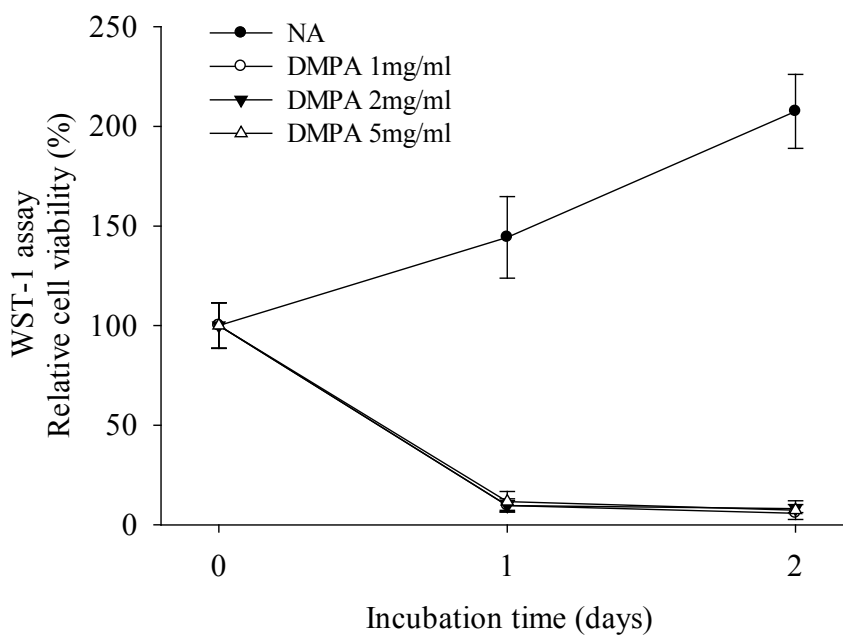


Figure 2.10: The effect of UV-exposed DMPA on HN4 cell viability. The cell culture media were first mixed with different concentrations of DMPA, and then the mixtures were exposed to the longwave UV at 365 nm with an intensity of 100 watts for 30 min. After the UV irradiation, the mixtures were immediately to treat HN4 cells for 0, 1 and 2 days. The cell viabilities were measured by WST-1 assay at the end of the treatment. The bars are mean \pm standard deviation.

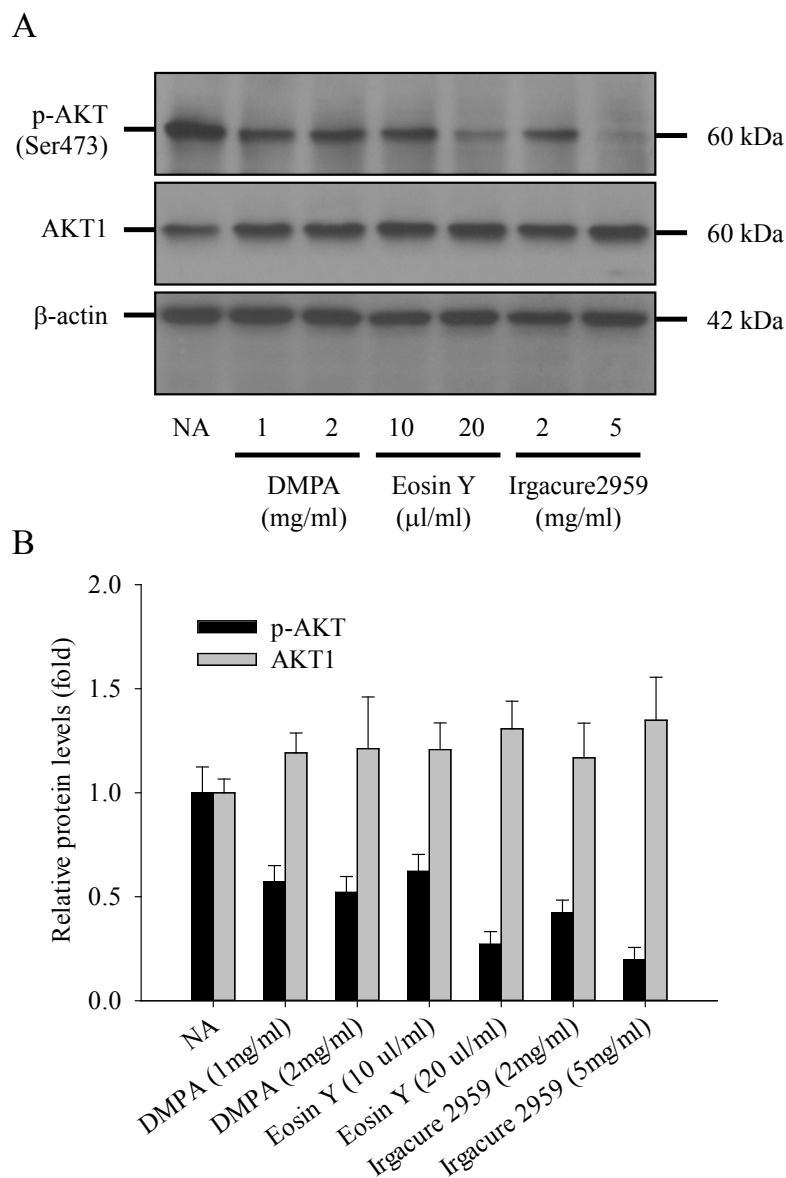


Figure 2.11: The effect of UV-exposed photoinitiators on intracellular AKT activity in HN4 cells.

The cell culture media were first mixed with different concentrations of eosin Y, Irgacure 2959 or DMPA, and then the mixtures were exposed to the longwave UV at 365 nm with an intensity of 100 watts for 30 min. After the UV irradiation, the mixtures were immediately to treat HN4 cells for 30 min and the total cell lysates were harvested. The intracellular phospho-AKT (p-AKT) and total AKT levels were analyzed by Western blot analysis (A). Each positive band was normalized to β -actin and was quantified by NIH ImageJ (B). The data represent typical one of three experiments. Each value represents mean \pm standard deviation.

mTOR signaling pathway in cell proliferation and p53 signaling pathway in cell survival, activating ROS signaling pathway in ER stress and caspase 9 signaling pathway in cell apoptosis [64]. For the potential use of photoinitiators to crosslink polymers in biomedical applications, it becomes crucial to optimize the concentration of photoinitiators and keep the minimal free radical residues after photopolymerization process.

2.3.4 The evaluation of free radicals stability on viability and intracellular AKT signaling transduction in HN4 cells

To further evaluate the stability of free radicals, the cell viability and intracellular AKT activity were determined in HN4 cells in response to the quenched eosin Y condition media. As shown in Figure 2.12, the quenched UV-exposed eosin Y exhibited more cytotoxicity than unquenched UV-exposed eosin Y, indicating the free radicals generated from UV irradiation of eosin Y were not diminished up to 48 hours of quencher. The reason is yet unclear, but it could be due to the interaction between free radicals and cell culture media. Such reaction then affects growth factors in the culture media which in turn inhibits cell signaling transductions. The evidence showed that the phosphorylation of AKT was significantly diminished in the HN4 cells treated with the quenched eosin Y condition media (Figure 2.13). These results suggest that free radicals may not only interact with cells but extracellular components as well. The actual cell survival in the 3-dimensional polymer scaffold might be higher than this simplistic 2-dimensional cell culture model in in vivo biomedical applications [81]. It depends on the ability of polymer scaffold to scavenge the free radicals generated from photopolymerization process.

Up to date, a few of papers have been published to demonstrate the biocompatibility of photoinitiators in different cell lines and conclude that Irgacure 2959 is the promising photoinitiator for cytocompatibility among Irgacure 184, Irgacure 907, Irgacure 651 and Irgacure 2959 [9, 81]. The biocompatible concentration range of Irgacure 2959 is within 0.5% (w/w) as reported [9, 81]. This conclusion is consistent

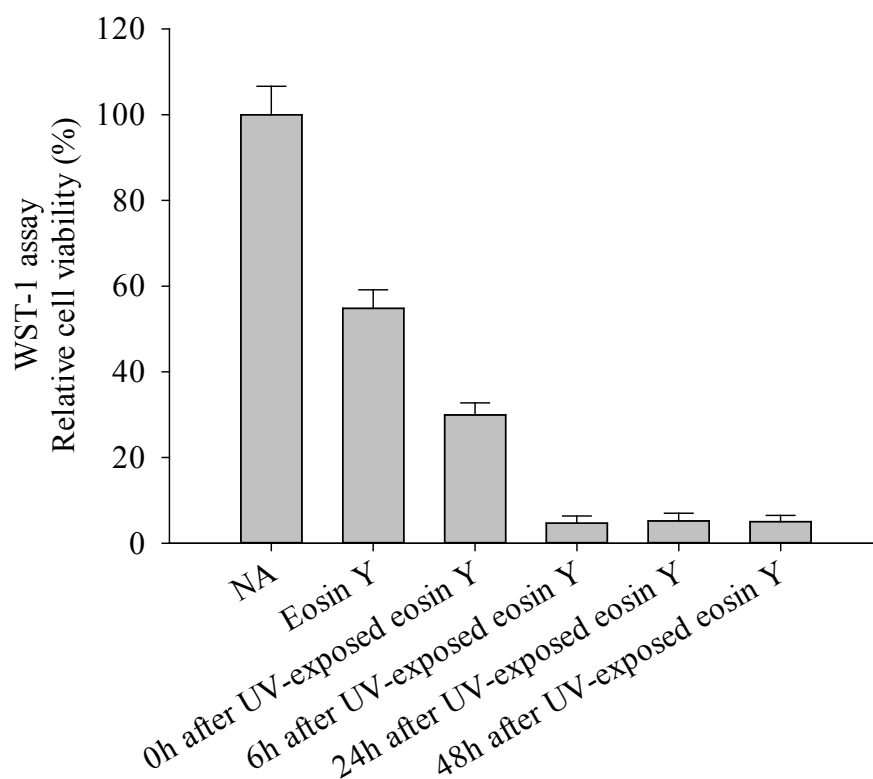


Figure 2.12: The effect of the free radicals stability on HN4 cell viability.

The cell culture media were first mixed with eosin Y to reach a final concentration of $20 \mu\text{l/ml}$, and the mixtures were exposed to the longwave UV at 365 nm with an intensity of 100 watts for 30 min. After the UV irradiation, the mixtures were stored in dark for 0, 6, 24 and 48 hours before the cell treatment. HN4 cells were then treated with no addition (NA), $20 \mu\text{l/ml}$ of eosin Y without UV irradiation or the UV exposed mixtures for 2 days. The cell viabilities were measured by WST-1 assay at the end of the treatment. The bars are mean \pm standard deviation.

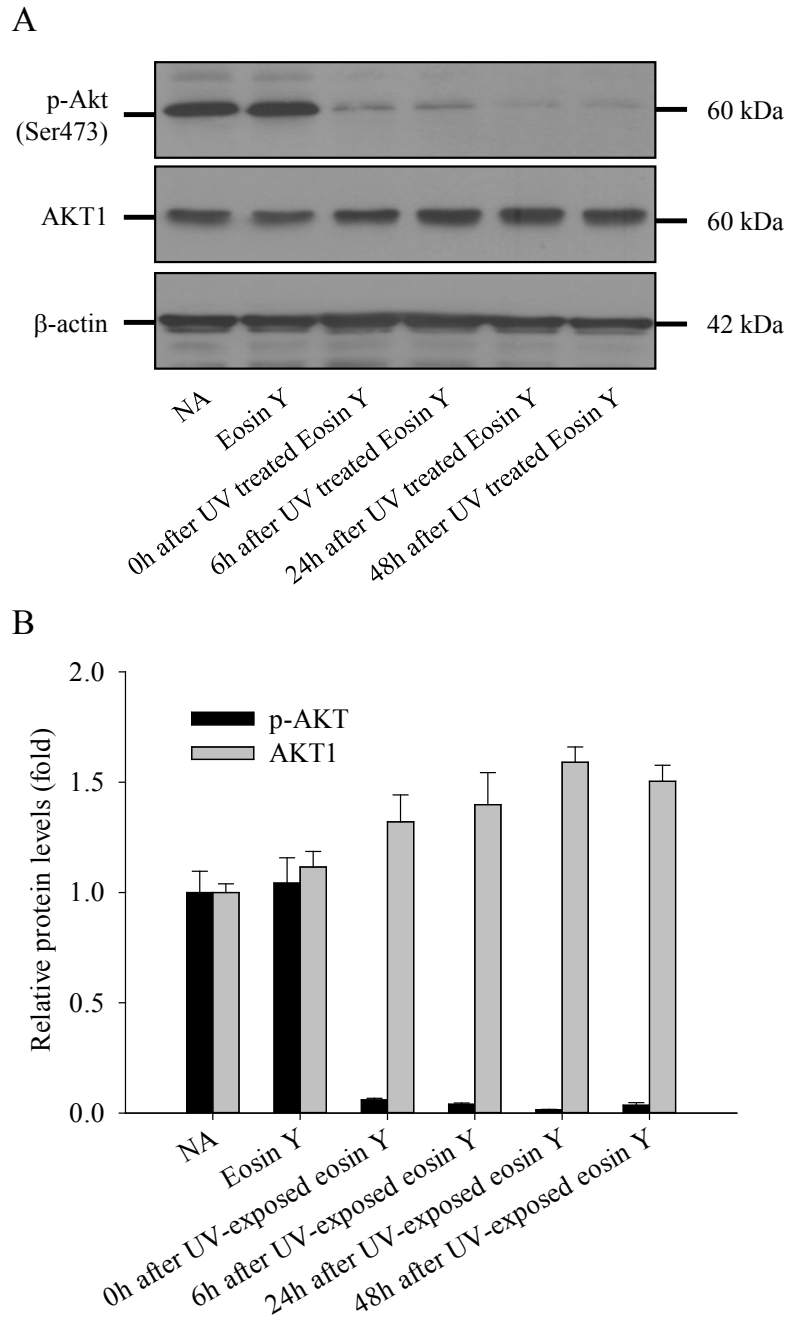


Figure 2.13: The effect of the free radicals stability on intracellular AKT activity in HN4 cells.

The preparation of the condition media was described in Figure 2.12. HN4 cells were then treated with no addition (NA), 20 $\mu\text{l}/\text{ml}$ of eosin Y without UV irradiation or the UV exposed mixtures for 30 min and the total cell lysates were harvested. The intracellular phospho-AKT (p-AKT) and total AKT levels were analyzed by Western blot analysis (A). Each positive band was normalized to β -actin and was quantified by NIH ImageJ (B). The data represent typical one of three experiments. Each value represents mean \pm standard deviation.

with our observations (Figures 2.2 and 2.5). However, the biocompatibility also depends on the materials of polymer and UV intensity during the photopolymerization [9]. Our finding agrees well with photoinitiator system of eosin Y with TEOA has little effect on cell viability [25]. In this work, it is the first time to illustrate the immediate response of cells regarding to the precursor and free radicals of photoinitiators. It was observed that free radicals significantly inhibited intracellular AKT signaling transduction (Figures 2.11 and 2.13), which was closely correlated to cytocompatibility in HN4 cells. Inhibition of AKT signaling transduction can further induce ROS formation and lead oxidative stress [72]. In order to diminish oxidative stress within the cells, antioxidants are commonly introduced to quench the activation of ROS signaling during the photopolymerization process. Nonetheless, it is of interest to test the intracellular AKT signaling transduction in the cells encapsulated within the photoinitiated crosslinking polymers along with the antioxidants. It is of importance to keep cells not only viable but migrating, proliferating and functioning in the photoinitiated crosslinking polymers as a function unit.

2.4 Conclusions

In this chapter, the effects of three photoinitiators and their free radicals on cytocompatibility and intracellular AKT signaling transduction were determined in HN4 cells. It was shown that the cytocompatibility of the photoinitiators was closely correlated to intracellular AKT signaling transduction within the cells. The most promising cytocompatible photoinitiator in this work was eosin Y at concentrations below 10 $\mu\text{l/ml}$. Eosin Y had minimal effect on intracellular AKT signaling transduction up to 25 $\mu\text{l/ml}$. Irgacure 2959 was also a promising cytocompatible photoinitiator only at concentration below 1 mg/ml. It was also shown that free radicals had significant effects on HN4 cells, including reducing cell viability and inhibiting intracellular AKT signaling transduction. These free radicals may interact with cell directly or indirectly via interaction with cell culture media. These findings could further enhance our understanding of the biocompatibility in the photoinitiator systems and provide

a novel way to look into the interaction between cells and photoinitiators or their free radicals.

Chapter 3

Fabrication of semi-interpenetrating network scaffolds for transbuccal mucosal delivery of insulin

3.1 Introduction

Insulin has been delivered to diabetic patients exclusively through the subcutaneous route since it was discovered. Due to the relatively short duration of action of 4 to 8 hours, patients in severe diabetic condition are required to take two to four daily injections. The stress and noncompliance of multiple daily injections attract numerous investigations to develop a safe and effective noninvasive route for insulin delivery. Oral administration of insulin is the first viable alternative to multiple daily injections. Oral administration of insulin can rapidly elevate insulin level in the portal blood, which simulates the physiological secretion pattern of the pancreas [71]. However, insulin has to travel through stomach, small intestine and the colon intact before reaching the blood stream. Subsequently, insulin has to be protected from the gastric enzymes, such as pepsin, trypsin and chymotrypsin in the duodenum as well as

exopeptidases when it reaches the brush border. Nanoparticle-based insulin delivery systems were reported to be able to overcome these barriers [71], and these systems have been received considerable attention. To date, there are three mechanisms for intestinal uptake of insulin encapsulated nanoparticles: (1) uptake by paracellular pathway, (2) transcytosis or receptor-mediated transcytosis through the epithelial cells of the intestinal mucosa, and (3) lymphatic uptake through the M cells of the Peyer's patches mostly abundant in the ileum [71].

Therefore, the properties of a successful drug carrier for insulin have been summarized as follows: (1) resistant against gastrointestinal enzymes and pH gradients, (2) stable and biocompatible to ensure that the main fraction of insulin remains biologically active from encapsulation to release, (3) highly permeable along with the intestinal membrane, (4) absorbable through the epithelial cell layer or the mucosal epithelium to enhance the absorption of drug, (6) fast release in the circulation to control the glucose concentration in blood, and (7) safe after oral administration [71].

Due to the large size, hydrophilicity, susceptibility to enzymatic degradation and poor intestinal absorption, oral delivery of free insulin has low bioavailability. A variety of formulations for oral insulin delivery have been developed in the last decade. Most strategies have shown promising results, such as pH sensitivity, enzymatic inhibition among others, but the bioavailability is still low as shown in Table 1.1.

Transbuccal mucosal administration could be a secondary alternative route to deliver insulin. It has been reported that co-administration of soybean-lecithin could enhance transbuccal mucosal delivery of insulin in rabbits and rats [77, 87]. In addition, poly(methacrylic acid)-grafted-poly(ethylene glycol) (P(MAA-g-EG)) hydrogel holds a great potential for transmucosal and intracellular delivery of insulin [41]. Both adhesion property and release kinetics can be modulated by tuning the polymer composition [41]. All of these interesting findings inspire our great interest to explore the transbuccal mucosal route for insulin delivery.

The anatomical and physiological properties of the oral mucosa have been generally reviewed as follows. The oral cavity contains lips, cheek, tongue, hard

palate, soft palate and floor of the mouth. The lining of the oral cavity is the oral mucosa that includes the buccal, sublingual, gingival, palatal and labial mucosa [58]. Among these mucosa, the buccal and sublingual mucosa have the largest surface area, which accounts for about 60% of the total oral mucosal surface area. The top layer of the oral mucosa comprises closely compacted epithelial cells, whose function is to protect the underlying tissue against potential harmful agents in the oral environment and from fluid loss [58]. Lamina propia and submucosa are under the epithelium, referred to as the basement membrane.

There are some significant challenges for systemic drug delivery through the oral cavity. (1) The drug has to be released from the carrier to the delivery site, such as buccal or sublingual mucosa, and the drug has to pass through the mucosal layers to enter the systemic circulation. (2) The drug has to remain bioactive in this process, including pH, fluid volume, enzyme activity and the permeability of oral mucosa in the oral cavity [58]. (3) The turnover of the mucosal surface is a determinant of this delivery route. The surface area of oral cavity is estimated at about 100 cm², with a local pH from 5.8 to 7.6. The relative drug absorption capacity is moderate in oral cavity comparing to stomach, small intestine, large intestine and rectum [58]. (4) The physiological environment of the oral cavity, including pH, fluid volume and composition, is determined by the secretion of saliva. Saliva provides a water rich environment of the oral cavity, which can be favorable for drug release from delivery systems, especially those based on hydrophilic polymers.

Biological polymers, such as collagen, gelatin, hyaluronic acid, and thrombin are widely employed as backbones in the construction of hydrogels or scaffolds for various biomedical applications [73]. Gelatin, a hydrophilic protein fragment derived from collagen, has been extensively investigated in drug delivery system, owing its biodegradability, its low level of immunogenicity and cytotoxicity, and its FDA approval as a clotting agent and exudate-absorbing construct. Several investigations indicate that gelatin can be chemically crosslinked with polyethylene glycol diacrylate (PEG-DA) to form a semi-interpenetrating network (sIPN) [73, 87, 27, 92]. This crosslinking process is driven by photopolymerization, which can physically enhance

the entanglement of polymer chains in three-dimensional structure. The application of photopolymerization techniques allows the ease of loading a desired drug dosage and control over crosslinking density [73]. It has been reported that (1) the degradation and drug release rate can be modulated by turning the weight percent of PEG-DA during the photopolymerization [92]; (2) increasing the gelatin content can significantly increase Young's modulus [27]; (3) the gelatin sIPN exhibits stability and adhesive strength to fresh tissue [87, 92, 10]; and (4) the adhesion values of gelatin IPN is up to 5.7 N [92]. Indeed, gelatin sIPN displays moisture absorbance, high tensile strength and elasticity, tissue integration and adhesion, and favorable tissue response, which can be for transbuccal mucosal drug delivery.

Electrospinning is a materials-processing method that is used to fabricate continuous ultrafine fibers with a diameter range from 50 nm to 10 μ m. Electrospinning is reported to be versatile, inexpensive, scalable, and reliable. Electrospun fibers are produced from a solution of natural or synthetic polymers, including collagens, gelatin, elastin, fibrinogen, hemoglobin and myoglobin and silk fibroin, or poly(dioxanone) (PDO), poly(ethylene oxide) (PEO), poly(ethylene terephthalate), poly(glyconate), PLGA, PLLA, PCL, poly(styrene), poly(vinyl alcohol) (PVA), chitosan, and hyaluronic acid (HA) [35, 63]. These electrospun fibers have been widely explored in biomedical applications such as tissue engineering, wound healing, orthopedics, biosensors and drug delivery [35, 32, 43, 82]. Electrospun fiber scaffold exhibits a high surface to volume ratio and direct local adhesion ability and holds a great potential for transbuccal mucosal drug delivery.

An electrospun gelatin fiber scaffold (GF) was developed to locally deliver nystatin for candidiasis [2]. GFs possess high biocompatibility and mucoadhesive property that allow local sustained release of drug at the absorption site [2, 7]. GF can be stabilized using a crosslinker of photocurable PEG-DA and form sIPN. The fiber morphology, mechanical and physical properties as well as drug release kinetics can be controlled by modulating the concentration of crosslinker [2]. However, the major limitation of photopolymerization techniques for these sIPN scaffolds or hydrogels is that the high-energy free radicals can create the potential of oxidative damage to the

photoencapsulated cell populations [9, 81]. The cytocompatibility of photoinitiators was investigated in Chapter 2. The results suggest that eosin Y is more cytocompatible than Irgacure 2959 and DMPA, with minimal effect on intracellular AKT signaling transduction in HN4 cells (Chapter 2).

In this chapter, a sIPN gelatin-co-insulin fiber scaffold (sIPN GIF) was fabricated by applying an optimized formulation of sIPN GF in respect to cytocompatibility and degradation rate. Enzyme-linked immunosorbent assay (ELISA) was used to monitor the insulin release kinetics of sIPN GIF. Western blot analysis and 3T3-L1 preadipocyte differentiation analysis were used to determine the bioactivity of insulin from sIPN GIF. The permeability of the insulin from sIPN GIF was evaluated through a porcine buccal mucosal membrane, which possesses analogous thickness, structure, morphology, and composition to normal human buccal epithelium [91]. Our results suggest that sIPN GIF holds a great potential for transbuccal mucosal delivery of insulin.

3.2 Materials and Methods

3.2.1 Materials

1-vinyl-2 pyrrolidinone (NVP), eosin Y, ethanol, human insulin, oil red O, phosphate buffer solution (PBS), Polyethylene glycol diacrylate (PEG-DA575, $M_n = 575$ g/mol), porcine type-A gelatin, and triethanolamine (TEOA) were purchased from Sigma-Aldrich (St. Louis, MO). 1,1,1,3,3,3-Hexafluoro-2-propanol (HFP) was purchased from TCI America (Portland, OR). Cell proliferation reagent WST-1 was purchased from Roche Applied Science (Indianapolis, IN). Insulin enzyme-linked immunosorbent assay (ELISA) kit was purchased from Calbiotech (Spring Valley, CA). Phospho-Akt (Ser473) (p-AKT) antibody was purchased from Cell Signaling Technology (Danvers, MA). AKT1 (559028) antibody was purchased from BD Biosciences Pharmingen (Mississauga, ON, Canada). β -actin (ACTBD11B7) antibody was purchased from Santa Cruz Biotechnology (Santa Cruz, CA). Goat anti-rabbit antibody

conjugated to horseradish peroxidase and goat anti-mouse antibody conjugated to horseradish peroxidase were purchased from Bio-Rad (Hercules, CA).

3.2.2 Cell culture

3T3-L1 preadipocytes were maintained in Dulbecco's Modification of Eagle's Medium (DMEM) (Life Technologies, Grand Island, NY) supplemented with high glucose, L-glutamine, 10% (v/v) fetal bovine serum (FBS) (Fisher Scientific, Pittsburgh, PA), 100 units/ml of penicillin (Thermo Fisher Scientific, Ashville, NC) and 100 $\mu\text{g}/\text{ml}$ of streptomycin (Thermo Fisher Scientific, Ashville, NC) at 37°C in a humid environment with 5% CO_2 .

3.2.3 Scaffold preparation

The preparation of gelatin fiber scaffold required two steps, referred to as electrospinning and cross-linking, as previously reported [2]. Briefly, 1 g of gelatin was first added into 10 ml of HFP solution, and the mixture was shaken continuously overnight to obtain a homogeneous transparent 10% (w/v) gelatin/HFP solution. To prepare gelatin-co-insulin solutions, 5 mg of insulin was added to 10 ml of the gelatin/HFP solution, and the mixture was shaken continuously overnight to obtain a homogenous 1:200 (w/w) insulin/gelatin solution.

3.2.4 Preparation of GF and GIF

To fabricate GF and GIF, a conventional electrospinning of gelatin solution was performed as shown in Figure 3.1. Briefly, a syringe of the gelatin solution or gelatin-co-insulin solution described above was placed in an electrostatic field with the applied voltage of 25 kV to a blunt needle (18 gauge 1.5"). A grounded aluminum collecting mandrel was placed 20 cm away from the tip of the needle; while a flat stainless steel collecting mandrel (7.5 \times 2.5 \times 0.5 cm, length \times width \times thickness) was placed 12.5 cm away from the needle. The gelatin solution was dispensed from the syringe into the electrostatic field at a rate of 6.37 ml/h. The electrospun fibers were accumulated

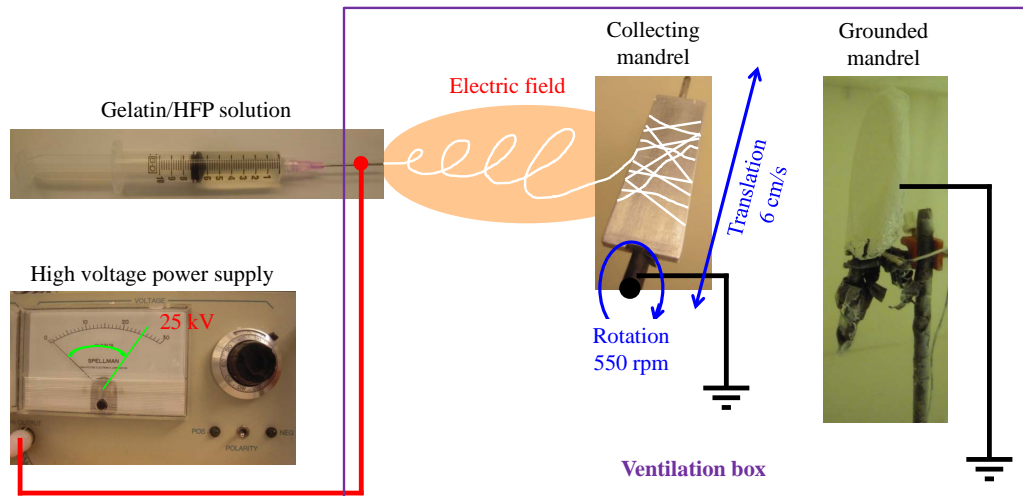


Figure 3.1: Experimental setup to schematically illustrate the conventional electrospinning.

on the collecting mandrel with a rotational speed of 550 rpm and a translational speeds of 6 cm/s over 12 cm.

3.2.5 Preparation of crosslinked GF and GIF

The eosin Y photoinitiator solution was prepared by 0.1% w/w eosin Y, 40% w/w TEOA and 4% w/w NVP in ethanol as previously reported [24, 29]. In order to obtain the optimal ratio of PEG-DA to eosin Y solution, (1) the electrospun GFs were cross-linked with various concentrations (0%, 1%, 2%, 5%, 10% and 20%; w/v) of PEG-DA in the presence of 5% (v/v) eosin Y solution; (2) the electrospun GFs were crosslinked with various concentrations (2%, 5% and 10%; v/v) of eosin Y solutions in the presence of 1% (w/v) PEG-DA. The crosslinking solutions were prepared by combining appropriate amounts of eosin Y solution and PEG-DA. Next, 600 μ l of crosslinking solution was poured onto a 200 mg of eletrospun gelatin fiber, followed by a 10 min of incubation to allow equilibrium. The scaffold was held under ultraviolet (UV) light (UVP Blak-Ray Long Wave Lamp, 100 Watts) from a 14 cm distance for 5 min on each side of the scaffold and then air-dried as previously reported [2].

3.2.6 Cytocompatibility assay

To evaluate the cytocompatibility of PEG-DA and PEG, both polymers were dissolved in ethanol first. 3T3-L1 preadipocytes were treated with 0, 17.4, 87, 174, 696 and 1739 M of PEG-DA or PEG for 2 days. To evaluate the cytocompatibility of the fabricated scaffolds, 20 mg of the fabricated scaffold was weighed and then individually immersed into a 5 ml of cell culture medium at 37°C for 2 hours. The elution media were collected at the end of incubation. 3T3-L1 preadipocytes were treated with these elution media for 2 days. At the end of each treatment, the cell viability was determined by WST-1 proliferation assay following the manufacturers protocol.

3.2.7 In vitro degradation studies

In vitro degradation of the fabricated scaffolds was evaluated in cell culture medium and simulated saliva fluid (SSF; 12 mM KH_2PO_4 , 40 mM NaCl, 1.5 mM CaCl_2 , with NaOH adjusted to pH 6.2) at 37 °C as previously reported [2]. Briefly, 20 mg of the fabricated scaffolds (n = 5) were weighed and then individually immersed in a tube filled with 5 ml of one of the two media mentioned above. Samples were taken out at 15, 30, 60 and 120 min, and centrifuged at 5,000 rpm for 5 min. After centrifugation, the residue was collected, freeze-dried and weighed.

3.2.8 Uniaxial tensile testing

Uniaxial tensile testing of electrospun scaffolds was performed as previously described [2, 50]. Briefly, dog-bone-shaped samples (n = 12-18) were obtained using a punch die (ODC Testing & Molds) with a dimension of 19.05 mm in length, 3.175 mm at narrowest point and 6.1 mm at widest point. The thickness of the samples was determined using a digital caliper. Mechanical properties of the samples were tested using an MTS Bionix 200 testing system with 100 N load cell (MTS Systems, Eden Prairie, MN). Samples were tested to failure at a 1.33 min^{-1} strain rate. TestWorks version 4 was used to calculate peak load, peak stress, modulus, strain at break and energy to break.

3.2.9 Scanning electron microscopy (SEM)

The fabricated and degraded scaffolds were placed on a 1 cm diameter stub, and the stub was placed on a specimen holder and prepared by gold sputtering. SEM images were taken on a JEOL LV-5610 scanning electron microscope in the Nanomaterials Core Characterization facility at Virginia Commonwealth University. The diameters of fibers were analyzed by NIH ImageJ (<http://rsbweb.nih.gov/ij/>) from 60 randomly chosen fibers in each SEM image as previously reported [2, 50].

3.2.10 Insulin release studies

Insulin released from the fabricated scaffolds was analyzed by ELISA and Western blot analysis as previously reported [84, 75, 70, 55]. Briefly, 20 mg of insulin-loaded scaffolds were immersed in 5 ml of DMEM at 37 °C. At the predetermined time points of 15, 30, 60, 120 and 240 min, a 25 μ l aliquot was withdrawn from the release medium. The cumulative drug release was then determined by ELISA according to the manufactory standard protocol. In order to evaluate the bioactivity of released insulin in each sample, 3T3-L1 preadipocytes were used as our model. 3T3-L1 preadipocytes were seeded onto a 6-well plate at 5×10^5 cells/well and cultured for 3 days to allow their attachment. The 3T3-L1 preadipocytes were then treated with the insulin released media at these predetermined time points for 10 min. The intracellular AKT signaling transduction in response to insulin treatment was determined by Western blot analysis.

3.2.11 Western blot analysis

Western blot analysis of total cellular protein was carried out by standard procedures, as described previously [89, 88]. Briefly, total cell lysates (30 μ g) were separated on a 10% SDS-PAGE gel and transferred onto a polyvinylidene difluoride (PVDF; Bio-Rad, Hercules, CA) membrane using Bio-Rad Mini-Blot transfer apparatus. The membrane was blocked for 2 hours in Tris-buffered solution (TBS) containing 5% of non-fat dried milk. The specific proteins on the membrane were determined by

incubating with the primary antibodies overnight at 4 °C with shaking. The membrane was washed three times and then incubated in a 1:3,000 dilution of a secondary antibody at room temperature for 1 hour in the washing buffer (Tris-buffered solution containing 0.5% Tween 20). The specific antigen-antibody interactions were detected using enhanced chemiluminescence (Pierce ECL Western Blotting Substrate; Thermo Scientific, Rockford, IL). The total cellular expression of β -actin was used as the loading control.

3.2.12 Oil red O staining

3T3-L1 cells were seeded onto a 6-well plate at 5×10^5 cells/well cultured for 3 days to allow their attachment. According to the standard protocol [65, 84], differentiation was initiated by incubating preseeded cells with DMEM containing 10% FBS, 10 g/mL of insulin, 10 g/mL of dexamethasone (DEX; Sigma-Aldrich, St. Louis, MO), and 0.5 mM of 3-isobutyl-1-methylxanthine (IBMX; Sigma-Aldrich, St. Louis, MO) or with insulin released media containing with 10% FBS, 10 μ g/mL of dexamethasone, and 0.5 mM of IBMX at Day 0. The induction media were replaced by DMEM containing 10% FBS and 10 μ g/mL of insulin or insulin released media containing with 10% FBS at Day 2. The cells were further incubated with DMEM containing with 10% FBS at Day 4, Day 6 and Day 8. The full maturation into adipocytes was achieved at Day 10. Differentiated adipocytes were rinsed in PBS for three times and then fixed with 10% formaldehyde for 2 hours. The cells were washed three times and immersed with 60% isopropanol for 2 min and then stained with 0.2% Oil Red O in 60% of isopropanol for 10 min. The cells were washed three times and then imaged under the microscope (Olympus, Tokyo, Japan) equipped with image recorder under $\times 20$ lenses [88, 45].

3.2.13 In vitro permeation studies

Porcine cheek tissues were obtained from freshly sacrificed pigs (Silver Ridge Slaughter House, Fredericksburg, VA) and transported to the lab within 2 hours. As previously

reported [91], the mucosa tissues were excised and cut into approximately 2 cm² and frozen on aluminum foil at -20 °C. Before permeation studies, the frozen specimens were equilibrated in PBS for 1 hour at room temperature to allow it completely thawed. Excesses of connective and adipose tissues were trimmed off to obtain a thickness of approximately 0.6 ± 0.1 mm. Buccal mucosa membrane was mounted onto a vertical Franz diffusion cell (PermeGear, Hellertown, PA) with the epithelium facing the donor chamber and the connective tissue facing the receiver chamber. The Franz diffusion cell had a diffusion area of 0.785 cm² with a donor chamber volume of 1 ml and a receiver chamber volume of 5 ml. The cell was placed in the water bath at 37 °C.

The permeation experiments were carried out using PBS in the receiver chamber and SSF in the donor chamber to mimic the in vivo physiological conditions. The sIPN GIF was placed on top of the mucosa membrane and immersed with 1 ml of SSF. At a given time point up to 4 hour, an aliquot of 1 ml from the receiver chamber was collected via syringe and analyzed with ELISA. Free insulin dissolved in SSF was used as a comparison. The permeability coefficient, P , was calculated as follows: $P = (dQ/dt)/AC$, where dQ/dt is the steady-state slope of a cumulative flux curve, C is the loading concentration of a permeant in the donor chamber, and A is the effective cross-sectional area (0.785 cm²) available for diffusion.

3.2.14 Statistical analysis

All the data were expressed as means ± standard deviation (SD) and subjected to one way analysis of variance (ANOVA) followed by Holm-Sidak method for significance using SigmaPlot 12. A value of $p < 0.05$ was considered as statistically significant. Statistical analysis data is provided in Appendix A (p120-141).

3.3 Results and discussion

3.3.1 Optimization of sINP GF scaffold

In order to optimize the sINP GF scaffold, the fabricated scaffolds were evaluated in respect to two aspects: cytocompatibility and degradation rate. Polyethylene glycol (PEG) is widely used in many applications from industrial manufacturing to medicine due to its excellent biocompatible properties. PEG-DA, a derivative of PEG, has also been widely used in biomedical applications, including hydrogels for drug delivery, tissue engineering and wound healing due to its crosslinking property [11, 27, 34, 40, 67]. However, a recent report indicated that the molecular weight of PEG-DA could affect cell viability in other ways [49]. It has been shown that PEG-DA (MW = 400) retained about 30% cell viability; while PEG-DA (MW = 3400) retained about 60% cell viability. The reason of this phenomenon could be the different diffusion rate of PEG-DA into the cells. A higher diffusion rate can cause more cell damage [49]. To conform these observations, the cytotoxicity of PEG-DA and PEG was determined first on 3T3-L1 preadipocytes. As shown in Figure 3.2, PEG monomers exhibited no or slightly cytotoxic effect on 3T3-L1 preadipocytes up to 174 μM ; in contrast, PEG-DA significantly reduced the 3T3-L1 preadipocyte viability at all the concentrations. The cytotoxic effect is most likely due to the functional terminals of PEG-DA chain. Thus, it is important to utilize these functional groups during the PEG-DA based photopolymerization process in order to make the material cytocompatible.

With the understanding of cytotoxicity of PEG-DA monomers, the cytocompatibility of the different formulation of GF scaffolds were determined. Eosin Y is a good photoinitiator candidate to crosslink polymers due to its excellent cytocompatibility as illustrated in Chapter 2. In this work, GF was crosslinked with a fixed 5% concentration of eosin Y and various concentrations from 0% to 20% of PEG-DA to obtain different formulations of GF scaffolds. An elution method was applied to test cytocompatibility of these fabricated GF scaffolds. As shown in Figure 3.3, GF

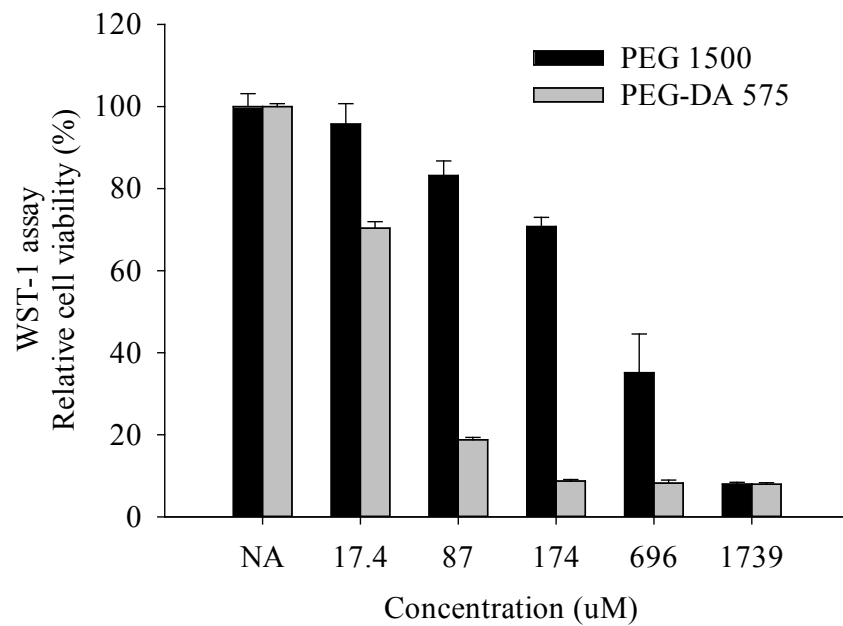


Figure 3.2: Effects of PEG and PEG-DA on cell viability.

3T3-L1 preadipocytes were treated with different concentrations of PEG or PEG-DA (0, 17.4, 87, 174, 696 and 1739 μM) for 2 days. The cell viabilities were measured by WST-1 assay at the end of the treatment ($n = 4$). The bars are mean \pm standard deviation.

incubated with 5% eosin Y alone has no cytotoxic effect on 3T3-L1 preadipocytes. It is consistent with the previous studies that eosin Y and GF are both cytocompatible biomaterials [68, 2]. Interestingly, a significant cytotoxic effect was observed when the concentration of PEG-DA was above 2%. It suggests that a significant proportion of PEG-DA remains uncrosslinked after crosslinking process, which could be a severely cytotoxic reagent to the cells. In respect of cytocompatibility, the optimal formulation of sIPN GF scaffold is GF crosslinked with 1% PEG-DA and 5% eosin Y photoinitiator solution. The ratio of eosin Y photoinitiator solution to PEG-DA is 5:1 (v/w), and it is sufficient to crosslink PEG-DA, subsequently to reduce the cytotoxic effect of PEG-DA monomers.

In order to determine the degradation rate, GF was crosslinked with a fixed 1% concentration of PEG-DA and various concentrations from 0% to 10% of eosin Y. The scaffold degradation rate was investigated in the cell culture media. As shown in Figure 3.4, the scaffold degradation rate was highly regulated by the concentration of eosin Y. The detail observation is explained as follows. GF was rapidly dissolved in the media within 30 min and totally lost its mass, and this is consistent with our previous results [2]. As expected, 1% PEG-DA could not crosslink with itself or GF in the absence of eosin Y in the crosslinking reaction, and GF/1% PEG-DA had same degradation rate as GF. The result has also shown crosslinking reaction was initiated in the presence of eosin Y and the crosslinking density was dependent on the concentration of eosin Y. GF/1% PEG-DA with 2% eosin Y scaffold was degraded within 60 min, but it could be potentially cytotoxic because the amount of eosin Y might be insufficient to utilize the functional group of PEG-DA. In turn, this scaffold could release the cytotoxic PEG-DA monomers into the cell culture media. In contrast, GF/1% PEG-DA with 10% eosin Y could be highly cytocompatible due to high crosslinking process and full utilization of functional groups of PEG-DA. However, GF/1% PEG-DA with 10% eosin Y exhibited a slow degradation rate, as the evidence showed that the mass of the scaffold was relatively stable during 120 min of incubation. This slow degradation rate could be insufficient to release

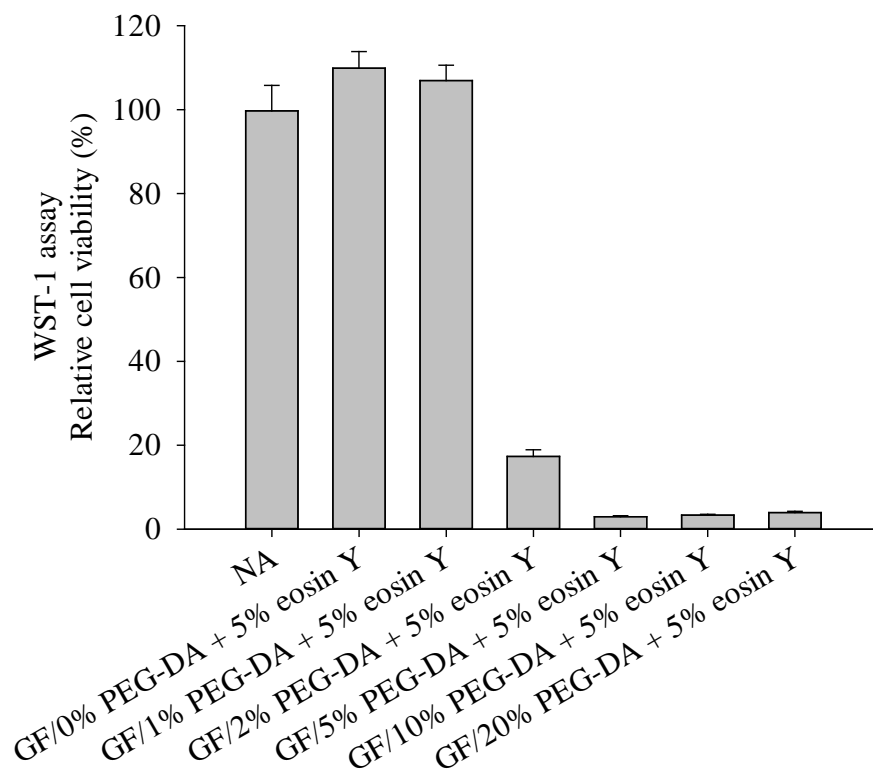


Figure 3.3: Effects of different formulations of GF scaffolds on cell viability.

Different concentrations of PEG-DA were used to crosslink GF to achieve the corresponding GF scaffolds. The elution method was used to test the cytocompatibility of these scaffolds. These fabricated scaffolds were immersed into the cell culture media for 2 hours. 3T3-L1 preadipocytes were then treated with these individual elution media for 2 days. The cell viabilities were measured by WST-1 assay at the end of the treatment ($n = 4$). The bars are mean \pm standard deviation.

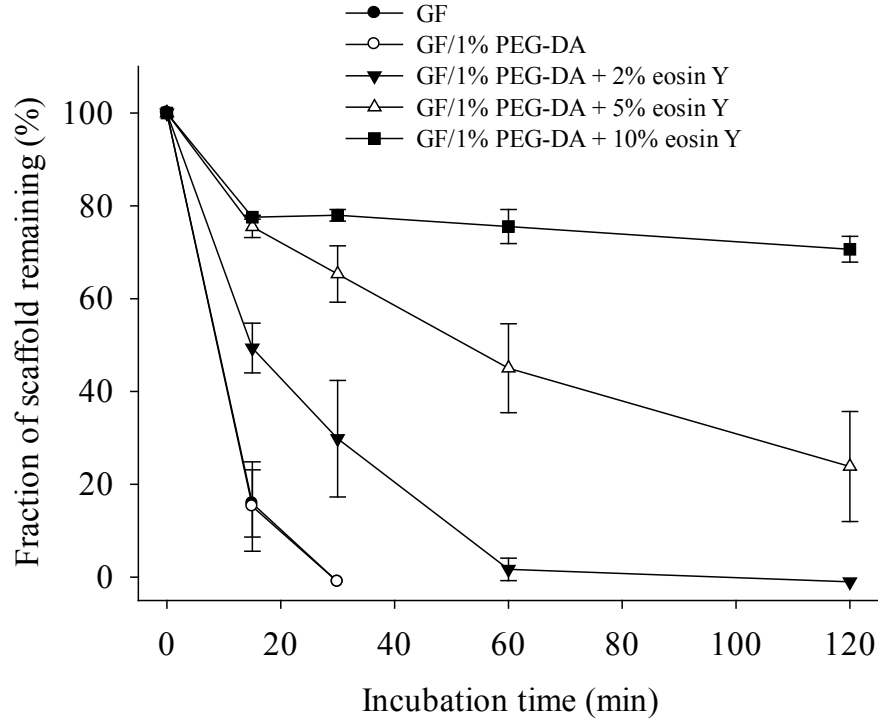


Figure 3.4: In vitro degradation of different fabricated GF scaffolds in the cell culture media.

20 mg of each fabricated GF scaffold was immersed into 5 ml of the cell culture media, and each sample was collected and weighed at the indicated time intervals ($n = 5$). The bars are mean \pm standard deviation.

insulin that is required for transbuccal mucosal delivery of insulin within the oral cavity. The formulation of scaffold was optimized as GF crosslinked with 1% PEG-DA and 5% eosin Y in respect to both cytocompatibility and degradation rate, and this formulation of scaffold was referred to as sINP GF in the rest of the work.

3.3.2 Mechanical properties of sINP GF scaffold

The mechanical properties were evaluated to confirm the crosslinking process of sINP GF. As shown in Figure 3.5A, the thickness of sINP GF was significantly smaller than the precursor GF. Most likely, the fibers fused together and crosslinked along or between the side chains. Similar observation was obtained using DMPA photoinitiator to crosslink GF with PEG-DA [2]. The mechanical properties, including the peak

load, peak stress, modulus, energy at break and strain at break, were significantly enhanced by 6.5, 7.9, 5.0, 17.1 and 2.4 fold in sIPN GF comparing with GF as shown in Figure 3.5B-F. The results confirmed 1% PEG-DA and 5% eosin Y were able to crosslink GF and increased its mechanical strength.

3.3.3 Morphology and fiber diameter of sIPN GF

The fiber morphology was evaluated by SEM to monitor the crosslinking process of sIPN GF. As shown in Figure 3.6, the morphology of GF displayed a well interconnective structure with fine continuous fibers and an undefined porosity, which was consistent with our previous reports [2, 7]. Interestingly, the morphology of sIPN GF showed that those continuous fibers of the scaffold were fused together and formed a much smaller porosity structure. At notice, some fibers were merged as side-by-side chains; while some fibers were crossed over the others. This observation supported the results from the tensile study that the thickness of sIPN GF was smaller than GF (Figure 3.5A). Such a small space between the crosslinked fibers was most likely resulted from the short chain of PEG-DA. Consequently, a significant increase of fiber diameter was observed in sIPN GF comparing to GF (Figure 3.7). It could also be observed clearly that two fibers were immersed together into one in sIPN GF (Figure 3.6). These results further confirmed the successful crosslinking process of sIPN GF.

3.3.4 Structure stability of sIPN GF

The structure stability of sIPN GF was investigated based on the degradation rate of sIPN GF in Figure 3.4, a set of SEM images of sIPN GF taken after 15, 30, 60 and 120 min of incubation in the cell culture media were compared to that of sIPN GF itself. As shown in Figure 3.8, the pore size significantly increased along with the incubation time. After 15 min of incubation, the fiber diameter was significantly reduced, and many small diameter fibers were observed, comparing to sIPN GF.

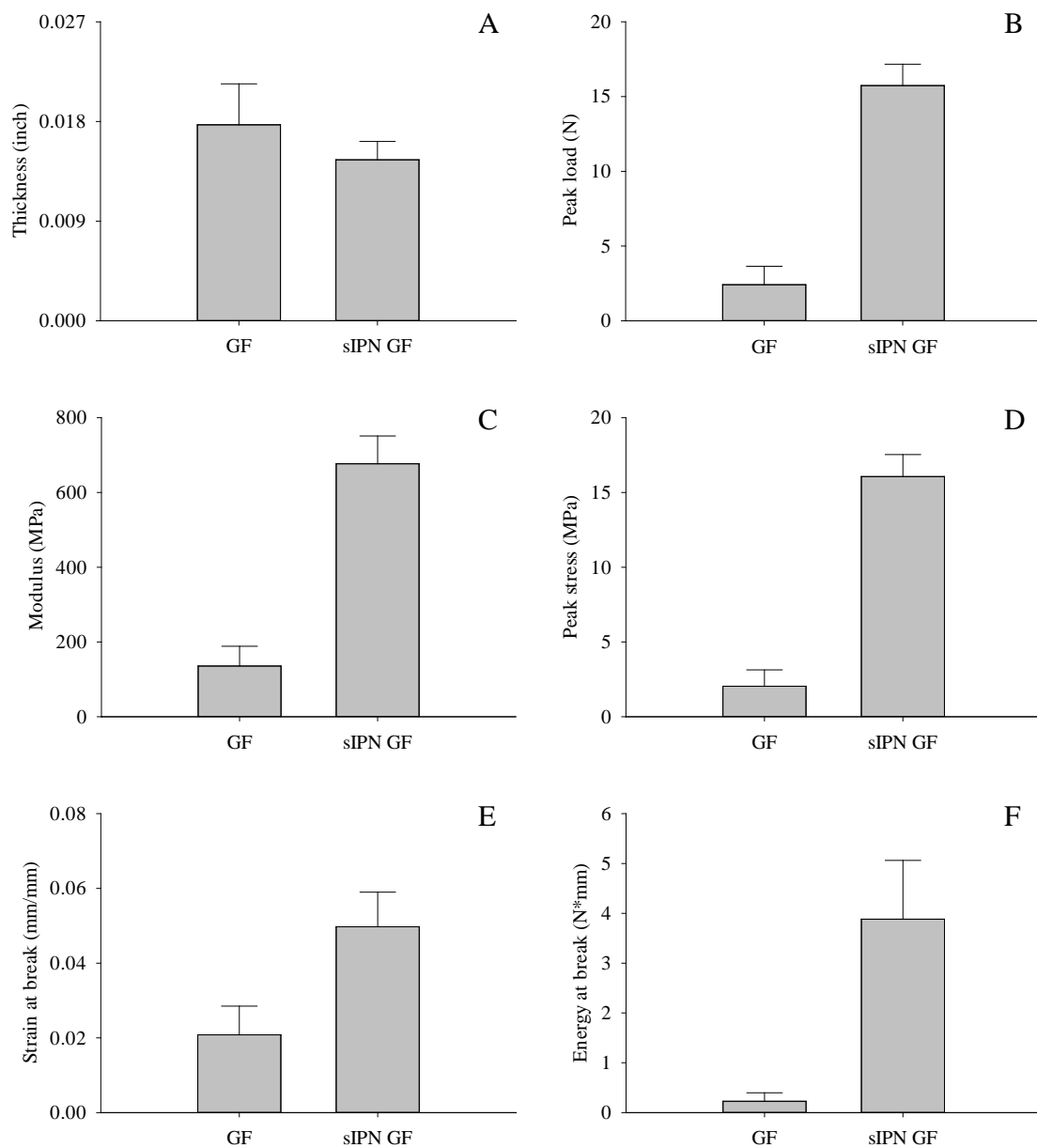


Figure 3.5: Mechanical properties of GF and sIPN GF.

The mechanical properties of GF (n = 18) and sIPN GF (n = 12) were evaluated by a uniaxial tensile test. (A) Thickness of the scaffolds. (B) Peak load of the scaffolds. (C) Peak stress of the scaffolds. (D) Modulus of the scaffolds. (E) Energy at break of the scaffolds. (F) Strain at break of the scaffolds. The bars are mean \pm standard deviation.

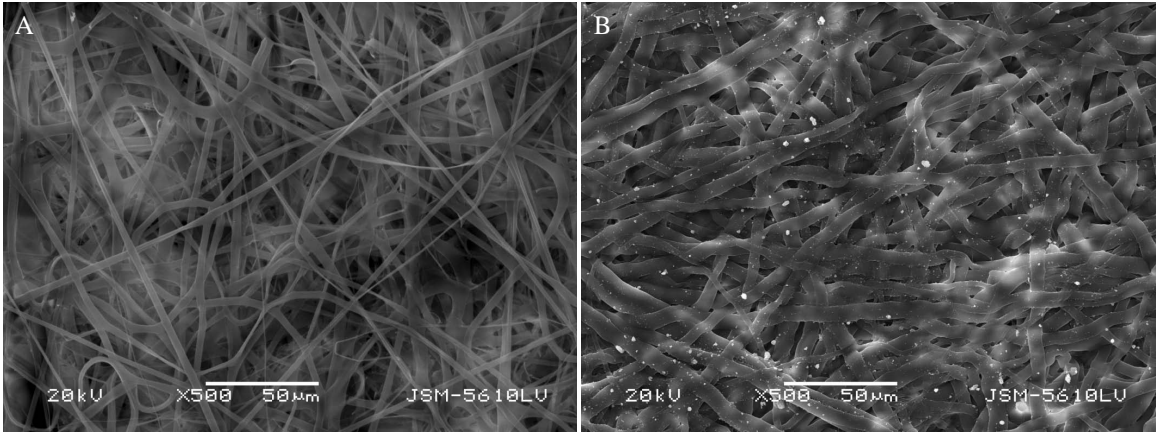


Figure 3.6: Morphology of GF and sIPN GF.

The scaffold morphology of (A) GF and (B) sIPN GF was observed by SEM (n = 3). Bars: 50 μ m.

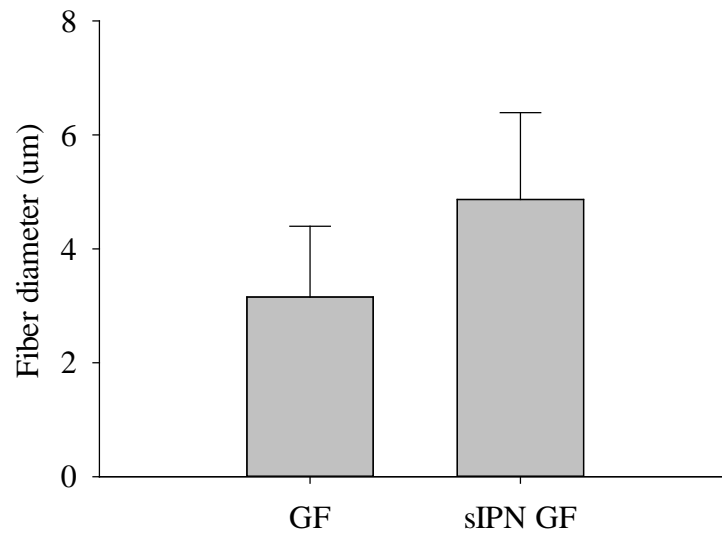


Figure 3.7: Fiber diameter of GF and sIPN GF.

Fiber diameters of GF and sIPN GF (n = 60) were measured by NIH ImageJ software from the SEM images. The bars are mean \pm standard deviation.

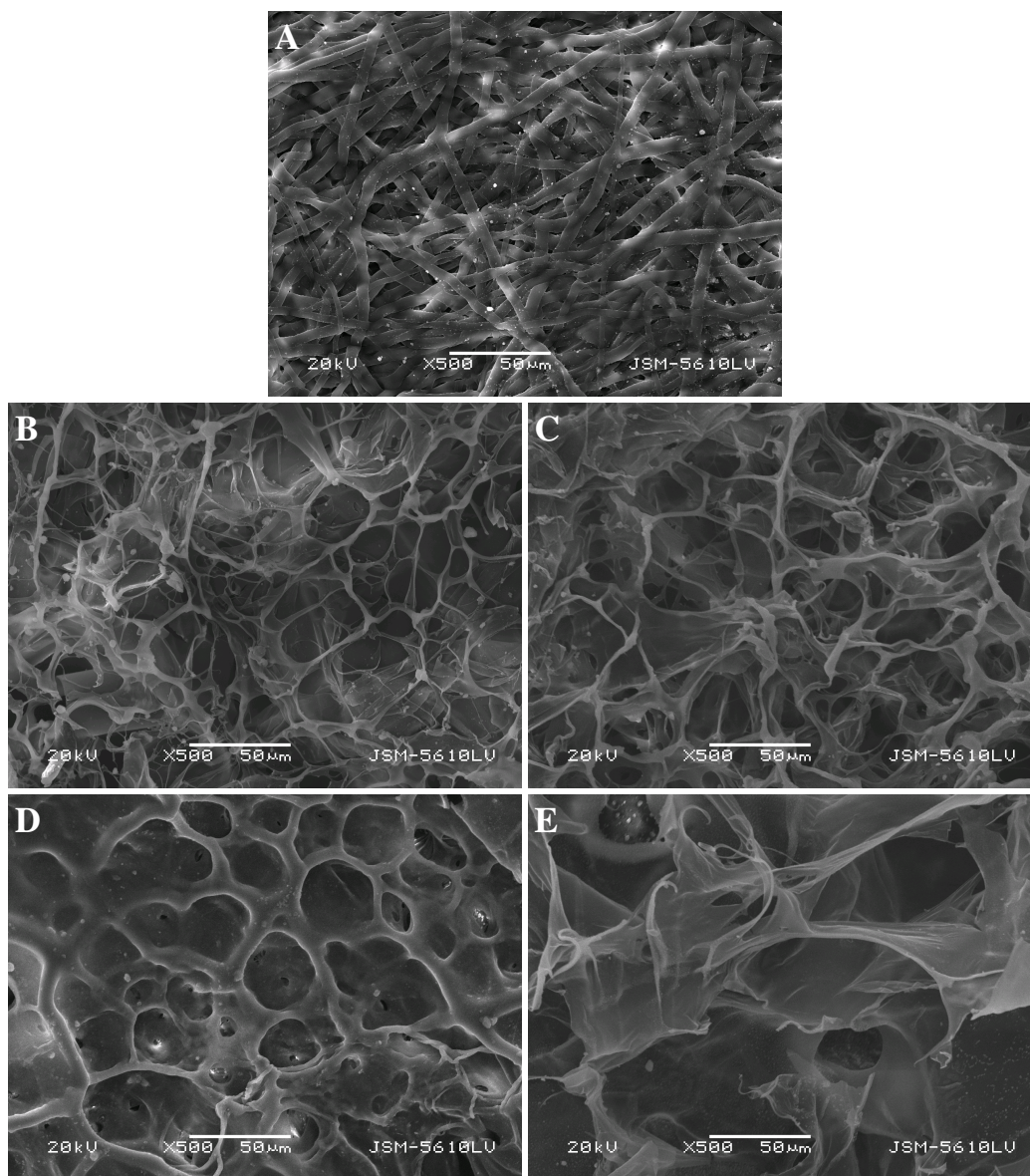


Figure 3.8: Morphology of sIPN GF after degradation.

20 mg of sIPN GF was immersed into 5 ml of cell culture media, and each sample was collected at the indicated time intervals of (A) 0 min, (B) 15 min, (C) 30 min, (D) 60 min and (E) 120 min. The remaining scaffold morphology was observed by SEM (n = 3). Bars: 50 μm .

After 30 min of incubation, most of the small diameter fibers were disappeared in the scaffold structure, while the structure remained three-dimensional. Most likely, these small diameter fibers were more easily degraded and dissolved into the media than the large diameter fibers. After 60 min of incubation, all the small diameter fibers were dissolved in the scaffold and the fiber diameter became larger. It was likely caused by the fact that some of the fibers were fused together to maintain the structure in the media. Lastly, after 120 min of incubation, the scaffold lost its defined three-dimensional structure and became separated pieces of polymers. These results were consistent with the degradation assay shown in Figure 3.4 that only 20% mass remained, and the scaffold lost its whole integrity after 120 min of incubation.

3.3.5 Insulin release kinetics of sIPN GIF

The fabricated sIPN GIF using optimized formulation described earlier was assessed to investigate the insulin release kinetics in response to the cell culture media. Cumulative insulin release studies were performed using ELISA. As shown in Figure 3.9, a fast insulin release was achieved from GIF that almost all insulin was released within 15 min. GIF, same as GF, can be instantaneously degraded and dissolved in the cell culture media within 30 min (Figure 3.4), which interprets all the insulin fabricated within GIF was released into the media within 30 min. The feeding ratio of insulin to gelatin was 5:1 (mg/g) according the formulation; and the resultant ratio of insulin to GIF was 3.25:1 (mg/g). Indeed, the loading efficiency of insulin after electrospinning was about 65%.

In contrast, a slower insulin release was observed from sIPN GIF within a 4-hour window of incubation in the cell culture media. These results were also consistent with the degradation rate (Figure 3.4) and the porosity of sIPN GF (Figure 3.8) described above. Nearly 20% of sIPN GIF mass has been degraded from the scaffold in the initial degradation at 15 min. The increase in porosity allows water molecules to come inside of scaffold, dissolve the gelatin fiber, and absorb insulin molecules. As shown in Figure 3.10, an initial burst release of insulin was observed about 70% of

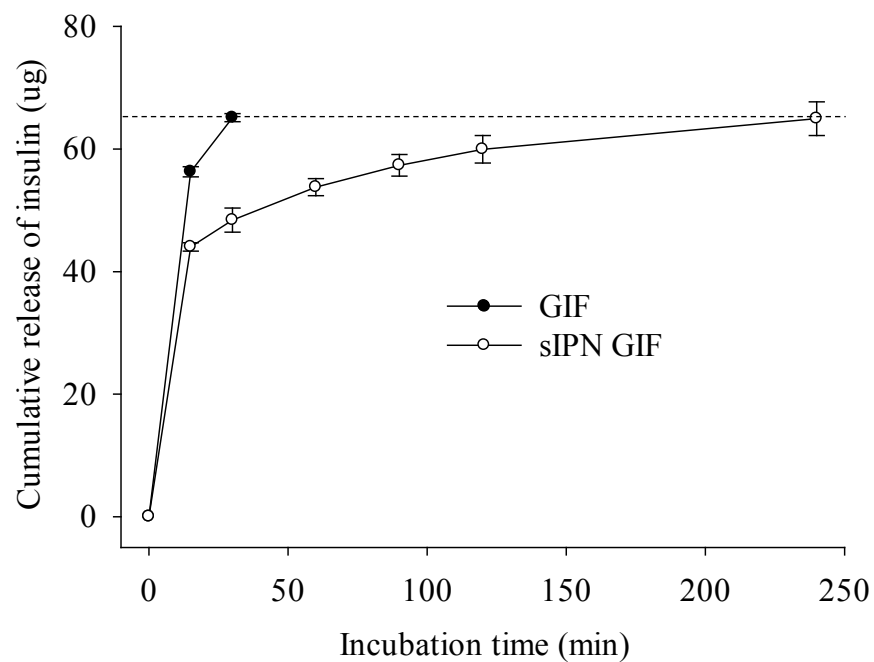


Figure 3.9: In vitro insulin release kinetics.

20 mg of GIF or sIPN GIF was immersed into 5 ml of cell culture media, and 25 μ l of release media was collected at the indicated time intervals. ELISA was employed to evaluate the insulin concentration from the release media. The bars are mean \pm standard deviation.

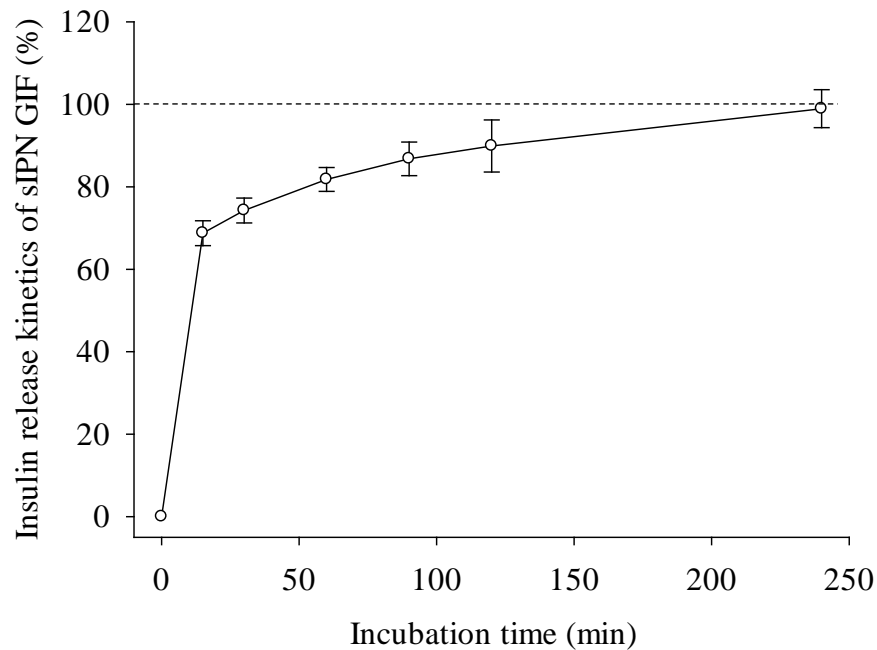


Figure 3.10: In vitro insulin release kinetics of sIPN GIF.

The insulin release kinetics of sIPN GIF was normalized by taking into account of 100% of insulin released from GIF within 30 min of incubation from Figure 3.10.

The bars are mean \pm standard deviation.

loading insulin from sIPN GIF within 15 min of incubation. The release rate of insulin was then reduced until 100% loading insulin was released from sIPN GIF, i.e., about 4 hours. This formulation of sIPN GF provides a fast release at the initial stage and a sustained slow release at the late stage, which can be benefit in oral mucosal delivery of insulin. Generally, an increase of both PEG-DA and eosin Y concentrations during the crosslinking process could help to enhance the scaffold stability and subsequently modulate the drug release kinetics. It is also important to keep the same ratio of PEG-DA to eosin Y as 1:5 (w/v) in order to maintain its biocompatibility.

3.3.6 Bioactivity of the insulin released from sIPN GIF

The bioactivity of insulin within sIPN GIF after electrospinning was examined in this work. It has been reported that proteins can be co-electrospun with polymers

without causing denature of the neutral protein. For instance, purified adipose tissue-derived extracellular matrix (At-ECM) can be electrospun alone or co-electrospun with PDO. The resultant scaffold forms a basement membrane-rich tissue engineering matrix that is capable of supporting stem cells [26]. Insulin is known as a peptide hormone that can bind to the extracellular portion of the alpha subunits of the insulin receptor and in turn trigger the signaling transduction within cells. Once the binding occurs, it causes a conformational change of the insulin receptor and then activates the kinase domain on the intracellular portion of the beta subunits. The activated kinase domain autophosphorylates IRS-1 protein, which subsequently activates phosphoinositol 3 kinase (PI3K). PI3K then catalyzes the reaction of PIP2 to PIP3, which can phosphorylate protein kinase B (PKB). PKB is also known as AKT that plays a key role in glucose metabolism, apoptosis, cell proliferation, transcription and cell migration [31, 80]. In this work, the phosphorylation of AKT was used as a marker to evaluate the bioactivity of released insulin. As shown in Figure 9, free insulin induced AKT phosphorylation as expected; while the release media from GIF also significantly induced AKT phosphorylation. It was also noticed that no significant change of p-AKT was observed in the release media from GF and sIPN GF. These results suggest that the insulin remains bioactive after electrospinning.

In the next step, sIPN GIF was examined for the ability to release bioactive insulin. As shown in Figure 3.12, phosphorylation of AKT displayed an incubation time-dependent manner of sIPN GIF. It was noticed that sIPN GIF in 15 min of incubation released a portion of insulin that was able to trigger AKT phosphorylation but not as high as that of 60 min of incubation. Together with insulin release kinetics (Figure 3.9), it supports that insulin bioactivity is close related to its release kinetics of sIPN GIF.

The differentiation of 3T3-L1 preadipocytes was also evaluated in regard to the insulin released from sIPN GIF. As expected, no adipocyte differentiation was observed in sIPN GF and negative control treatment groups; whereas a significant

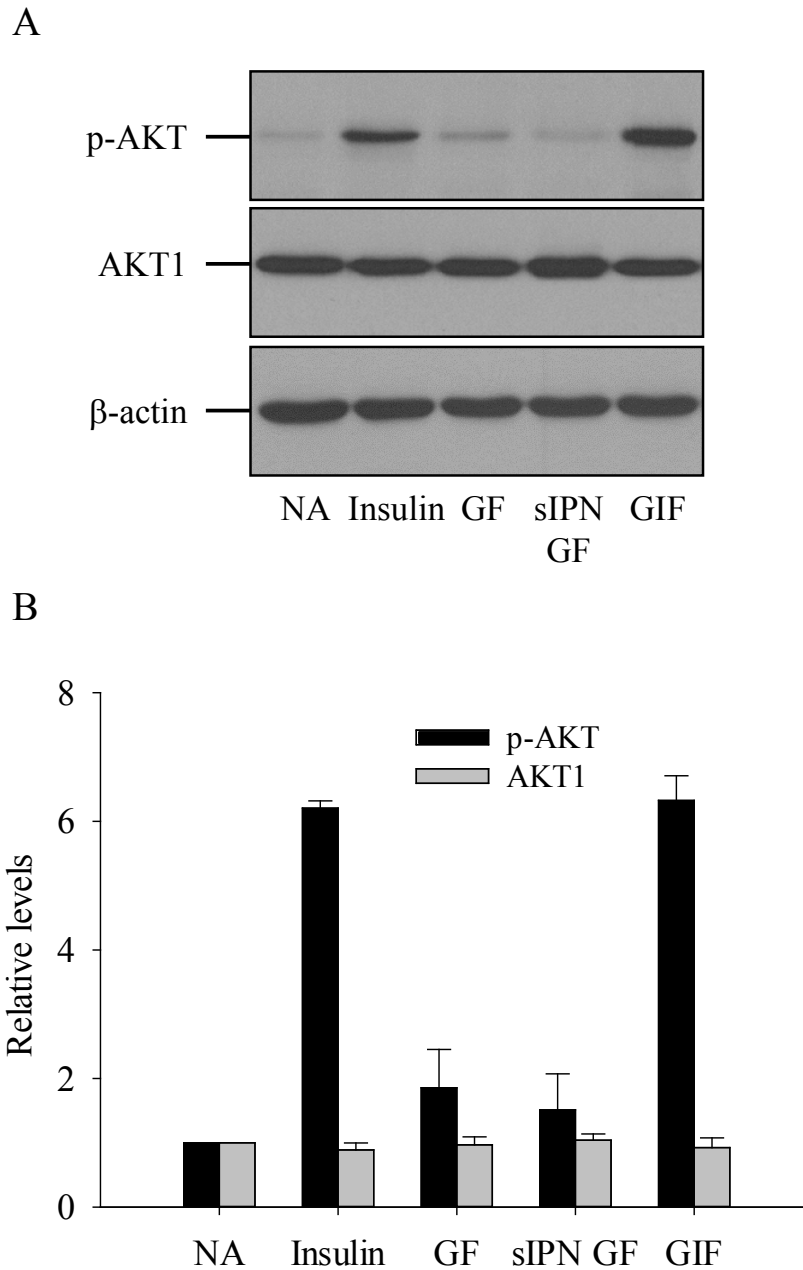


Figure 3.11: Western blot analysis of intracellular AKT activity in responding to the fabricated GF scaffolds.

20 mg of each fabricated GF scaffold (GF, sIPN GF and GIF) was immersed into 5 ml of cell culture media for 30 min. 3T3-L1 preadipocytes were then treated with these individual elution media or free insulin for 10 min. The intracellular phospho-AKT (p-AKT) and total AKT levels were analyzed by Western blot analysis (A). Each positive band was normalized to β -actin and was quantified by NIH ImageJ (B). The data represents typical one of three experiments. The bars are mean \pm standard deviation.

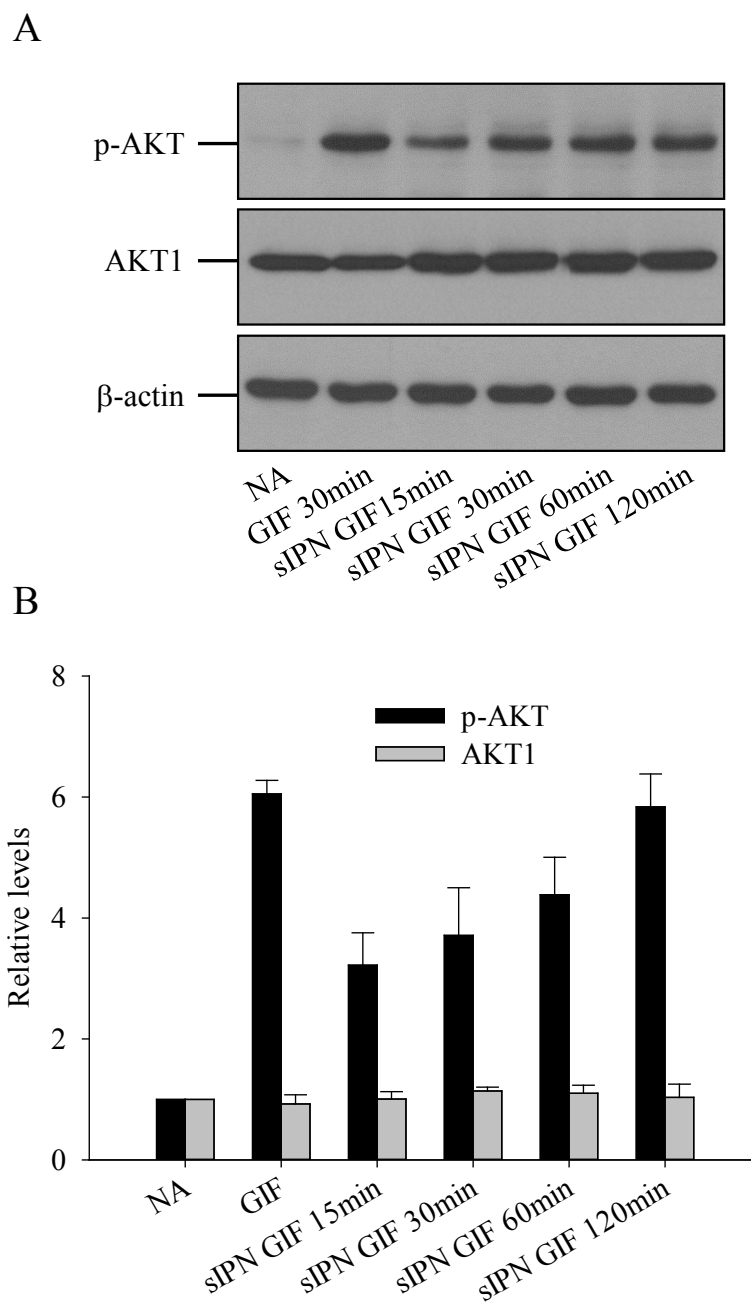


Figure 3.12: Western blot analysis of intracellular AKT activity in responding to sIPN GIF.

20 mg of sIPN GIF was immersed into 5 ml of cell culture media for 15 min, 30 min, 60 min and 120 min; while 20 mg of GIF was immersed into 5 ml of cell culture media for 30 min. 3T3-L1 preadipocytes were then treated with these individual elution media for 10 min. The intracellular phospho-AKT (p-AKT) and total AKT levels were analyzed by Western blot analysis (A). Each positive band was normalized to β -actin and was quantified by NIH ImageJ (B). The data represents typical one of three experiments. The bars are mean \pm standard deviation.

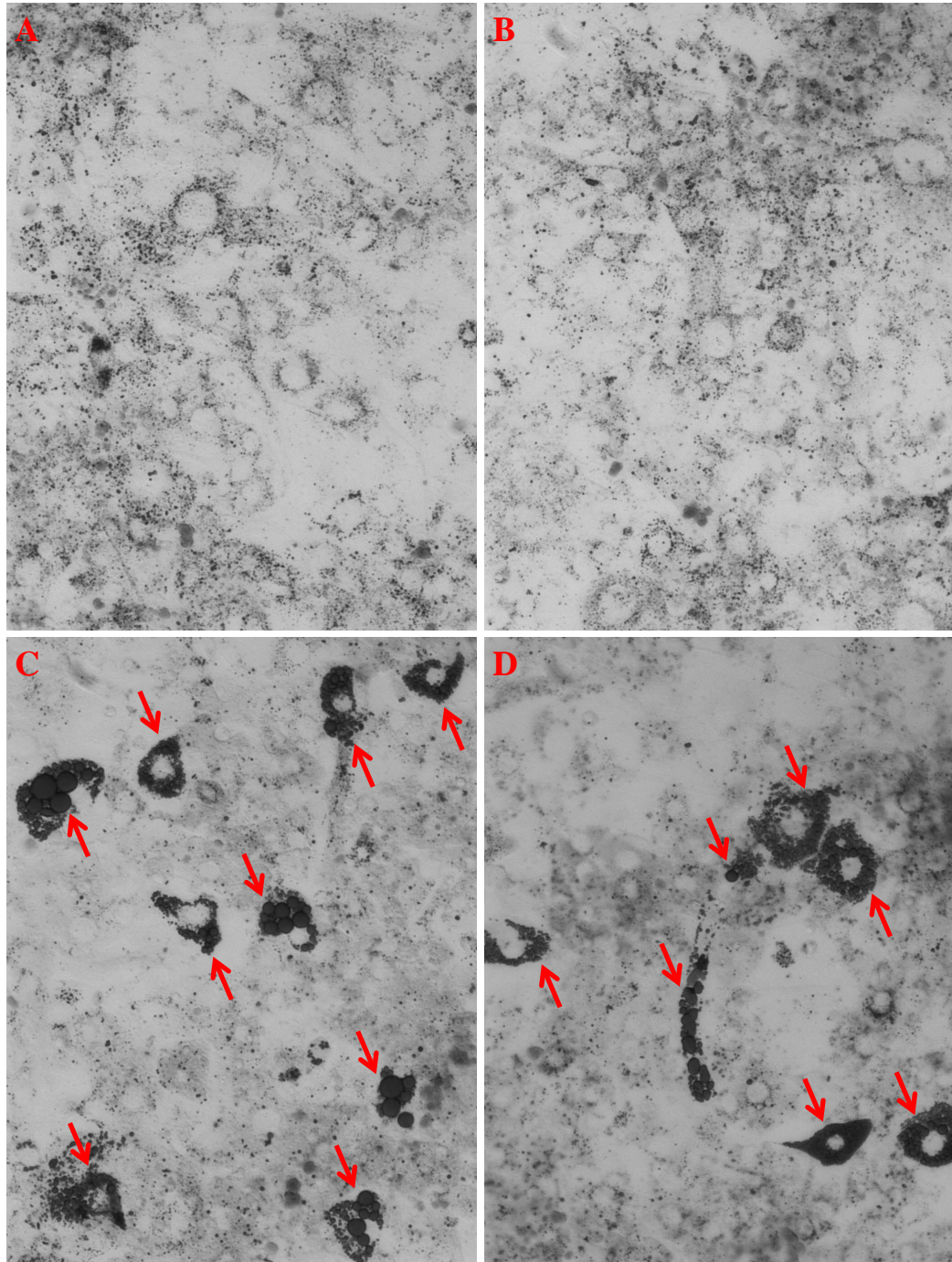


Figure 3.13: Oil red O staining of 3T3-L1 preadipocytes in responding to sIPN GIF.

20 mg of sIPN GIF or sIPN GF was immersed into 5 ml of cell culture media for 120 min. 3T3-L1 preadipocytes were then treated with these individual elution media or free insulin along with DEX and IBMX for 2 days. After additional 8 days incubation, the cells are fixed and total intracellular neutral lipids were stained with

Oil Red O. (A) NA, (B) sIPN GF, (C) sIPN GIF and (D) free insulin. Arrows indicate stained lipid inclusions.

adipocyte differentiation was achieved in sIPN GIF and free insulin groups as shown in Figure 3.13. It confirmed from the biological aspect that the insulin can be co-electrospun with gelatin and remain its bioactivity. The insulin release kinetics can be modulated by applying crosslink reaction to GIF.

3.3.7 Diffusion rate of insulin from sIPN GIF across porcine buccal mucosa

Hydrophilic molecules across buccal membrane is generally via a paracellular route that is driven by passive diffusion. Due to its good biodegradability, moderate stiffness and satisfactory tissue adhesiveness properties [73, 92], gelatin/PEG sIPN are investigated to deliver biomacromolecules and release them in a controlled release manner [10]. Firstly, it has been reported that mucoadhesive hydrogels can open up the tight junctions of the epithelium by dehydrating the cells as they swell, which in turn increases the permeability of the loaded drug [60]. Secondly, a direct contact of gels and mucosa could give a high localization of drug onto the mucosal surface, which in turn facilitates drug buccal transport. Based on the understanding of these mechanisms, a gelatin/PEG sIPN was developed to enhance transbuccal delivery of dendritic nanoparticles through an in vitro model [91]. Although PEG-only hydrogel has shown a slightly higher degree of enhanced transbuccal delivery of dendritic nanoparticles, it is a lack of mucosal adhesiveness property that makes PEG-only hydrogel unsuitable platform for buccal administration formulations [91].

In this work, the permeability of insulin from sIPN GIF was evaluated via a vertical Franz diffusion cell with a porcine epithelium membrane. First, the degradation rate of sIPN GF was determined in SSF, which simulates oral saliva condition. As shown in Figure 3.14, the degradation rate of sIPN GF in SSF is similar to that in the cell culture media (Figure 3.4). However, the composition of in vivo saliva remains different as that of in vitro SSF. The saliva contains the enzymes secreted from the salivary glands, such as amylase and lipase. These enzymes may have the potential to accelerate the degradation of sIPN GF. Second, the diffusion rates of in-

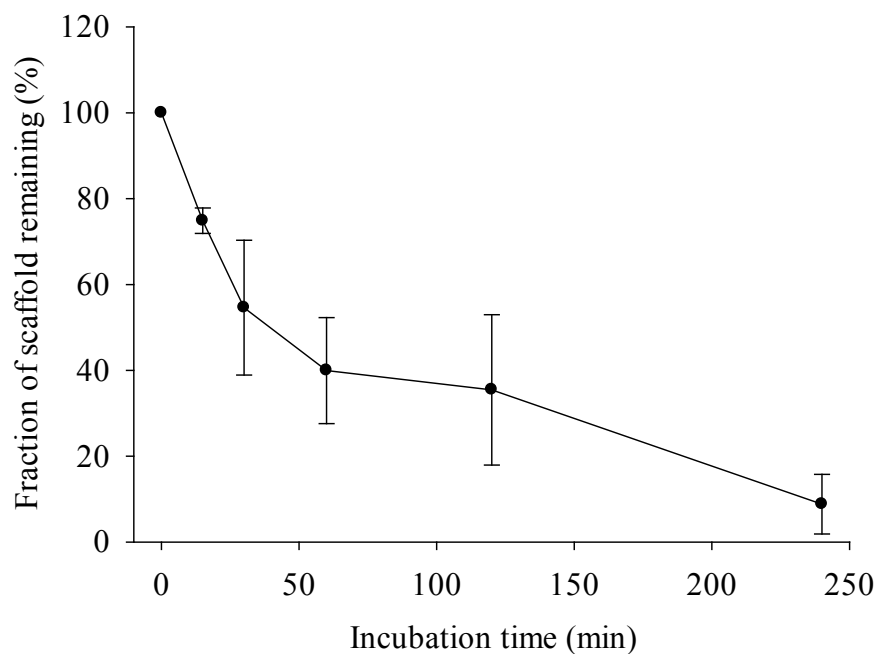


Figure 3.14: In vitro degradation of sIPN GF in SSF.

20 mg of sIPN GF was immersed into 5 ml of SSF, and each sample was collected and weighed at the indicated time intervals ($n = 8$). The bars are mean \pm standard deviation.

Insulin from sIPN GF and free insulin were determined through porcine buccal mucosa. As shown in Figure 3.15, the positive control benzylamine displayed a high transport rate, consistent with the previous report [2]. As shown in Figure 3.16, the cumulative flux curves of both sIPN GF and free insulin exhibited a linear range during the first 2 hours, indicating a steady state transport of the insulin via the paracellular route. Permeability was then calculated from the linear range of the cumulative flux curves. The permeability of insulin from sIPN GF was determined to be 1.00×10^{-7} cm/s; whereas the permeability of free insulin was 7.67×10^{-8} cm/s. A 30% enhancement of permeability was achieved by sIPN GF.

Although the enhanced permeability of insulin from sIPN GF has been shown, some challenges and future directions remain as follow. (1) It would be critical if the mucosal endothelial cells remain as intact and tight conjunct after freeze-thaw cycle.

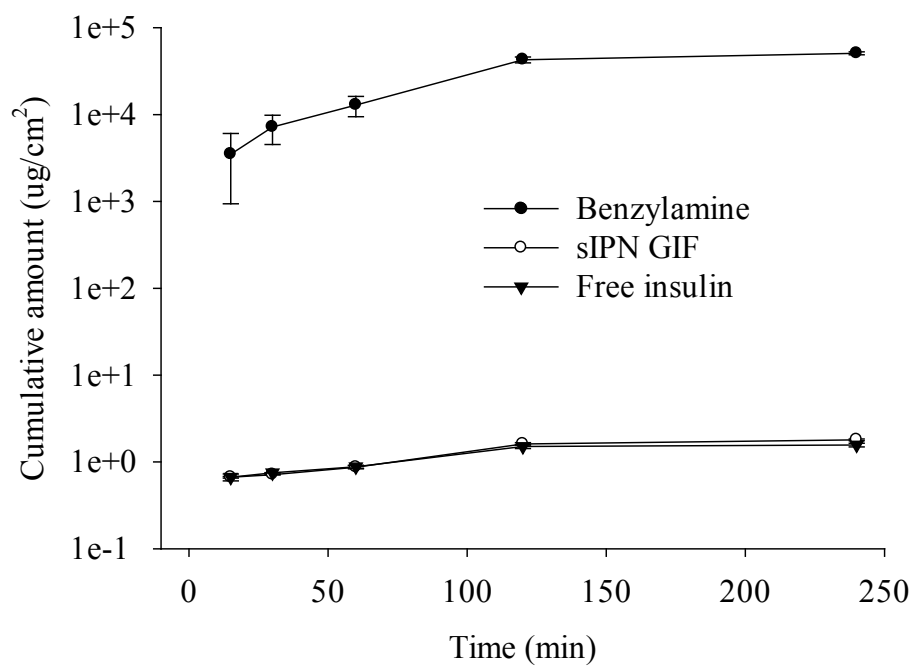


Figure 3.15: Transport of insulin or benzylamine across porcine buccal mucosa.

At the indicated time intervals, the transbuccal mucosal insulin from sIPN GIF or free insulin was determined by ELISA, and benzylamine was determined by UV-Vis (n = 3). The bars are mean standard deviation.

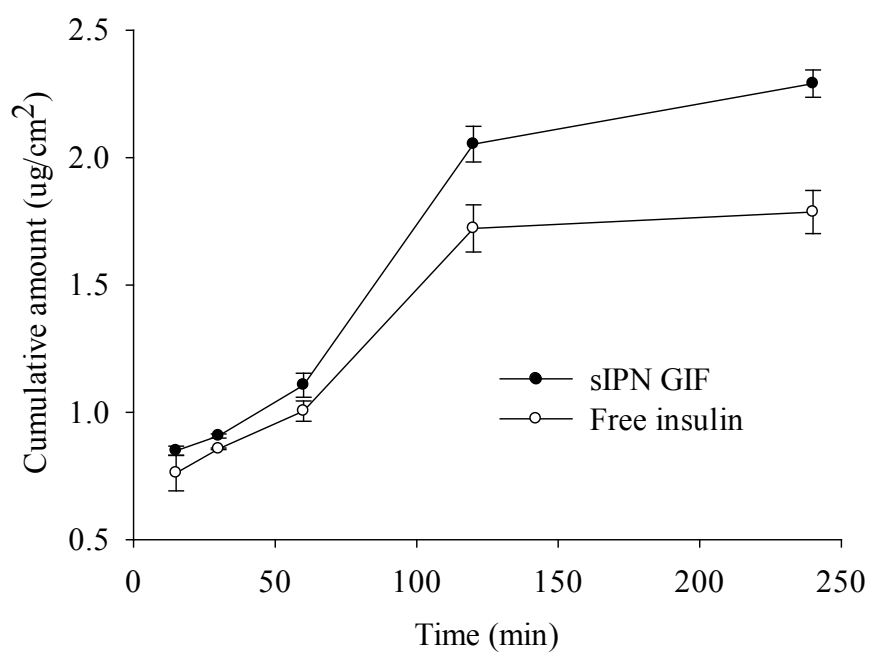


Figure 3.16: Transport of insulin across porcine buccal mucosa.

At the indicated time intervals, the transbuccal mucosal insulin from sIPN GIF or free insulin was determined by ELISA ($n = 3$). The bars are mean standard deviation.

(2) It is of interest to investigate whether the mucosal endothelial cells can uptake insulin during the diffusion process. (3) The continued work could be determination of the mucosal adhesion properties of sIPN GF. (4) Future studies include optimization of sIPN GIF loaded with permeation enhancer, such as sodium glycodeoxycholate (NaGDC), since it has been reported that bile salts hold a great potential to enhance transbuccal permeability of drug [91]. (5) The studies may also include the testing of pharmacokinetics and pharmacodynamics (PK/PD) of sIPN GIF following buccal administration in pig.

3.4 Conclusions

In this work, sIPN GF was fabricated by crosslinking GF with PEG-DA via photopolymerization process. The optimal ratio of PEG-DA to eosin Y is 1:5 (w/v) with respect to biocompatibility, degradation rate and structure stability. This formulation of sIPN GF exhibits high biocompatibility and possesses mucoadhesion property. It could be a good candidate for buccal mucosal delivery of insulin. The insulin release kinetics was modulated to achieve a desired bioactivity. Based on our preliminary in vitro investigation, sIPN GIF significantly enhanced transbuccal diffusion rate of insulin through the porcine mucosal membrane. The in vivo mucosal administration of insulin on sIPN GIF will be evaluated in our future studies.

Chapter 4

General conclusions and future directions

4.1 General conclusions

To explore the potential application of sIPN GF in transbuccal mucosal delivery of insulin, a general review was provided on adhesion property and release kinetics from polymeric insulin delivery systems (Chapter 3). Several factors may impact insulin transbuccal mucosal behaviors from polymeric matrices, including matrix factors, solute factors and experimental conditions. Among these factors, material degradation rate and insulin release kinetics and permeability are the key driving forces. With a better understanding of buccal mucosal transport mechanism, our objective was to optimize sIPN GF with the most appropriate biological and physical properties for transbuccal mucosal delivery of insulin.

sIPN GF is commonly formed by crosslinking GF with PEG-DA. This crosslinking process is driven by photopolymerization. Photoinitiators play an important role within photopolymerization. Photoinitiators can be dissociated into high-energy free radicals by exposure to specific wavelengths of light. Subsequently, these free radicals induce the polymerization of a macromer solution. However, these high-energy free radicals are toxic molecules that can induce oxidative stress to the cells. Chapter 2 illustrated that eosin Y was less cytotoxic than Irgacure 2959 and DMPA, and eosin Y

possessed minimal effect on intracellular AKT signaling transduction up to 25 $\mu\text{l/ml}$. It has been shown that the cytocompatibility of photoinitiators was closely correlated to the intracellular AKT signaling transduction within the cells. Free radicals can directly or indirectly interact with cells, inhibit the intracellular AKT signaling transduction and decrease cell viability. In summary, eosin Y can serve as a photoinitiator for the photopolymerization of sIPN GF, by owing its high cytocompatible property. The amount ratio of eosin Y to GF and PEG-DA needs to be optimized in order to minimize the cytotoxic effect induced by free radicals.

PEG-DA and PEG are widely used in biomedical applications, including drug delivery, tissue engineering and wound healing. A smaller molecular weight of PEG-DA has a higher diffusion rate into the cells, which can cause more damage of the cells. It has been shown the PEG-DA enhanced cytotoxic effect to the cells comparing to its precursor PEG (Chapter 3). This increase of toxicity is most likely caused by the acrylate modification at the terminals of PEG monomer chains. It becomes important to optimize the amount of both PEG-DA and eosin Y in the formulation of sIPN GF in respect to cytocompatibility.

Another important factor for transbuccal mucosal delivery of insulin is the degradation rate of polymeric matrices. Photopolymerization can physically enhance the entanglement of polymer chains in a three-dimensional structure. By controlling the crosslinking density, polymeric matrices can achieve a desired degradation rate.

In respect to both cytocompatibility and degradation rate of the scaffold, the formulation of sIPN GF was optimized by crosslinking GF with 1% PEG-DA and 5% eosin Y (Chapter 3). The optimized sIPN GF possessed no cytotoxic effect and exhibited a moderate degradation rate within 4-hour window (Chapter 3).

This optimized formulation was used to fabricate sIPN GIF for transbuccal mucosal delivery of insulin. Several important factors of sIPN GIF have been determined. 1) sIPN GIF achieved a 65% loading efficiency of insulin after electrospinning and crosslinking. 2) The insulin release kinetics was modulated after crosslinking in sIPN GIF. 3) The insulin released from sIPN GIF remained bioactive to activate intracellular AKT signaling transduction and differentiate 3T3-L1 preadipocytes. 4)

The permeability of the insulin released from sIPN GIF was on the order of 10^{-7} cm/s using a vertical Franz diffusion cell system mounted with porcine buccal mucosa (Chapter 3).

Insulin is commercially available in a concentration of 100 or 500 units/ml, which is designated U-100 and U-500, respectively. U-500 is only used in rare cases of insulin resistance when the patient requires extremely large doses of insulin [5]. The bolus dose for food coverage is prescribed as an insulin to carbohydrate ratio. The insulin to carbohydrate ratio represents the amounts of carbohydrate are covered by 1 unit of insulin. Here, 1 unit of insulin is equivalent to about 36 μ g of insulin. Generally, 1 unit of insulin will dispose of 12-15 g of carbohydrate. This range can vary from 6-30 g or more of carbohydrate depending on the insulin sensitivity, which can vary according to the time of day, from person to person, and is affected by physical activity and stress. According to the formulation of sIPN GIF, 65 μ g of insulin was incorporated within 20 mg of sIPN GIF, which is equal to 1.8 units of insulin. In order to achieve a common unit of insulin (10 units) taken each time, about 110 mg of sIPN GIF is required. The size of 110 of sIPN GIF is within 5 cm² range, which is a reasonable size of pill for oral mucosal administration. These results suggest that sIPN GIF holds a great potential for transbuccal mucosal delivery of insulin.

4.2 Future directions

The accomplishments from this work can inspire the further suggestions for continuing this work.

4.2.1 Evaluation of sIPN GIF in in vivo model

Porcine buccal tissues were utilized for studying the permeability of insulin from sIPN GIF in this work. Porcine buccal mucosa has been well established to be the closest to human mucosa. In vivo evaluation of sIPN GIF in transbuccal mucosal delivery of insulin will be conducted in pig in our future investigations. The bioavailability of

insulin will be studied by pharmacokinetics and pharmacodynamics. This in vivo pig study can provide direct evidence to evaluate the buccal mucosal permeability and biocompatibility from sIPN GF formulation.

4.2.2 Potential application of sIPN GF for wound healing

The outcome of these studies demonstrated the potential of developing such natural/synthetic hybrid materials into dermal equivalence. As a natural protein, insulin was successfully co-electrospun with gelatin in this work. The loading efficacy of insulin was about 65%, and the insulin remained bioactive after electrospinning and crosslinking process. These results inspire our great interests to further explore sIPN GF in the biomedical applications, such as wound healing.

Wounds can extend partially through the dermis and have capabilities to regenerate. However, the body cannot heal deep dermal injuries adequately. In some cases, such as full thickness burns or deep ulcers, there are no remaining sources of cells for regeneration except peripheral cells from the wound. Therefore, it takes a long time to complete re-epithelialization, and it is complicated by scarring of the base [18].

Matrix metalloproteinases, referred to as MMPs, play a major role in wound healing. MMPs can degrade all components of the extracellular matrix as well as regulate vascularization and inflammatory response [61, 53, 30]. It has been reported that MMP-2 regulates the formation of a glial scar and white matter sparing and/or axonal plasticity [30]. MMP-2 in turn can facilitate wound healing and promote functional recovery after spinal cord injury [61]. Thus, MMP-2 is exploited as a therapeutic target in the treatment of wound healing.

Electrospun nano- or macro-fiber scaffolds hold a great potential in the treatment of dermal wounds through layered application [33, 36, 18, 16]. It is of interest to explore sIPN GF incorporating with MMP-2 (sIPN GF/MMP-2) in the treatment of wound healing. The formulation of sIPN GF is required to be optimized in respect to the degradation rate. In the treatment of wound healing, the ratio of PEG-DA to eosin Y will be further modulated in order to achieve a slow degradation rate of the

sIPN GF and a slow release kinetics of MMP-2. It is important to investigate the efficacy of sIPN GF/MMP-2 in modulating host inflammatory response and healing outcome in a disease-relevant animal model, such as db/db mice with full thickness wounds.

Bibliography

- [1] Ryu Abe, Koujirou Hara, Kazuhiro Sayama, Kazunari Domen, and Hironori Arakawa. Steady hydrogen evolution from water on eosin y-fixed tio₂ photocatalyst using a silane-coupling reagent under visible light irradiation. *Journal of Photochemistry and Photobiology A: Chemistry*, 137(1):63–69, 2000.
- [2] Donald Aduba Jr, Jeremy A Hammer, Quan Yuan, W Andrew Yeudall, Gary L Bowlin, and Hu Yang. Semi-interpenetrating network (sipn) gelatin nanofiber scaffolds for oral mucosal drug delivery. *Acta Biomaterialia*, 2013.
- [3] Cameron Alexander. Synthetic polymer systems in drug delivery. *Expert opinion on emerging drugs*, 6(2):345–363, 2001.
- [4] DA Altomare and AR Khaled. Homeostasis and the importance for a balance between akt/mtor activity and intracellular signaling. *Current medicinal chemistry*, 19(22):3748, 2012.
- [5] American Diabetes Association. Insulin administration. *Diabetes Care*, 24(11):1984–1987, 2001.
- [6] CS Bahney, Trevor J Lujan, CW Hsu, M Bottlang, JL West, and B Johnstone. Visible light photoinitiation of mesenchymal stem cell-laden bioresponsive hydrogels. *European Cells and Materials*, 22:43–55, 2011.

- [7] Catherine P Barnes, Scott A Sell, Eugene D Boland, David G Simpson, and Gary L Bowlin. Nanofiber technology: designing the next generation of tissue engineering scaffolds. *Advanced drug delivery reviews*, 59(14):1413–1433, 2007.
- [8] Izabela M Barszczewska-Rybarek and Monika Krasowska. Fractal analysis of heterogeneous polymer networks formed by photopolymerization of dental dimethacrylates. *Dental Materials*, 2012.
- [9] Stephanie J Bryant, Charles R Nuttelman, and Kristi S Anseth. Cytocompatibility of uv and visible light photoinitiating systems on cultured nih/3t3 fibroblasts in vitro. *Journal of Biomaterials Science, Polymer Edition*, 11(5):439–457, 2000.
- [10] Jeanine A Burmania, Kelly R Stevens, and Weiyuan John Kao. Cell interaction with protein-loaded interpenetrating networks containing modified gelatin and poly (ethylene glycol) diacrylate. *Biomaterials*, 24(22):3921–3930, 2003.
- [11] Shenshen Cai, Yanchun Liu, Xiao Zheng Shu, and Glenn D Prestwich. Injectable glycosaminoglycan hydrogels for controlled release of human basic fibroblast growth factor. *Biomaterials*, 26(30):6054–6067, 2005.
- [12] Jeffrey W Card and Bernadene A Magnuson. A review of the efficacy and safety of nanoparticle-based oral insulin delivery systems. *American Journal of Physiology-Gastrointestinal and Liver Physiology*, 301(6):G956–G967, 2011.
- [13] Roberta Censi, Tina Vermonden, Mies J van Steenberg, Hendrik Deschout, Kevin Braeckmans, Stefaan C De Smedt, Cornelus F van Nostrum, Piera Di Martino, and WE Hennink. Photopolymerized thermosensitive hydrogels for tailorable diffusion-controlled protein delivery. *Journal of controlled release*, 140(3):230–236, 2009.
- [14] Kishore B Chalasani, GJ Russell-Jones, Sarath K Yandrapu, Prakash V Diwan, and Sanjay K Jain. A novel vitamin b₁₂-nanosphere conjugate carrier system for peroral delivery of insulin. *Journal of controlled release*, 117(3):421–429, 2007.

- [15] Kishore B Chalasani, Gregory J Russell-Jones, Akhlesh K Jain, Prakash V Diwan, and Sanjay K Jain. Effective oral delivery of insulin in animal models using vitamin b12-coated dextran nanoparticles. *Journal of Controlled Release*, 122(2):141–150, 2007.
- [16] Jyh-Ping Chen, Gwo-Yun Chang, and Jan-Kan Chen. Electrospun collagen/chitosan nanofibrous membrane as wound dressing. *Colloids and Surfaces A: Physicochemical and Engineering Aspects*, 313:183–188, 2008.
- [17] Mei-Chin Chen, Kiran Sonaje, Ko-Jie Chen, and Hsing-Wen Sung. A review of the prospects for polymeric nanoparticle platforms in oral insulin delivery. *Biomaterials*, 32(36):9826–9838, 2011.
- [18] EJ Chong, TT Phan, IJ Lim, YZ Zhang, BH Bay, S Ramakrishna, and CT Lim. Evaluation of electrospun pcl/gelatin nanofibrous scaffold for wound healing and layered dermal reconstitution. *Acta Biomaterialia*, 3(3):321–330, 2007.
- [19] Fu-de Cui, An-jin Tao, Dong-mei Cun, Li-qiang Zhang, and Kai Shi. Preparation of insulin loaded plga-hp55 nanoparticles for oral delivery. *Journal of pharmaceutical sciences*, 96(2):421–427, 2007.
- [20] Fude Cui, Kai Shi, Liqiang Zhang, Anjin Tao, and Yoshiaki Kawashima. Biodegradable nanoparticles loaded with insulin-phospholipid complex for oral delivery: preparation, in vitro characterization and in vivo evaluation. *Journal of controlled release*, 114(2):242–250, 2006.
- [21] Christiane Damgé, Philippe Maincent, and Nathalie Ubrich. Oral delivery of insulin associated to polymeric nanoparticles in diabetic rats. *Journal of controlled release*, 117(2):163–170, 2007.
- [22] Heidi A Declercq, Tomasz L Gorski, Séverine P Tielens, Etienne H Schacht, and Maria J Cornelissen. Encapsulation of osteoblast seeded microcarriers into injectable, photopolymerizable three-dimensional scaffolds based on d, l-lactide and ϵ -caprolactone. *Biomacromolecules*, 6(3):1608–1614, 2005.

- [23] Luis del Peso, Maribel González-García, Carmen Page, Román Herrera, and Gabriel Nuñez. Interleukin-3-induced phosphorylation of bad through the protein kinase akt. *Science*, 278(5338):687–689, 1997.
- [24] Pooja N Desai, Quan Yuan, and Hu Yang. Synthesis and characterization of photocurable polyamidoamine dendrimer hydrogels as a versatile platform for tissue engineering and drug delivery. *Biomacromolecules*, 11(3):666–673, 2010.
- [25] John P Fisher, David Dean, Paul S Engel, and Antonios G Mikos. Photoinitiated polymerization of biomaterials. *Annual review of materials research*, 31(1):171–181, 2001.
- [26] Michael P Francis, Patrick C Sachs, Parthasarathy A Madurantakam, Scott A Sell, Lynne W Elmore, Gary L Bowlin, and Shawn E Holt. Electrospinning adipose tissue-derived extracellular matrix for adipose stem cell culture. *Journal of Biomedical Materials Research Part A*, 100(7):1716–1724, 2012.
- [27] Yao Fu and Weiyuan John Kao. Drug release kinetics and transport mechanisms from semi-interpenetrating networks of gelatin and poly (ethylene glycol) diacrylate. *Pharmaceutical research*, 26(9):2115–2124, 2009.
- [28] Sherita Hill Golden and Tamar Sapir. Methods for insulin delivery and glucose monitoring in diabetes: Summary of a comparative effectiveness review. *Continuing Education*, 18(6), 2012.
- [29] Christopher A Holden, Puneet Tyagi, Ashish Thakur, Rajendra Kadam, Gajanan Jadhav, Uday B Kompella, and Hu Yang. Polyamidoamine dendrimer hydrogel for enhanced delivery of antiglaucoma drugs. *Nanomedicine: Nanotechnology, Biology and Medicine*, 8(5):776–783, 2012.
- [30] Jung-Yu C Hsu, Robert McKeon, Staci Goussev, Zena Werb, Jung-Uek Lee, Alpa Trivedi, and Linda J Noble-Haesslein. Matrix metalloproteinase-2 facilitates wound healing events that promote functional recovery after spinal cord injury. *The Journal of neuroscience*, 26(39):9841–9850, 2006.

- [31] Zhen Y Jiang, Qiong L Zhou, Kerri A Coleman, Queta Boese, and Michael P Czech. Insulin signaling through akt/protein kinase b analyzed by small interfering rna-mediated gene silencing. *Proceedings of the National Academy of Sciences*, 100(13):7569–7574, 2003.
- [32] Lin Jin, Ting Wang, Mei-Ling Zhu, Michelle K Leach, Youssef I Naim, Joseph M Corey, Zhang-Qi Feng, and Qing Jiang. Electrospun fibers and tissue engineering. *Journal of Biomedical Nanotechnology*, 8(1):1–9, 2012.
- [33] Dharendra S Katti, Kyle W Robinson, Frank K Ko, and Cato T Laurencin. Bioresorbable nanofiber-based systems for wound healing and drug delivery: Optimization of fabrication parameters. *Journal of Biomedical Materials Research Part B: Applied Biomaterials*, 70(2):286–296, 2004.
- [34] Vandana Keskar, Nicholas W Marion, Jeremy J Mao, and Richard A Gemeinhart. In vitro evaluation of macroporous hydrogels to facilitate stem cell infiltration, growth, and mineralization. *Tissue Engineering Part A*, 15(7):1695–1707, 2009.
- [35] Dhan B Khadka and Donald T Haynie. Protein-and peptide-based electrospun nanofibers in medical biomaterials. *Nanomedicine: Nanotechnology, Biology and Medicine*, 8(8):1242–1262, 2012.
- [36] Myung-Seob Khil, Dong-Il Cha, Hak-Yong Kim, In-Shik Kim, and Narayan Bhattarai. Electrospun nanofibrous polyurethane membrane as wound dressing. *Journal of Biomedical Materials Research Part B: Applied Biomaterials*, 67(2):675–679, 2003.
- [37] Albert H Kim, Gus Khursigara, Xuan Sun, Thomas F Franke, and Moses V Chao. Akt phosphorylates and negatively regulates apoptosis signal-regulating kinase 1. *Science Signaling*, 21(3):893, 2001.
- [38] Alexander H Krauland, Davide Guggi, and Andreas Bernkop-Schnürch. Oral insulin delivery: the potential of thiolated chitosan-insulin tablets on non-diabetic rats. *Journal of controlled release*, 95(3):547–555, 2004.

- [39] Xiaoyang Li, Jianping Qi, Yunchang Xie, Xi Zhang, Shunwen Hu, Ying Xu, Yi Lu, and Wei Wu. Nanoemulsions coated with alginate/chitosan as oral insulin delivery systems: preparation, characterization, and hypoglycemic effect in rats. *International journal of nanomedicine*, 8:23, 2013.
- [40] Youyun Liang, Tor W Jensen, Edward J Roy, Chaenyung Cha, Ross J DeVolder, Richie E Kohman, Bao Zhong Zhang, Kyle B Textor, Laretta A Rund, Lawrence B Schook, et al. Tuning the non-equilibrium state of a drug-encapsulated poly (ethylene glycol) hydrogel for stem and progenitor cell mobilization. *Biomaterials*, 32(7):2004–2012, 2011.
- [41] William B Liechty, Mary Caldorera-Moore, Margaret A Phillips, Cody Schoener, and Nicholas A Peppas. Advanced molecular design of biopolymers for transmucosal and intracellular delivery of chemotherapeutic agents and biological therapeutics. *Journal of Controlled Release*, 155(2):119–127, 2011.
- [42] Chien-Chi Lin and Kristi S Anseth. Glucagon-like peptide-1 functionalized peg hydrogels promote survival and function of encapsulated pancreatic β -cells. *Biomacromolecules*, 10(9):2460–2467, 2009.
- [43] Wenying Liu, Stavros Thomopoulos, and Younan Xia. Electrospun nanofibers for regenerative medicine. *Advanced healthcare materials*, 1(1):10–25, 2012.
- [44] LG Lovell, BJ Elliott, JR Brown, and CN Bowman. The effect of wavelength on the polymerization of multi (meth) acrylates with disulfide/benzilketal combinations. *Polymer*, 42(2):421–429, 2001.
- [45] Yongjie Ma, Leyuan Xu, Daniel Rodriguez-Agudo, Xiaobo Li, Douglas M Heuman, Phillip B Hylemon, William M Pandak, and Shunlin Ren. 25-hydroxycholesterol-3-sulfate regulates macrophage lipid metabolism via the lxr/srebp-1 signaling pathway. *American Journal of Physiology-Endocrinology And Metabolism*, 295(6):E1369–E1379, 2008.

- [46] Tomoko Magoshi and Takehisa Matsuda. Formation of polymerized mixed heparin/albumin surface layer and cellular adhesional responses. *Biomacromolecules*, 3(5):976–983, 2002.
- [47] Brendan D Manning and Lewis C Cantley. Akt/pkb signaling: navigating downstream. *Cell*, 129(7):1261, 2007.
- [48] F Masson, C Decker, S Andre, and X Andrieu. Uv-curable formulations for uv-transparent optical fiber coatings: I. acrylic resins. *Progress in organic coatings*, 49(1):1–12, 2004.
- [49] Jason P Mazzoccoli, Donald L Feke, Harihara Baskaran, and Peter N Pintauro. Mechanical and cell viability properties of crosslinked low-and high-molecular weight poly (ethylene glycol) diacrylate blends. *Journal of biomedical materials research Part A*, 93(2):558–566, 2010.
- [50] Michael J McClure, Patricia S Wolfe, David G Simpson, Scott A Sell, and Gary L Bowlin. The use of air-flow impedance to control fiber deposition patterns during electrospinning. *Biomaterials*, 33(3):771–779, 2012.
- [51] Fwu-Long Mi, Yong-Yi Wu, Yu-Hsin Lin, Kiran Sonaje, Yi-Cheng Ho, Chiung-Tong Chen, Jyuhn-Huarng Juang, and Hsing-Wen Sung. Oral delivery of peptide drugs using nanoparticles self-assembled by poly (γ -glutamic acid) and a chitosan derivative functionalized by trimethylation. *Bioconjugate chemistry*, 19(6):1248–1255, 2008.
- [52] Ana Isabel Mouquinho, Krasimira Petrova, Maria Teresa Barros, and João Sotomayor. New polymer networks for pdlc films application. 2012.
- [53] M Muller, C Trocme, B Lardy, F Morel, S Halimi, and PY Benhamou. Matrix metalloproteinases and diabetic foot ulcers: the ratio of mmp-1 to timp-1 is a predictor of wound healing. *Diabetic Medicine*, 25(4):419–426, 2008.

- [54] Mayura Oak and Jagdish Singh. Chitosan-zinc-insulin complex incorporated thermosensitive polymer for controlled delivery of basal insulin in vivo. *Journal of Controlled Release*, 2012.
- [55] Alicia K Olivier, Yaling Yi, Xingshen Sun, Hongshu Sui, Bo Liang, Shanming Hu, Weiliang Xie, John T Fisher, Nicholas W Keiser, Diana Lei, et al. Abnormal endocrine pancreas function at birth in cystic fibrosis ferrets. *The Journal of clinical investigation*, 122(10):3755–3768, 2012.
- [56] Anna-Karin Olsson, Anna Dimberg, Johan Kreuger, and Lena Claesson-Welsh. Vegf receptor signalling? in control of vascular function. *Nature Reviews Molecular Cell Biology*, 7(5):359–371, 2006.
- [57] Yan Pan, Ying-jian Li, Hui-ying Zhao, Jun-min Zheng, Hui Xu, Gang Wei, Jin-song Hao, and Fu-de Cui. Bioadhesive polysaccharide in protein delivery system: chitosan nanoparticles improve the intestinal absorption of insulin in vivo. *International journal of pharmaceutics*, 249(1):139–147, 2002.
- [58] Viralkumar F Patel, Fang Liu, and Marc B Brown. Advances in oral transmucosal drug delivery. *Journal of Controlled Release*, 153(2):106–116, 2011.
- [59] Masanori Sakamoto, Mamoru Fujistuka, and Tetsuro Majima. Light as a construction tool of metal nanoparticles: synthesis and mechanism. *Journal of Photochemistry and Photobiology C: Photochemistry Reviews*, 10(1):33–56, 2009.
- [60] Nazila Salamat-Miller, Montakarn Chittchang, and Thomas P Johnston. The use of mucoadhesive polymers in buccal drug delivery. *Advanced Drug Delivery Reviews*, 57(11):1666–1691, 2005.
- [61] Tuula Salo, M Mäkelä, M Kylmäniemi, H Autio-Harmainen, and H Larjava. Expression of matrix metalloproteinase-2 and-9 during early human wound healing. *Laboratory investigation; a journal of technical methods and pathology*, 70(2):176–182, 1994.

- [62] Bruno Sarmento, António Ribeiro, Francisco Veiga, Domingos Ferreira, and Ronald Neufeld. Oral bioavailability of insulin contained in polysaccharide nanoparticles. *Biomacromolecules*, 8(10):3054–3060, 2007.
- [63] Scott A Sell, Michael J McClure, Koyal Garg, Patricia S Wolfe, and Gary L Bowlin. Electrospinning of collagen/biopolymers for regenerative medicine and cardiovascular tissue engineering. *Advanced drug delivery reviews*, 61(12):1007–1019, 2009.
- [64] Gregg L Semenza. Targeting hif-1 for cancer therapy. *Nature Reviews Cancer*, 3(10):721–732, 2003.
- [65] Tsuyoshi Shimada, Nobuhiko Hiramatsu, Ayumi Kasai, Mai Mukai, Maro Okamura, Jian Yao, Tao Huang, Minori Tamai, Shuhei Takahashi, Tomoyuki Nakamura, et al. Suppression of adipocyte differentiation by cordyceps militaris through activation of the aryl hydrocarbon receptor. *American Journal of Physiology-Endocrinology And Metabolism*, 295(4):E859–E867, 2008.
- [66] Jennifer E Skeen, Prashanth T Bhaskar, Chia-Chen Chen, William S Chen, Xiaoding Peng, Veronique Nogueira, Annett Hahn-Windgassen, Hiroaki Kiyokawa, and Nissim Hay. Akt deficiency impairs normal cell proliferation and suppresses oncogenesis in a p53-independent and mtorc1-dependent manner. *Cancer cell*, 10(4):269–280, 2006.
- [67] Sonja Sokic and Georgia Papavasiliou. Fgf-1 and proteolytically mediated cleavage site presentation influence three-dimensional fibroblast invasion in biomimetic pegda hydrogels. *Acta Biomaterialia*, 8(6):2213–2222, 2012.
- [68] So-Ra Son, Rose-Ann Franco, Sang-Ho Bae, Young-Ki Min, and Byong-Taek Lee. Electrospun plga/gelatin fibrous tubes for the application of biodegradable intestinal stent in rat model. *Journal of Biomedical Materials Research Part B: Applied Biomaterials*, 2013.

- [69] Kiran Sonaje, Yu-Hsin Lin, Jyuhn-Huarng Juang, Shiao-Pyng Wey, Chiung-Tong Chen, and Hsing-Wen Sung. In vivo evaluation of safety and efficacy of self-assembled nanoparticles for oral insulin delivery. *Biomaterials*, 30(12):2329–2339, 2009.
- [70] Diane H Song, Lisa Getty-Kaushik, Eva Tseng, Jonathan Simon, Barbara E Corkey, and M Michael Wolfe. Glucose-dependent insulinotropic polypeptide enhances adipocyte development and glucose uptake in part through akt activation. *Gastroenterology*, 133(6):1796–1805, 2007.
- [71] TA Sonia and Chandra P Sharma. An overview of natural polymers for oral insulin delivery. *Drug discovery today*, 2012.
- [72] Olivier Soppera, Colette Turck, and Daniel J Lougnot. Fabrication of micro-optical devices by self-guiding photopolymerization in the near ir. *Optics letters*, 34(4):461–463, 2009.
- [73] Kelly R Stevens, Nicole J Einerson, Jeanine A Burmania, and Weiyuan John Kao. In vivo biocompatibility of gelatin-based hydrogels and interpenetrating networks. *Journal of Biomaterials Science, Polymer Edition*, 13(12):1353–1366, 2002.
- [74] Julie Støy, Emma L Edghill, Sarah E Flanagan, Honggang Ye, Veronica P Paz, Anna Pluzhnikov, Jennifer E Below, M Geoffrey Hayes, Nancy J Cox, Gregory M Lipkind, et al. Insulin gene mutations as a cause of permanent neonatal diabetes. *Proceedings of the National Academy of Sciences*, 104(38):15040–15044, 2007.
- [75] Scott A Summers, Eileen L Whiteman, Han Cho, Lorraine Lipfert, and Morris J Birnbaum. Differentiation-dependent suppression of platelet-derived growth factor signaling in cultured adipocytes. *Journal of Biological Chemistry*, 274(34):23858–23867, 1999.
- [76] Hsing-Wen Sung, Kiran Sonaje, Zi-Xian Liao, Li-Wen Hsu, and Er-Yuan Chuang. pH-responsive nanoparticles shelled with chitosan for oral delivery of insulin:

- from mechanism to therapeutic applications. *Accounts of chemical research*, 45(4):619–629, 2012.
- [77] Weiqun Tian, Qiaolin Hu, Ying Xu, and Yi Xu. Effect of soybean-lecithin as an enhancer of buccal mucosa absorption of insulin. *Bio-Medical Materials and Engineering*, 22(1):171–178, 2012.
- [78] Sophie Turban and Eric Hajduch. Protein kinase c isoforms: mediators of reactive lipid metabolites in the development of insulin resistance. *FEBS letters*, 585(2):269–274, 2011.
- [79] Huixin Wang, Vyomesh Patel, Hiroshi Miyazaki, J Silvio Gutkind, and W Andrew Yeudall. Role for eps8 in squamous carcinogenesis. *Carcinogenesis*, 30(1):165–174, 2009.
- [80] Eileen L Whiteman, Han Cho, and Morris J Birnbaum. Role of akt/protein kinase b in metabolism. *Trends in Endocrinology & Metabolism*, 13(10):444–451, 2002.
- [81] Christopher G Williams, Athar N Malik, Tae Kyun Kim, Paul N Manson, and Jennifer H Elisseeff. Variable cytocompatibility of six cell lines with photoinitiators used for polymerizing hydrogels and cell encapsulation. *Biomaterials*, 26(11):1211–1218, 2005.
- [82] Gareth R Williams, Nicholas P Chatterton, Tahir Nazir, Deng-Guang Yu, Li-Min Zhu, and Christopher J Branford-White. Electrospun nanofibers in drug delivery: recent developments and perspectives. *Therapeutic Delivery*, 3(4):515–533, 2012.
- [83] Camile B Woitiski, Ronald J Neufeld, Francisco Veiga, Rui A Carvalho, and Isabel V Figueiredo. Pharmacological effect of orally delivered insulin facilitated by multilayered stable nanoparticles. *European Journal of Pharmaceutical Sciences*, 41(3):556–563, 2010.

- [84] Jinshyun R Wu-Wong, Cathleen E Berg, Jiahong Wang, William J Chiou, and Brian Fissel. Endothelin stimulates glucose uptake and glut4 translocation via activation of endothelin eta receptor in 3t3-l1 adipocytes. *Journal of Biological Chemistry*, 274(12):8103–8110, 1999.
- [85] Stephan Wullschleger, Robbie Loewith, and Michael N Hall. Tor signaling in growth and metabolism. *Cell*, 124(3):471–484, 2006.
- [86] Xiang Yuan Xiong, Yu Ping Li, Zi Ling Li, Chun Li Zhou, Kam Chiu Tam, Zhi Yong Liu, and Guo Xiu Xie. Vesicles from pluronic/poly (lactic acid) block copolymers as new carriers for oral insulin delivery. *Journal of controlled release*, 120(1):11–17, 2007.
- [87] Hui-Bi Xu, Kai-Xun Huang, Yu-Shan Zhu, Qiu-Hua Gao, Qing-Zhi Wu, Wei-Qun Tian, Xi-Qun Sheng, Ze-Xian Chen, and Zhong-Hong Gao. Hypoglycaemic effect of a novel insulin buccal formulation on rabbits. *Pharmacological research*, 46(5):459–467, 2002.
- [88] Leyuan Xu, Qianming Bai, Daniel Rodriguez-Agudo, Phillip B Hylemon, Douglas M Heuman, William M Pandak, and Shunlin Ren. Regulation of hepatocyte lipid metabolism and inflammatory response by 25-hydroxycholesterol and 25-hydroxycholesterol-3-sulfate. *lipids*, 45(9):821–832, 2010.
- [89] Leyuan Xu, Shanwei Shen, Yongjie Ma, Jin Koung Kim, Daniel Rodriguez-Agudo, Douglas M Heuman, Phillip B Hylemon, William M Pandak, and Shunlin Ren. 25-hydroxycholesterol-3-sulfate attenuates inflammatory response via ppar γ signaling in human thp-1 macrophages. *American Journal of Physiology-Endocrinology And Metabolism*, 302(7):E788–E799, 2012.
- [90] Elizabeth Yeh, Melissa Cunningham, Hugh Arnold, Dawn Chasse, Teresa Monteith, Giovanni Ivaldi, William C Hahn, P Todd Stukenberg, Shirish Shenolikar, Takafumi Uchida, et al. A signalling pathway controlling c-myc degradation that impacts oncogenic transformation of human cells. *Nature cell biology*, 6(4):308–318, 2004.

- [91] Quan Yuan, Yao Fu, Weiyuan John Kao, Damir Janigro, and Hu Yang. Transbuccal delivery of cns therapeutic nanoparticles: Synthesis, characterization, and in vitro permeation studies. *ACS chemical neuroscience*, 2(11):676–683, 2011.
- [92] Jodi L Zilinski and Weiyuan John Kao. Tissue adhesiveness and host response of in situ photopolymerizable interpenetrating networks containing methylprednisolone acetate. *Journal of Biomedical Materials Research Part A*, 68(2):392–400, 2004.

Appendix A

Statistical analysis of the experimental data

Figure 2.1 eosin Y

One Way Analysis of Variance

Data source: Data 1 in Fig.1 eosinY

Normality Test (Shapiro-Wilk) Failed (P < 0.050)

Equal Variance Test: Passed (P = 0.094)

Group Name	N	Missing	Mean	Std Dev	SEM
0d	3	0	100	6.811	3.932
NA 1d	3	0	144.147	13.87	8.008
2.5ul/ml 1d	3	0	148.997	4.013	2.317
5ul/ml 1d	3	0	128.93	3.29	1.899
10ul/ml 1d	3	0	141.472	8.704	5.025
25ul/ml 1d	3	0	72.408	10.81	6.241
NA 2d	3	0	206.02	53.979	31.165
2.5ul/ml 2d	3	0	202.174	39.727	22.937
5ul/ml 2d	3	0	139.13	18.966	10.95
10ul/ml 2d	3	0	121.906	24.643	14.228
25ul/ml 2d	3	0	18.896	2.027	1.171
NA 3d	3	0	259.532	18.813	10.862
2.5ul/ml 3d	3	0	239.632	32.436	18.727
5ul/ml 3d	3	0	187.291	20.331	11.738
10ul/ml 3d	3	0	91.806	18.724	10.81
25ul/ml 3d	3	0	4.849	1.613	0.931
NA 4d	3	0	323.077	31.883	18.408
2.5ul/ml 4d	3	0	290.468	28.254	16.313
5ul/ml 4d	3	0	143.144	18.208	10.513
10ul/ml 4d	3	0	38.127	7.287	4.207
25ul/ml 4d	3	0	5.017	0.869	0.502

Source of Variation	DF	SS	MS	F	P
Between Groups	20	483604.7	24180.23	49.327	<0.001
Residual	42	20588.36	490.199		
Total	62	504193			

The differences in the mean values among the treatment groups are greater than would be expected by chance; there is a statistically significant difference (P = <0.001).

Power of performed test with alpha = 0.050: 1.000

All Pairwise Multiple Comparison Procedures (Holm-Sidak method):

Overall significance level = 0.05

Comparisons for factor:

Comparison	Diff of Me t	P	P<0.050
------------	--------------	---	---------

NA 4d vs. 25ul/ml 3d	318.227	17.603	<0.001	Yes
NA 4d vs. 25ul/ml 4d	318.06	17.594	<0.001	Yes
NA 4d vs. 25ul/ml 2d	304.181	16.826	<0.001	Yes
2.5ul/ml 4d vs. 25ul/ml 3d	285.619	15.8	<0.001	Yes
2.5ul/ml 4d vs. 25ul/ml 4d	285.452	15.79	<0.001	Yes
NA 4d vs. 10ul/ml 4d	284.95	15.763	<0.001	Yes
2.5ul/ml 4d vs. 25ul/ml 2d	271.572	15.023	<0.001	Yes
NA 3d vs. 25ul/ml 3d	254.682	14.088	<0.001	Yes
NA 3d vs. 25ul/ml 4d	254.515	14.079	<0.001	Yes
2.5ul/ml 4d vs. 10ul/ml 4d	252.341	13.959	<0.001	Yes
NA 4d vs. 25ul/ml 1d	250.669	13.866	<0.001	Yes
NA 3d vs. 25ul/ml 2d	240.635	13.311	<0.001	Yes
2.5ul/ml 3d vs. 25ul/ml 3d	234.783	12.987	<0.001	Yes
2.5ul/ml 3d vs. 25ul/ml 4d	234.615	12.978	<0.001	Yes
NA 4d vs. 10ul/ml 3d	231.271	12.793	<0.001	Yes
NA 4d vs. 0d	223.077	12.34	<0.001	Yes
NA 3d vs. 10ul/ml 4d	221.405	12.247	<0.001	Yes
2.5ul/ml 3d vs. 25ul/ml 2d	220.736	12.21	<0.001	Yes
2.5ul/ml 4d vs. 25ul/ml 1d	218.06	12.062	<0.001	Yes
2.5ul/ml 3d vs. 10ul/ml 4d	201.505	11.147	<0.001	Yes
NA 4d vs. 10ul/ml 2d	201.171	11.128	<0.001	Yes
NA 2d vs. 25ul/ml 3d	201.171	11.128	<0.001	Yes
NA 2d vs. 25ul/ml 4d	201.003	11.119	<0.001	Yes
2.5ul/ml 4d vs. 10ul/ml 3d	198.662	10.989	<0.001	Yes
2.5ul/ml 2d vs. 25ul/ml 3d	197.324	10.915	<0.001	Yes
2.5ul/ml 2d vs. 25ul/ml 4d	197.157	10.906	<0.001	Yes
NA 4d vs. 5ul/ml 1d	194.147	10.74	<0.001	Yes
2.5ul/ml 4d vs. 0d	190.468	10.536	<0.001	Yes
NA 3d vs. 25ul/ml 1d	187.124	10.351	<0.001	Yes
NA 2d vs. 25ul/ml 2d	187.124	10.351	<0.001	Yes
NA 4d vs. 5ul/ml 2d	183.946	10.175	<0.001	Yes
2.5ul/ml 2d vs. 25ul/ml 2d	183.278	10.138	<0.001	Yes
5ul/ml 3d vs. 25ul/ml 3d	182.441	10.092	<0.001	Yes
5ul/ml 3d vs. 25ul/ml 4d	182.274	10.083	<0.001	Yes
NA 4d vs. 10ul/ml 1d	181.605	10.046	<0.001	Yes
NA 4d vs. 5ul/ml 4d	179.933	9.953	<0.001	Yes
NA 4d vs. NA 1d	178.93	9.898	<0.001	Yes
NA 4d vs. 2.5ul/ml 1d	174.08	9.63	<0.001	Yes
2.5ul/ml 4d vs. 10ul/ml 2d	168.562	9.324	<0.001	Yes
5ul/ml 3d vs. 25ul/ml 2d	168.395	9.315	<0.001	Yes
NA 2d vs. 10ul/ml 4d	167.893	9.287	<0.001	Yes
NA 3d vs. 10ul/ml 3d	167.726	9.278	<0.001	Yes
2.5ul/ml 3d vs. 25ul/ml 1d	167.224	9.25	<0.001	Yes
2.5ul/ml 2d vs. 10ul/ml 4d	164.047	9.075	<0.001	Yes
2.5ul/ml 4d vs. 5ul/ml 1d	161.538	8.936	<0.001	Yes
NA 3d vs. 0d	159.532	8.825	<0.001	Yes
2.5ul/ml 4d vs. 5ul/ml 2d	151.338	8.372	<0.001	Yes
5ul/ml 3d vs. 10ul/ml 4d	149.164	8.251	<0.001	Yes
2.5ul/ml 4d vs. 10ul/ml 1d	148.997	8.242	<0.001	Yes

2.5ul/ml 3d vs. 10ul/ml 3d	147.826	8.177 <0.001	Yes
2.5ul/ml 4d vs. 5ul/ml 4d	147.324	8.15 <0.001	Yes
2.5ul/ml 4d vs. NA 1d	146.321	8.094 <0.001	Yes
2.5ul/ml 1d vs. 25ul/ml 3d	144.147	7.974 <0.001	Yes
2.5ul/ml 1d vs. 25ul/ml 4d	143.98	7.965 <0.001	Yes
2.5ul/ml 4d vs. 2.5ul/ml 1d	141.472	7.826 <0.001	Yes
2.5ul/ml 3d vs. 0d	139.632	7.724 <0.001	Yes
NA 1d vs. 25ul/ml 3d	139.298	7.706 <0.001	Yes
NA 1d vs. 25ul/ml 4d	139.13	7.696 <0.001	Yes
5ul/ml 4d vs. 25ul/ml 3d	138.294	7.65 <0.001	Yes
5ul/ml 4d vs. 25ul/ml 4d	138.127	7.641 <0.001	Yes
NA 3d vs. 10ul/ml 2d	137.625	7.613 <0.001	Yes
10ul/ml 1d vs. 25ul/ml 3d	136.622	7.558 <0.001	Yes
10ul/ml 1d vs. 25ul/ml 4d	136.455	7.548 <0.001	Yes
NA 4d vs. 5ul/ml 3d	135.786	7.511 <0.001	Yes
5ul/ml 2d vs. 25ul/ml 3d	134.281	7.428 <0.001	Yes
5ul/ml 2d vs. 25ul/ml 4d	134.114	7.419 <0.001	Yes
NA 2d vs. 25ul/ml 1d	133.612	7.391 <0.001	Yes
NA 3d vs. 5ul/ml 1d	130.602	7.225 <0.001	Yes
2.5ul/ml 1d vs. 25ul/ml 2d	130.1	7.197 <0.001	Yes
2.5ul/ml 2d vs. 25ul/ml 1d	129.766	7.178 <0.001	Yes
NA 1d vs. 25ul/ml 2d	125.251	6.929 <0.001	Yes
5ul/ml 4d vs. 25ul/ml 2d	124.247	6.873 <0.001	Yes
5ul/ml 1d vs. 25ul/ml 3d	124.08	6.864 <0.001	Yes
5ul/ml 1d vs. 25ul/ml 4d	123.913	6.855 <0.001	Yes
10ul/ml 1d vs. 25ul/ml 2d	122.575	6.781 <0.001	Yes
NA 4d vs. 2.5ul/ml 2d	120.903	6.688 <0.001	Yes
NA 3d vs. 5ul/ml 2d	120.401	6.66 <0.001	Yes
5ul/ml 2d vs. 25ul/ml 2d	120.234	6.651 <0.001	Yes
NA 3d vs. 10ul/ml 1d	118.06	6.531 <0.001	Yes
2.5ul/ml 3d vs. 10ul/ml 2d	117.726	6.512 <0.001	Yes
NA 4d vs. NA 2d	117.057	6.475 <0.001	Yes
10ul/ml 2d vs. 25ul/ml 3d	117.057	6.475 <0.001	Yes
10ul/ml 2d vs. 25ul/ml 4d	116.89	6.466 <0.001	Yes
NA 3d vs. 5ul/ml 4d	116.388	6.438 <0.001	Yes
NA 3d vs. NA 1d	115.385	6.383 <0.001	Yes
5ul/ml 3d vs. 25ul/ml 1d	114.883	6.355 <0.001	Yes
NA 2d vs. 10ul/ml 3d	114.214	6.318 <0.001	Yes
2.5ul/ml 1d vs. 10ul/ml 4d	110.87	6.133 <0.001	Yes
2.5ul/ml 3d vs. 5ul/ml 1d	110.702	6.124 <0.001	Yes
NA 3d vs. 2.5ul/ml 1d	110.535	6.114 <0.001	Yes
2.5ul/ml 2d vs. 10ul/ml 3d	110.368	6.105 <0.001	Yes
5ul/ml 1d vs. 25ul/ml 2d	110.033	6.087 <0.001	Yes
NA 1d vs. 10ul/ml 4d	106.02	5.865 <0.001	Yes
NA 2d vs. 0d	106.02	5.865 <0.001	Yes
5ul/ml 4d vs. 10ul/ml 4d	105.017	5.809 <0.001	Yes
10ul/ml 1d vs. 10ul/ml 4d	103.344	5.717 <0.001	Yes
2.5ul/ml 4d vs. 5ul/ml 3d	103.177	5.707 <0.001	Yes
10ul/ml 2d vs. 25ul/ml 2d	103.01	5.698 <0.001	Yes

2.5ul/ml 2d vs. 0d	102.174	5.652	<0.001	Yes
5ul/ml 2d vs. 10ul/ml 4d	101.003	5.587	<0.001	Yes
2.5ul/ml 3d vs. 5ul/ml 2d	100.502	5.559	<0.001	Yes
2.5ul/ml 3d vs. 10ul/ml 1d	98.161	5.43	<0.001	Yes
2.5ul/ml 3d vs. 5ul/ml 4d	96.488	5.337	<0.001	Yes
5ul/ml 3d vs. 10ul/ml 3d	95.485	5.282	<0.001	Yes
2.5ul/ml 3d vs. NA 1d	95.485	5.282	<0.001	Yes
0d vs. 25ul/ml 3d	95.151	5.263	<0.001	Yes
0d vs. 25ul/ml 4d	94.983	5.254	<0.001	Yes
5ul/ml 1d vs. 10ul/ml 4d	90.803	5.023	0.001	Yes
2.5ul/ml 3d vs. 2.5ul/ml 1d	90.635	5.014	0.001	Yes
2.5ul/ml 4d vs. 2.5ul/ml 2d	88.294	4.884	0.002	Yes
5ul/ml 3d vs. 0d	87.291	4.829	0.002	Yes
10ul/ml 3d vs. 25ul/ml 3d	86.957	4.81	0.002	Yes
10ul/ml 3d vs. 25ul/ml 4d	86.789	4.801	0.002	Yes
2.5ul/ml 4d vs. NA 2d	84.448	4.671	0.003	Yes
NA 2d vs. 10ul/ml 2d	84.114	4.653	0.003	Yes
10ul/ml 2d vs. 10ul/ml 4d	83.779	4.634	0.003	Yes
NA 4d vs. 2.5ul/ml 3d	83.445	4.616	0.003	Yes
0d vs. 25ul/ml 2d	81.104	4.486	0.005	Yes
2.5ul/ml 2d vs. 10ul/ml 2d	80.268	4.44	0.006	Yes
NA 2d vs. 5ul/ml 1d	77.09	4.264	0.01	Yes
2.5ul/ml 1d vs. 25ul/ml 1d	76.589	4.237	0.011	Yes
2.5ul/ml 2d vs. 5ul/ml 1d	73.244	4.052	0.019	Yes
10ul/ml 3d vs. 25ul/ml 2d	72.91	4.033	0.02	Yes
NA 3d vs. 5ul/ml 3d	72.241	3.996	0.022	Yes
NA 1d vs. 25ul/ml 1d	71.739	3.968	0.024	Yes
5ul/ml 4d vs. 25ul/ml 1d	70.736	3.913	0.027	Yes
10ul/ml 1d vs. 25ul/ml 1d	69.064	3.82	0.036	Yes
25ul/ml 1d vs. 25ul/ml 3d	67.559	3.737	0.045	Yes
25ul/ml 1d vs. 25ul/ml 4d	67.391	3.728	0.046	Yes
NA 2d vs. 5ul/ml 2d	66.89	3.7	0.049	Yes
5ul/ml 2d vs. 25ul/ml 1d	66.722	3.691	0.05	Yes
5ul/ml 3d vs. 10ul/ml 2d	65.385	3.617	0.061	No
NA 2d vs. 10ul/ml 1d	64.548	3.571	0.068	No
NA 4d vs. NA 3d	63.545	3.515	0.079	No
2.5ul/ml 2d vs. 5ul/ml 2d	63.043	3.487	0.084	No
NA 2d vs. 5ul/ml 4d	62.876	3.478	0.085	No
NA 2d vs. NA 1d	61.873	3.423	0.098	No
0d vs. 10ul/ml 4d	61.873	3.423	0.097	No
2.5ul/ml 2d vs. 10ul/ml 1d	60.702	3.358	0.114	No
2.5ul/ml 2d vs. 5ul/ml 4d	59.03	3.265	0.144	No
5ul/ml 3d vs. 5ul/ml 1d	58.361	3.228	0.156	No
2.5ul/ml 2d vs. NA 1d	58.027	3.21	0.161	No
NA 3d vs. 2.5ul/ml 2d	57.358	3.173	0.175	No
2.5ul/ml 1d vs. 10ul/ml 3d	57.191	3.164	0.177	No
NA 2d vs. 2.5ul/ml 1d	57.023	3.154	0.178	No
5ul/ml 1d vs. 25ul/ml 1d	56.522	3.127	0.188	No
10ul/ml 3d vs. 10ul/ml 4d	53.679	2.969	0.27	No

NA 3d vs. NA 2d	53.512	2.96	0.273 No
25ul/ml 1d vs. 25ul/ml 2d	53.512	2.96	0.269 No
2.5ul/ml 2d vs. 2.5ul/ml 1d	53.177	2.942	0.277 No
NA 1d vs. 10ul/ml 3d	52.341	2.895	0.303 No
2.5ul/ml 3d vs. 5ul/ml 3d	52.341	2.895	0.298 No
5ul/ml 4d vs. 10ul/ml 3d	51.338	2.84	0.332 No
2.5ul/ml 4d vs. 2.5ul/ml 3d	50.836	2.812	0.347 No
10ul/ml 1d vs. 10ul/ml 3d	49.666	2.747	0.391 No
10ul/ml 2d vs. 25ul/ml 1d	49.498	2.738	0.393 No
2.5ul/ml 1d vs. 0d	48.997	2.71	0.409 No
5ul/ml 3d vs. 5ul/ml 2d	48.161	2.664	0.441 No
5ul/ml 2d vs. 10ul/ml 3d	47.324	2.618	0.473 No
5ul/ml 3d vs. 10ul/ml 1d	45.819	2.535	0.539 No
5ul/ml 3d vs. 5ul/ml 4d	44.147	2.442	0.615 No
NA 1d vs. 0d	44.147	2.442	0.607 No
5ul/ml 3d vs. NA 1d	43.144	2.387	0.649 No
5ul/ml 4d vs. 0d	43.144	2.387	0.641 No
10ul/ml 1d vs. 0d	41.472	2.294	0.714 No
5ul/ml 2d vs. 0d	39.13	2.165	0.809 No
5ul/ml 3d vs. 2.5ul/ml 1d	38.294	2.118	0.835 No
2.5ul/ml 3d vs. 2.5ul/ml 2d	37.458	2.072	0.858 No
5ul/ml 1d vs. 10ul/ml 3d	37.124	2.054	0.863 No
25ul/ml 1d vs. 10ul/ml 4d	34.281	1.896	0.936 No
2.5ul/ml 3d vs. NA 2d	33.612	1.859	0.945 No
10ul/ml 4d vs. 25ul/ml 3d	33.278	1.841	0.947 No
10ul/ml 4d vs. 25ul/ml 4d	33.11	1.832	0.946 No
NA 4d vs. 2.5ul/ml 4d	32.609	1.804	0.951 No
2.5ul/ml 4d vs. NA 3d	30.936	1.711	0.972 No
10ul/ml 2d vs. 10ul/ml 3d	30.1	1.665	0.978 No
5ul/ml 1d vs. 0d	28.93	1.6	0.985 No
0d vs. 25ul/ml 1d	27.592	1.526	0.991 No
2.5ul/ml 1d vs. 10ul/ml 2d	27.09	1.499	0.992 No
NA 1d vs. 10ul/ml 2d	22.241	1.23	1 No
10ul/ml 2d vs. 0d	21.906	1.212	1 No
5ul/ml 4d vs. 10ul/ml 2d	21.237	1.175	1 No
2.5ul/ml 1d vs. 5ul/ml 1d	20.067	1.11	1 No
NA 3d vs. 2.5ul/ml 3d	19.9	1.101	1 No
10ul/ml 1d vs. 10ul/ml 2d	19.565	1.082	1 No
10ul/ml 3d vs. 25ul/ml 1d	19.398	1.073	1 No
10ul/ml 4d vs. 25ul/ml 2d	19.231	1.064	1 No
NA 2d vs. 5ul/ml 3d	18.729	1.036	1 No
5ul/ml 2d vs. 10ul/ml 2d	17.224	0.953	1 No
NA 1d vs. 5ul/ml 1d	15.217	0.842	1 No
2.5ul/ml 2d vs. 5ul/ml 3d	14.883	0.823	1 No
5ul/ml 4d vs. 5ul/ml 1d	14.214	0.786	1 No
25ul/ml 2d vs. 25ul/ml 3d	14.047	0.777	1 No
25ul/ml 2d vs. 25ul/ml 4d	13.88	0.768	1 No
10ul/ml 1d vs. 5ul/ml 1d	12.542	0.694	1 No
5ul/ml 2d vs. 5ul/ml 1d	10.201	0.564	1 No

2.5ul/ml 1d vs. 5ul/ml 2d	9.866	0.546	1 No
0d vs. 10ul/ml 3d	8.194	0.453	1 No
2.5ul/ml 1d vs. 10ul/ml 1d	7.525	0.416	1 No
5ul/ml 1d vs. 10ul/ml 2d	7.023	0.389	1 No
2.5ul/ml 1d vs. 5ul/ml 4d	5.853	0.324	1 No
NA 1d vs. 5ul/ml 2d	5.017	0.278	1 No
2.5ul/ml 1d vs. NA 1d	4.849	0.268	1 No
5ul/ml 4d vs. 5ul/ml 2d	4.013	0.222	1 No
NA 2d vs. 2.5ul/ml 2d	3.846	0.213	1 No
NA 1d vs. 10ul/ml 1d	2.676	0.148	1 No
10ul/ml 1d vs. 5ul/ml 2d	2.341	0.13	1 No
5ul/ml 4d vs. 10ul/ml 1d	1.672	0.0925	1 No
NA 1d vs. 5ul/ml 4d	1.003	0.0555	0.998 No
25ul/ml 4d vs. 25ul/ml 3d	1.67E-01	9.25E-03	0.993 No

Figure 2.2 Irgacure2959

One Way Analysis of Variance

Data source: Data 1 in Irgacure 2959 viability

Normality Test (Shapiro-Wilk) Failed (P < 0.050)

Equal Variance Test: Passed (P = 0.147)

Group Name	N	Missing	Mean	Std Dev	SEM
0d	3	0	100	6.811	3.932
NA 1d	3	0	141.472	6.56	3.788
1mg/ml 1d	3	0	144.649	13.76	7.944
2mg/ml 1d	3	0	96.488	7.396	4.27
5mg/ml 1d	3	0	8.528	1.003	0.579
10mg/ml 1d	3	0	5.518	2.299	1.327
NA 2d	3	0	207.191	16.147	9.323
1mg/ml 2d	3	0	208.696	9.291	5.364
2mg/ml 2d	3	0	148.662	21.132	12.2
5mg/ml 2d	3	0	2.843	0.766	0.442
10mg/ml 2d	3	0	5.351	2.262	1.306
NA 3d	3	0	265.552	14.491	8.366
1mg/ml 3d	3	0	236.789	22.17	12.8
2mg/ml 3d	3	0	193.478	7.206	4.16
5mg/ml 3d	3	0	7.358	1.263	0.729
10mg/ml 3d	3	0	9.699	1.159	0.669
NA 4d	3	0	350.334	17.668	10.201
1mg/ml 4d	3	0	348.328	53.584	30.936
2mg/ml 4d	3	0	220.736	14.618	8.439
5mg/ml 4d	3	0	5.184	2.262	1.306
10mg/ml 4d	3	0	2.508	2.508	1.448

Source of Variation	DF	SS	MS	F	P
Between Groups	20	829222.5	41461.13	164.16	<0.001
Residual	42	10607.77	252.566		
Total	62	839830.3			

The differences in the mean values among the treatment groups are greater than would be expected by chance; there is a statistically significant difference (P = <0.001).

Power of performed test with alpha = 0.050: 1.000

All Pairwise Multiple Comparison Procedures (Holm-Sidak method):
Overall significance level = 0.05

Comparisons for factor:

Comparison	Diff of Me t	P	P<0.050
------------	--------------	---	---------

NA 4d vs. 10mg/ml 4d	347.826	26.805	<0.001	Yes
NA 4d vs. 5mg/ml 2d	347.492	26.78	<0.001	Yes
1mg/ml 4d vs. 10mg/ml 4d	345.819	26.651	<0.001	Yes
1mg/ml 4d vs. 5mg/ml 2d	345.485	26.625	<0.001	Yes
NA 4d vs. 5mg/ml 4d	345.151	26.599	<0.001	Yes
NA 4d vs. 10mg/ml 2d	344.983	26.586	<0.001	Yes
NA 4d vs. 10mg/ml 1d	344.816	26.573	<0.001	Yes
1mg/ml 4d vs. 5mg/ml 4d	343.144	26.444	<0.001	Yes
NA 4d vs. 5mg/ml 3d	342.977	26.432	<0.001	Yes
1mg/ml 4d vs. 10mg/ml 2d	342.977	26.432	<0.001	Yes
1mg/ml 4d vs. 10mg/ml 1d	342.809	26.419	<0.001	Yes
NA 4d vs. 5mg/ml 1d	341.806	26.341	<0.001	Yes
1mg/ml 4d vs. 5mg/ml 3d	340.97	26.277	<0.001	Yes
NA 4d vs. 10mg/ml 3d	340.635	26.251	<0.001	Yes
1mg/ml 4d vs. 5mg/ml 1d	339.799	26.187	<0.001	Yes
1mg/ml 4d vs. 10mg/ml 3d	338.629	26.096	<0.001	Yes
NA 3d vs. 10mg/ml 4d	263.043	20.271	<0.001	Yes
NA 3d vs. 5mg/ml 2d	262.709	20.246	<0.001	Yes
NA 3d vs. 5mg/ml 4d	260.368	20.065	<0.001	Yes
NA 3d vs. 10mg/ml 2d	260.201	20.052	<0.001	Yes
NA 3d vs. 10mg/ml 1d	260.033	20.04	<0.001	Yes
NA 3d vs. 5mg/ml 3d	258.194	19.898	<0.001	Yes
NA 3d vs. 5mg/ml 1d	257.023	19.808	<0.001	Yes
NA 3d vs. 10mg/ml 3d	255.853	19.717	<0.001	Yes
NA 4d vs. 2mg/ml 1d	253.846	19.563	<0.001	Yes
1mg/ml 4d vs. 2mg/ml 1d	251.839	19.408	<0.001	Yes
NA 4d vs. 0d	250.334	19.292	<0.001	Yes
1mg/ml 4d vs. 0d	248.328	19.137	<0.001	Yes
1mg/ml 3d vs. 10mg/ml 4d	234.281	18.055	<0.001	Yes
1mg/ml 3d vs. 5mg/ml 2d	233.946	18.029	<0.001	Yes
1mg/ml 3d vs. 5mg/ml 4d	231.605	17.849	<0.001	Yes
1mg/ml 3d vs. 10mg/ml 2d	231.438	17.836	<0.001	Yes
1mg/ml 3d vs. 10mg/ml 1d	231.271	17.823	<0.001	Yes
1mg/ml 3d vs. 5mg/ml 3d	229.431	17.681	<0.001	Yes
1mg/ml 3d vs. 5mg/ml 1d	228.261	17.591	<0.001	Yes
1mg/ml 3d vs. 10mg/ml 3d	227.09	17.501	<0.001	Yes
2mg/ml 4d vs. 10mg/ml 4d	218.227	16.818	<0.001	Yes
2mg/ml 4d vs. 5mg/ml 2d	217.893	16.792	<0.001	Yes
2mg/ml 4d vs. 5mg/ml 4d	215.552	16.612	<0.001	Yes
2mg/ml 4d vs. 10mg/ml 2d	215.385	16.599	<0.001	Yes
2mg/ml 4d vs. 10mg/ml 1d	215.217	16.586	<0.001	Yes
2mg/ml 4d vs. 5mg/ml 3d	213.378	16.444	<0.001	Yes
2mg/ml 4d vs. 5mg/ml 1d	212.207	16.354	<0.001	Yes
2mg/ml 4d vs. 10mg/ml 3d	211.037	16.264	<0.001	Yes
NA 4d vs. NA 1d	208.863	16.096	<0.001	Yes
1mg/ml 4d vs. NA 1d	206.856	15.941	<0.001	Yes
1mg/ml 2d vs. 10mg/ml 4d	206.187	15.89	<0.001	Yes
1mg/ml 2d vs. 5mg/ml 2d	205.853	15.864	<0.001	Yes
NA 4d vs. 1mg/ml 1d	205.686	15.851	<0.001	Yes

NA 2d vs. 10mg/ml 4d	204.682	15.774	<0.001	Yes
NA 2d vs. 5mg/ml 2d	204.348	15.748	<0.001	Yes
1mg/ml 4d vs. 1mg/ml 1d	203.679	15.697	<0.001	Yes
1mg/ml 2d vs. 5mg/ml 4d	203.512	15.684	<0.001	Yes
1mg/ml 2d vs. 10mg/ml 2d	203.344	15.671	<0.001	Yes
1mg/ml 2d vs. 10mg/ml 1d	203.177	15.658	<0.001	Yes
NA 2d vs. 5mg/ml 4d	202.007	15.568	<0.001	Yes
NA 2d vs. 10mg/ml 2d	201.839	15.555	<0.001	Yes
NA 4d vs. 2mg/ml 2d	201.672	15.542	<0.001	Yes
NA 2d vs. 10mg/ml 1d	201.672	15.542	<0.001	Yes
1mg/ml 2d vs. 5mg/ml 3d	201.338	15.516	<0.001	Yes
1mg/ml 2d vs. 5mg/ml 1d	200.167	15.426	<0.001	Yes
NA 2d vs. 5mg/ml 3d	199.833	15.4	<0.001	Yes
1mg/ml 4d vs. 2mg/ml 2d	199.666	15.387	<0.001	Yes
1mg/ml 2d vs. 10mg/ml 3d	198.997	15.336	<0.001	Yes
NA 2d vs. 5mg/ml 1d	198.662	15.31	<0.001	Yes
NA 2d vs. 10mg/ml 3d	197.492	15.22	<0.001	Yes
2mg/ml 3d vs. 10mg/ml 4d	190.97	14.717	<0.001	Yes
2mg/ml 3d vs. 5mg/ml 2d	190.635	14.691	<0.001	Yes
2mg/ml 3d vs. 5mg/ml 4d	188.294	14.511	<0.001	Yes
2mg/ml 3d vs. 10mg/ml 2d	188.127	14.498	<0.001	Yes
2mg/ml 3d vs. 10mg/ml 1d	187.96	14.485	<0.001	Yes
2mg/ml 3d vs. 5mg/ml 3d	186.12	14.343	<0.001	Yes
2mg/ml 3d vs. 5mg/ml 1d	184.95	14.253	<0.001	Yes
2mg/ml 3d vs. 10mg/ml 3d	183.779	14.163	<0.001	Yes
NA 3d vs. 2mg/ml 1d	169.064	13.029	<0.001	Yes
NA 3d vs. 0d	165.552	12.758	<0.001	Yes
NA 4d vs. 2mg/ml 3d	156.856	12.088	<0.001	Yes
1mg/ml 4d vs. 2mg/ml 3d	154.849	11.934	<0.001	Yes
2mg/ml 2d vs. 10mg/ml 4d	146.154	11.263	<0.001	Yes
2mg/ml 2d vs. 5mg/ml 2d	145.819	11.238	<0.001	Yes
2mg/ml 2d vs. 5mg/ml 4d	143.478	11.057	<0.001	Yes
2mg/ml 2d vs. 10mg/ml 2d	143.311	11.044	<0.001	Yes
NA 4d vs. NA 2d	143.144	11.031	<0.001	Yes
2mg/ml 2d vs. 10mg/ml 1d	143.144	11.031	<0.001	Yes
1mg/ml 1d vs. 10mg/ml 4d	142.14	10.954	<0.001	Yes
1mg/ml 1d vs. 5mg/ml 2d	141.806	10.928	<0.001	Yes
NA 4d vs. 1mg/ml 2d	141.639	10.915	<0.001	Yes
2mg/ml 2d vs. 5mg/ml 3d	141.304	10.89	<0.001	Yes
1mg/ml 4d vs. NA 2d	141.137	10.877	<0.001	Yes
1mg/ml 3d vs. 2mg/ml 1d	140.301	10.812	<0.001	Yes
2mg/ml 2d vs. 5mg/ml 1d	140.134	10.799	<0.001	Yes
1mg/ml 4d vs. 1mg/ml 2d	139.632	10.761	<0.001	Yes
1mg/ml 1d vs. 5mg/ml 4d	139.465	10.748	<0.001	Yes
1mg/ml 1d vs. 10mg/ml 2d	139.298	10.735	<0.001	Yes
1mg/ml 1d vs. 10mg/ml 1d	139.13	10.722	<0.001	Yes
NA 1d vs. 10mg/ml 4d	138.963	10.709	<0.001	Yes
2mg/ml 2d vs. 10mg/ml 3d	138.963	10.709	<0.001	Yes
NA 1d vs. 5mg/ml 2d	138.629	10.683	<0.001	Yes

1mg/ml 1d vs. 5mg/ml 3d	137.291	10.58	<0.001	Yes
1mg/ml 3d vs. 0d	136.789	10.542	<0.001	Yes
NA 1d vs. 5mg/ml 4d	136.288	10.503	<0.001	Yes
NA 1d vs. 10mg/ml 2d	136.12	10.49	<0.001	Yes
1mg/ml 1d vs. 5mg/ml 1d	136.12	10.49	<0.001	Yes
NA 1d vs. 10mg/ml 1d	135.953	10.477	<0.001	Yes
1mg/ml 1d vs. 10mg/ml 3d	134.95	10.4	<0.001	Yes
NA 1d vs. 5mg/ml 3d	134.114	10.335	<0.001	Yes
NA 1d vs. 5mg/ml 1d	132.943	10.245	<0.001	Yes
NA 1d vs. 10mg/ml 3d	131.773	10.155	<0.001	Yes
NA 4d vs. 2mg/ml 4d	129.599	9.988	<0.001	Yes
1mg/ml 4d vs. 2mg/ml 4d	127.592	9.833	<0.001	Yes
2mg/ml 4d vs. 2mg/ml 1d	124.247	9.575	<0.001	Yes
NA 3d vs. NA 1d	124.08	9.562	<0.001	Yes
NA 3d vs. 1mg/ml 1d	120.903	9.317	<0.001	Yes
2mg/ml 4d vs. 0d	120.736	9.305	<0.001	Yes
NA 3d vs. 2mg/ml 2d	116.89	9.008	<0.001	Yes
NA 4d vs. 1mg/ml 3d	113.545	8.75	<0.001	Yes
1mg/ml 2d vs. 2mg/ml 1d	112.207	8.647	<0.001	Yes
1mg/ml 4d vs. 1mg/ml 3d	111.538	8.596	<0.001	Yes
NA 2d vs. 2mg/ml 1d	110.702	8.531	<0.001	Yes
1mg/ml 2d vs. 0d	108.696	8.377	<0.001	Yes
NA 2d vs. 0d	107.191	8.261	<0.001	Yes
0d vs. 10mg/ml 4d	97.492	7.513	<0.001	Yes
0d vs. 5mg/ml 2d	97.157	7.487	<0.001	Yes
2mg/ml 3d vs. 2mg/ml 1d	96.99	7.475	<0.001	Yes
1mg/ml 3d vs. NA 1d	95.318	7.346	<0.001	Yes
0d vs. 5mg/ml 4d	94.816	7.307	<0.001	Yes
0d vs. 10mg/ml 2d	94.649	7.294	<0.001	Yes
0d vs. 10mg/ml 1d	94.482	7.281	<0.001	Yes
2mg/ml 1d vs. 10mg/ml 4d	93.98	7.243	<0.001	Yes
2mg/ml 1d vs. 5mg/ml 2d	93.645	7.217	<0.001	Yes
2mg/ml 3d vs. 0d	93.478	7.204	<0.001	Yes
0d vs. 5mg/ml 3d	92.642	7.139	<0.001	Yes
1mg/ml 3d vs. 1mg/ml 1d	92.14	7.101	<0.001	Yes
0d vs. 5mg/ml 1d	91.472	7.049	<0.001	Yes
2mg/ml 1d vs. 5mg/ml 4d	91.304	7.036	<0.001	Yes
2mg/ml 1d vs. 10mg/ml 2d	91.137	7.024	<0.001	Yes
2mg/ml 1d vs. 10mg/ml 1d	90.97	7.011	<0.001	Yes
0d vs. 10mg/ml 3d	90.301	6.959	<0.001	Yes
2mg/ml 1d vs. 5mg/ml 3d	89.13	6.869	<0.001	Yes
1mg/ml 3d vs. 2mg/ml 2d	88.127	6.792	<0.001	Yes
2mg/ml 1d vs. 5mg/ml 1d	87.96	6.779	<0.001	Yes
2mg/ml 1d vs. 10mg/ml 3d	86.789	6.688	<0.001	Yes
NA 4d vs. NA 3d	84.783	6.534	<0.001	Yes
1mg/ml 4d vs. NA 3d	82.776	6.379	<0.001	Yes
2mg/ml 4d vs. NA 1d	79.264	6.109	<0.001	Yes
2mg/ml 4d vs. 1mg/ml 1d	76.087	5.864	<0.001	Yes
NA 3d vs. 2mg/ml 3d	72.074	5.554	<0.001	Yes

2mg/ml 4d vs. 2mg/ml 2d	72.074	5.554	<0.001	Yes
1mg/ml 2d vs. NA 1d	67.224	5.181	<0.001	Yes
NA 2d vs. NA 1d	65.719	5.065	<0.001	Yes
1mg/ml 2d vs. 1mg/ml 1d	64.047	4.936	<0.001	Yes
NA 2d vs. 1mg/ml 1d	62.542	4.82	0.001	Yes
1mg/ml 2d vs. 2mg/ml 2d	60.033	4.626	0.002	Yes
NA 2d vs. 2mg/ml 2d	58.528	4.511	0.003	Yes
NA 3d vs. NA 2d	58.361	4.498	0.003	Yes
NA 3d vs. 1mg/ml 2d	56.856	4.382	0.004	Yes
2mg/ml 2d vs. 2mg/ml 1d	52.174	4.021	0.013	Yes
2mg/ml 3d vs. NA 1d	52.007	4.008	0.013	Yes
2mg/ml 3d vs. 1mg/ml 1d	48.829	3.763	0.026	Yes
2mg/ml 2d vs. 0d	48.662	3.75	0.027	Yes
1mg/ml 1d vs. 2mg/ml 1d	48.161	3.712	0.03	Yes
NA 1d vs. 2mg/ml 1d	44.983	3.467	0.058	No
NA 3d vs. 2mg/ml 4d	44.816	3.454	0.059	No
2mg/ml 3d vs. 2mg/ml 2d	44.816	3.454	0.058	No
1mg/ml 1d vs. 0d	44.649	3.441	0.059	No
1mg/ml 3d vs. 2mg/ml 3d	43.311	3.338	0.077	No
NA 1d vs. 0d	41.472	3.196	0.11	No
1mg/ml 3d vs. NA 2d	29.599	2.281	0.701	No
NA 3d vs. 1mg/ml 3d	28.763	2.217	0.746	No
1mg/ml 3d vs. 1mg/ml 2d	28.094	2.165	0.779	No
2mg/ml 4d vs. 2mg/ml 3d	27.258	2.101	0.818	No
1mg/ml 3d vs. 2mg/ml 4d	16.054	1.237	1	No
1mg/ml 2d vs. 2mg/ml 3d	15.217	1.173	1	No
NA 2d vs. 2mg/ml 3d	13.712	1.057	1	No
2mg/ml 4d vs. NA 2d	13.545	1.044	1	No
2mg/ml 4d vs. 1mg/ml 2d	12.04	0.928	1	No
10mg/ml 3d vs. 10mg/ml 4d	7.191	0.554	1	No
2mg/ml 2d vs. NA 1d	7.191	0.554	1	No
10mg/ml 3d vs. 5mg/ml 2d	6.856	0.528	1	No
5mg/ml 1d vs. 10mg/ml 4d	6.02	0.464	1	No
5mg/ml 1d vs. 5mg/ml 2d	5.686	0.438	1	No
5mg/ml 3d vs. 10mg/ml 4d	4.849	0.374	1	No
5mg/ml 3d vs. 5mg/ml 2d	4.515	0.348	1	No
10mg/ml 3d vs. 5mg/ml 4d	4.515	0.348	1	No
10mg/ml 3d vs. 10mg/ml 2d	4.348	0.335	1	No
10mg/ml 3d vs. 10mg/ml 1d	4.181	0.322	1	No
2mg/ml 2d vs. 1mg/ml 1d	4.013	0.309	1	No
0d vs. 2mg/ml 1d	3.512	0.271	1	No
5mg/ml 1d vs. 5mg/ml 4d	3.344	0.258	1	No
5mg/ml 1d vs. 10mg/ml 2d	3.177	0.245	1	No
1mg/ml 1d vs. NA 1d	3.177	0.245	1	No
10mg/ml 1d vs. 10mg/ml 4d	3.01	0.232	1	No
5mg/ml 1d vs. 10mg/ml 1d	3.01	0.232	1	No
10mg/ml 2d vs. 10mg/ml 4d	2.843	0.219	1	No
10mg/ml 1d vs. 5mg/ml 2d	2.676	0.206	1	No
5mg/ml 4d vs. 10mg/ml 4d	2.676	0.206	1	No

10mg/ml 2d vs. 5mg/ml 2d	2.508	0.193	1 No
5mg/ml 4d vs. 5mg/ml 2d	2.341	0.18	1 No
10mg/ml 3d vs. 5mg/ml 3d	2.341	0.18	1 No
5mg/ml 3d vs. 5mg/ml 4d	2.174	0.168	1 No
NA 4d vs. 1mg/ml 4d	2.007	0.155	1 No
5mg/ml 3d vs. 10mg/ml 2d	2.007	0.155	1 No
5mg/ml 3d vs. 10mg/ml 1d	1.839	0.142	1 No
1mg/ml 2d vs. NA 2d	1.505	0.116	1 No
5mg/ml 1d vs. 5mg/ml 3d	1.171	0.0902	1 No
10mg/ml 3d vs. 5mg/ml 1d	1.171	0.0902	1 No
10mg/ml 1d vs. 5mg/ml 4d	0.334	0.0258	1 No
5mg/ml 2d vs. 10mg/ml 4d	0.334	0.0258	1 No
10mg/ml 1d vs. 10mg/ml 2d	0.167	0.0129	1 No
10mg/ml 2d vs. 5mg/ml 4d	1.67E-01	1.29E-02	0.99 No

Figure 2.3 DMPA

One Way Analysis of Variance

Data source: Data 1 in DMPA viability

Normality Test (Shapiro-Wilk) Failed (P < 0.050)

Equal Variance Test: Passed (P = 0.414)

Group Name	N	Missing	Mean	Std Dev	SEM
0d	3	0	100	8.822	5.093
NA 1d	3	0	144.245	6.41	3.701
0.5mg/ml 1d	3	0	2.691	1.186	0.685
1mg/ml 1d	3	0	4.634	2.883	1.665
2mg/ml 1d	3	0	4.933	0.777	0.448
5mg/ml 1d	3	0	5.082	1.698	0.98
NA 2d	3	0	211.211	7.883	4.551
0.5mg/ml 2d	3	0	4.185	1.812	1.046
1mg/ml 2d	3	0	6.278	2.497	1.442
2mg/ml 2d	3	0	5.83	1.186	0.685
5mg/ml 2d	3	0	3.737	1.37	0.791
NA 3d	3	0	274.29	13.069	7.545
0.5mg/ml 3d	3	0	4.036	0	0
1mg/ml 3d	3	0	2.541	0.518	0.299
2mg/ml 3d	3	0	1.046	1.812	1.046
5mg/ml 3d	3	0	0.598	1.036	0.598
NA 4d	3	0	386.846	32.77	18.92
0.5mg/ml 4d	3	0	2.84	1.867	1.078
1mg/ml 4d	3	0	5.082	2.55	1.472
2mg/ml 4d	3	0	4.783	0.933	0.539
5mg/ml 4d	3	0	2.242	2.055	1.186

Source of Variation	DF	SS	MS	F	P
Between Groups	20	703765.9	35188.29	502.197	<0.001
Residual	42	2942.884	70.069		
Total	62	706708.8			

The differences in the mean values among the treatment groups are greater than would be expected by chance; there is a statistically significant difference (P = <0.001).

Power of performed test with alpha = 0.050: 1.000

All Pairwise Multiple Comparison Procedures (Holm-Sidak method):
Overall significance level = 0.05

Comparisons for factor:

Comparison	Diff of Me t	P	P<0.050
------------	--------------	---	---------

NA 4d vs. 5mg/ml 3d	386.248	56.513	<0.001	Yes
NA 4d vs. 2mg/ml 3d	385.8	56.448	<0.001	Yes
NA 4d vs. 5mg/ml 4d	384.604	56.273	<0.001	Yes
NA 4d vs. 1mg/ml 3d	384.305	56.229	<0.001	Yes
NA 4d vs. 0.5mg/ml 1d	384.155	56.207	<0.001	Yes
NA 4d vs. 0.5mg/ml 4d	384.006	56.185	<0.001	Yes
NA 4d vs. 5mg/ml 2d	383.109	56.054	<0.001	Yes
NA 4d vs. 0.5mg/ml 3d	382.81	56.01	<0.001	Yes
NA 4d vs. 0.5mg/ml 2d	382.661	55.988	<0.001	Yes
NA 4d vs. 1mg/ml 1d	382.212	55.923	<0.001	Yes
NA 4d vs. 2mg/ml 4d	382.063	55.901	<0.001	Yes
NA 4d vs. 2mg/ml 1d	381.913	55.879	<0.001	Yes
NA 4d vs. 1mg/ml 4d	381.764	55.857	<0.001	Yes
NA 4d vs. 5mg/ml 1d	381.764	55.857	<0.001	Yes
NA 4d vs. 2mg/ml 2d	381.016	55.748	<0.001	Yes
NA 4d vs. 1mg/ml 2d	380.568	55.682	<0.001	Yes
NA 4d vs. 0d	286.846	41.969	<0.001	Yes
NA 3d vs. 5mg/ml 3d	273.692	40.045	<0.001	Yes
NA 3d vs. 2mg/ml 3d	273.244	39.979	<0.001	Yes
NA 3d vs. 5mg/ml 4d	272.048	39.804	<0.001	Yes
NA 3d vs. 1mg/ml 3d	271.749	39.76	<0.001	Yes
NA 3d vs. 0.5mg/ml 1d	271.599	39.739	<0.001	Yes
NA 3d vs. 0.5mg/ml 4d	271.45	39.717	<0.001	Yes
NA 3d vs. 5mg/ml 2d	270.553	39.586	<0.001	Yes
NA 3d vs. 0.5mg/ml 3d	270.254	39.542	<0.001	Yes
NA 3d vs. 0.5mg/ml 2d	270.105	39.52	<0.001	Yes
NA 3d vs. 1mg/ml 1d	269.656	39.454	<0.001	Yes
NA 3d vs. 2mg/ml 4d	269.507	39.432	<0.001	Yes
NA 3d vs. 2mg/ml 1d	269.357	39.411	<0.001	Yes
NA 3d vs. 5mg/ml 1d	269.208	39.389	<0.001	Yes
NA 3d vs. 1mg/ml 4d	269.208	39.389	<0.001	Yes
NA 3d vs. 2mg/ml 2d	268.46	39.279	<0.001	Yes
NA 3d vs. 1mg/ml 2d	268.012	39.214	<0.001	Yes
NA 4d vs. NA 1d	242.601	35.496	<0.001	Yes
NA 2d vs. 5mg/ml 3d	210.613	30.815	<0.001	Yes
NA 2d vs. 2mg/ml 3d	210.164	30.75	<0.001	Yes
NA 2d vs. 5mg/ml 4d	208.969	30.575	<0.001	Yes
NA 2d vs. 1mg/ml 3d	208.67	30.531	<0.001	Yes
NA 2d vs. 0.5mg/ml 1d	208.52	30.509	<0.001	Yes
NA 2d vs. 0.5mg/ml 4d	208.371	30.487	<0.001	Yes
NA 2d vs. 5mg/ml 2d	207.474	30.356	<0.001	Yes
NA 2d vs. 0.5mg/ml 3d	207.175	30.312	<0.001	Yes
NA 2d vs. 0.5mg/ml 2d	207.025	30.291	<0.001	Yes
NA 2d vs. 1mg/ml 1d	206.577	30.225	<0.001	Yes
NA 2d vs. 2mg/ml 4d	206.428	30.203	<0.001	Yes
NA 2d vs. 2mg/ml 1d	206.278	30.181	<0.001	Yes
NA 2d vs. 5mg/ml 1d	206.129	30.159	<0.001	Yes
NA 2d vs. 1mg/ml 4d	206.129	30.159	<0.001	Yes
NA 2d vs. 2mg/ml 2d	205.381	30.05	<0.001	Yes

NA 2d vs. 1mg/ml 2d	204.933	29.984	<0.001	Yes
NA 4d vs. NA 2d	175.635	25.698	<0.001	Yes
NA 3d vs. 0d	174.29	25.501	<0.001	Yes
NA 1d vs. 5mg/ml 3d	143.647	21.017	<0.001	Yes
NA 1d vs. 2mg/ml 3d	143.199	20.952	<0.001	Yes
NA 1d vs. 5mg/ml 4d	142.003	20.777	<0.001	Yes
NA 1d vs. 1mg/ml 3d	141.704	20.733	<0.001	Yes
NA 1d vs. 0.5mg/ml 1d	141.555	20.711	<0.001	Yes
NA 1d vs. 0.5mg/ml 4d	141.405	20.689	<0.001	Yes
NA 1d vs. 5mg/ml 2d	140.508	20.558	<0.001	Yes
NA 1d vs. 0.5mg/ml 3d	140.209	20.514	<0.001	Yes
NA 1d vs. 0.5mg/ml 2d	140.06	20.493	<0.001	Yes
NA 1d vs. 1mg/ml 1d	139.611	20.427	<0.001	Yes
NA 1d vs. 2mg/ml 4d	139.462	20.405	<0.001	Yes
NA 1d vs. 2mg/ml 1d	139.312	20.383	<0.001	Yes
NA 1d vs. 5mg/ml 1d	139.163	20.361	<0.001	Yes
NA 1d vs. 1mg/ml 4d	139.163	20.361	<0.001	Yes
NA 1d vs. 2mg/ml 2d	138.416	20.252	<0.001	Yes
NA 1d vs. 1mg/ml 2d	137.967	20.186	<0.001	Yes
NA 3d vs. NA 1d	130.045	19.027	<0.001	Yes
NA 4d vs. NA 3d	112.556	16.468	<0.001	Yes
NA 2d vs. 0d	111.211	16.272	<0.001	Yes
0d vs. 5mg/ml 3d	99.402	14.544	<0.001	Yes
0d vs. 2mg/ml 3d	98.954	14.478	<0.001	Yes
0d vs. 5mg/ml 4d	97.758	14.303	<0.001	Yes
0d vs. 1mg/ml 3d	97.459	14.26	<0.001	Yes
0d vs. 0.5mg/ml 1d	97.309	14.238	<0.001	Yes
0d vs. 0.5mg/ml 4d	97.16	14.216	<0.001	Yes
0d vs. 5mg/ml 2d	96.263	14.085	<0.001	Yes
0d vs. 0.5mg/ml 3d	95.964	14.041	<0.001	Yes
0d vs. 0.5mg/ml 2d	95.815	14.019	<0.001	Yes
0d vs. 1mg/ml 1d	95.366	13.953	<0.001	Yes
0d vs. 2mg/ml 4d	95.217	13.931	<0.001	Yes
0d vs. 2mg/ml 1d	95.067	13.91	<0.001	Yes
0d vs. 5mg/ml 1d	94.918	13.888	<0.001	Yes
0d vs. 1mg/ml 4d	94.918	13.888	<0.001	Yes
0d vs. 2mg/ml 2d	94.17	13.778	<0.001	Yes
0d vs. 1mg/ml 2d	93.722	13.713	<0.001	Yes
NA 2d vs. NA 1d	66.966	9.798	<0.001	Yes
NA 3d vs. NA 2d	63.079	9.229	<0.001	Yes
NA 1d vs. 0d	44.245	6.474	<0.001	Yes
1mg/ml 2d vs. 5mg/ml 3d	5.68	0.831		1 No
1mg/ml 2d vs. 2mg/ml 3d	5.232	0.765		1 No
2mg/ml 2d vs. 5mg/ml 3d	5.232	0.765		1 No
2mg/ml 2d vs. 2mg/ml 3d	4.783	0.7		1 No
1mg/ml 4d vs. 5mg/ml 3d	4.484	0.656		1 No
5mg/ml 1d vs. 5mg/ml 3d	4.484	0.656		1 No
2mg/ml 1d vs. 5mg/ml 3d	4.335	0.634		1 No
2mg/ml 4d vs. 5mg/ml 3d	4.185	0.612		1 No

5mg/ml 1d vs. 2mg/ml 3d	4.036	0.591	1 No
1mg/ml 2d vs. 5mg/ml 4d	4.036	0.591	1 No
1mg/ml 4d vs. 2mg/ml 3d	4.036	0.591	1 No
1mg/ml 1d vs. 5mg/ml 3d	4.036	0.591	1 No
2mg/ml 1d vs. 2mg/ml 3d	3.886	0.569	1 No
2mg/ml 4d vs. 2mg/ml 3d	3.737	0.547	1 No
1mg/ml 2d vs. 1mg/ml 3d	3.737	0.547	1 No
0.5mg/ml 2d vs. 5mg/ml 3d	3.587	0.525	1 No
2mg/ml 2d vs. 5mg/ml 4d	3.587	0.525	1 No
1mg/ml 1d vs. 2mg/ml 3d	3.587	0.525	1 No
1mg/ml 2d vs. 0.5mg/ml 1d	3.587	0.525	1 No
0.5mg/ml 3d vs. 5mg/ml 3d	3.438	0.503	1 No
1mg/ml 2d vs. 0.5mg/ml 4d	3.438	0.503	1 No
2mg/ml 2d vs. 1mg/ml 3d	3.288	0.481	1 No
2mg/ml 2d vs. 0.5mg/ml 1d	3.139	0.459	1 No
0.5mg/ml 2d vs. 2mg/ml 3d	3.139	0.459	1 No
5mg/ml 2d vs. 5mg/ml 3d	3.139	0.459	1 No
2mg/ml 2d vs. 0.5mg/ml 4d	2.99	0.437	1 No
0.5mg/ml 3d vs. 2mg/ml 3d	2.99	0.437	1 No
5mg/ml 1d vs. 5mg/ml 4d	2.84	0.416	1 No
1mg/ml 4d vs. 5mg/ml 4d	2.84	0.416	1 No
2mg/ml 1d vs. 5mg/ml 4d	2.691	0.394	1 No
5mg/ml 2d vs. 2mg/ml 3d	2.691	0.394	1 No
1mg/ml 4d vs. 1mg/ml 3d	2.541	0.372	1 No
2mg/ml 4d vs. 5mg/ml 4d	2.541	0.372	1 No
1mg/ml 2d vs. 5mg/ml 2d	2.541	0.372	1 No
5mg/ml 1d vs. 1mg/ml 3d	2.541	0.372	1 No
1mg/ml 4d vs. 0.5mg/ml 1d	2.392	0.35	1 No
1mg/ml 1d vs. 5mg/ml 4d	2.392	0.35	1 No
2mg/ml 1d vs. 1mg/ml 3d	2.392	0.35	1 No
5mg/ml 1d vs. 0.5mg/ml 1d	2.392	0.35	1 No
2mg/ml 4d vs. 1mg/ml 3d	2.242	0.328	1 No
0.5mg/ml 4d vs. 5mg/ml 3d	2.242	0.328	1 No
2mg/ml 1d vs. 0.5mg/ml 1d	2.242	0.328	1 No
1mg/ml 2d vs. 0.5mg/ml 3d	2.242	0.328	1 No
1mg/ml 4d vs. 0.5mg/ml 4d	2.242	0.328	1 No
5mg/ml 1d vs. 0.5mg/ml 4d	2.242	0.328	1 No
1mg/ml 1d vs. 1mg/ml 3d	2.093	0.306	1 No
1mg/ml 2d vs. 0.5mg/ml 2d	2.093	0.306	1 No
2mg/ml 1d vs. 0.5mg/ml 4d	2.093	0.306	1 No
2mg/ml 4d vs. 0.5mg/ml 1d	2.093	0.306	1 No
2mg/ml 2d vs. 5mg/ml 2d	2.093	0.306	1 No
0.5mg/ml 1d vs. 5mg/ml 3d	2.093	0.306	1 No
0.5mg/ml 2d vs. 5mg/ml 4d	1.943	0.284	1 No
1mg/ml 1d vs. 0.5mg/ml 1d	1.943	0.284	1 No
2mg/ml 4d vs. 0.5mg/ml 4d	1.943	0.284	1 No
1mg/ml 3d vs. 5mg/ml 3d	1.943	0.284	1 No
0.5mg/ml 3d vs. 5mg/ml 4d	1.794	0.262	1 No
0.5mg/ml 4d vs. 2mg/ml 3d	1.794	0.262	1 No

1mg/ml 1d vs. 0.5mg/ml 4d	1.794	0.262	1 No
2mg/ml 2d vs. 0.5mg/ml 3d	1.794	0.262	1 No
5mg/ml 4d vs. 5mg/ml 3d	1.644	0.241	1 No
1mg/ml 2d vs. 1mg/ml 1d	1.644	0.241	1 No
0.5mg/ml 2d vs. 1mg/ml 3d	1.644	0.241	1 No
0.5mg/ml 1d vs. 2mg/ml 3d	1.644	0.241	1 No
2mg/ml 2d vs. 0.5mg/ml 2d	1.644	0.241	1 No
0.5mg/ml 2d vs. 0.5mg/ml 1d	1.495	0.219	1 No
1mg/ml 2d vs. 2mg/ml 4d	1.495	0.219	1 No
5mg/ml 2d vs. 5mg/ml 4d	1.495	0.219	1 No
1mg/ml 3d vs. 2mg/ml 3d	1.495	0.219	1 No
0.5mg/ml 3d vs. 1mg/ml 3d	1.495	0.219	1 No
0.5mg/ml 2d vs. 0.5mg/ml 4d	1.345	0.197	1 No
1mg/ml 2d vs. 2mg/ml 1d	1.345	0.197	1 No
5mg/ml 1d vs. 5mg/ml 2d	1.345	0.197	1 No
1mg/ml 4d vs. 5mg/ml 2d	1.345	0.197	1 No
0.5mg/ml 3d vs. 0.5mg/ml 1d	1.345	0.197	1 No
5mg/ml 4d vs. 2mg/ml 3d	1.196	0.175	1 No
5mg/ml 2d vs. 1mg/ml 3d	1.196	0.175	1 No
2mg/ml 2d vs. 1mg/ml 1d	1.196	0.175	1 No
1mg/ml 2d vs. 5mg/ml 1d	1.196	0.175	1 No
0.5mg/ml 3d vs. 0.5mg/ml 4d	1.196	0.175	1 No
2mg/ml 1d vs. 5mg/ml 2d	1.196	0.175	1 No
1mg/ml 2d vs. 1mg/ml 4d	1.196	0.175	1 No
2mg/ml 2d vs. 2mg/ml 4d	1.046	0.153	1 No
2mg/ml 4d vs. 5mg/ml 2d	1.046	0.153	1 No
5mg/ml 1d vs. 0.5mg/ml 3d	1.046	0.153	1 No
5mg/ml 2d vs. 0.5mg/ml 1d	1.046	0.153	1 No
1mg/ml 4d vs. 0.5mg/ml 3d	1.046	0.153	1 No
2mg/ml 1d vs. 0.5mg/ml 3d	0.897	0.131	1 No
1mg/ml 1d vs. 5mg/ml 2d	0.897	0.131	1 No
5mg/ml 1d vs. 0.5mg/ml 2d	0.897	0.131	1 No
1mg/ml 4d vs. 0.5mg/ml 2d	0.897	0.131	1 No
5mg/ml 2d vs. 0.5mg/ml 4d	0.897	0.131	1 No
2mg/ml 2d vs. 2mg/ml 1d	0.897	0.131	1 No
2mg/ml 1d vs. 0.5mg/ml 2d	0.747	0.109	1 No
2mg/ml 2d vs. 5mg/ml 1d	0.747	0.109	1 No
2mg/ml 4d vs. 0.5mg/ml 3d	0.747	0.109	1 No
2mg/ml 2d vs. 1mg/ml 4d	0.747	0.109	1 No
0.5mg/ml 4d vs. 5mg/ml 4d	0.598	0.0875	1 No
1mg/ml 1d vs. 0.5mg/ml 3d	0.598	0.0875	1 No
2mg/ml 4d vs. 0.5mg/ml 2d	0.598	0.0875	1 No
0.5mg/ml 1d vs. 5mg/ml 4d	0.448	0.0656	1 No
1mg/ml 2d vs. 2mg/ml 2d	0.448	0.0656	1 No
2mg/ml 3d vs. 5mg/ml 3d	0.448	0.0656	1 No
1mg/ml 4d vs. 1mg/ml 1d	0.448	0.0656	1 No
1mg/ml 1d vs. 0.5mg/ml 2d	0.448	0.0656	1 No
5mg/ml 1d vs. 1mg/ml 1d	0.448	0.0656	1 No
0.5mg/ml 2d vs. 5mg/ml 2d	0.448	0.0656	1 No

1mg/ml 4d vs. 2mg/ml 4d	0.299	0.0437	1 No
5mg/ml 1d vs. 2mg/ml 4d	0.299	0.0437	1 No
1mg/ml 3d vs. 5mg/ml 4d	0.299	0.0437	1 No
0.5mg/ml 3d vs. 5mg/ml 2d	0.299	0.0437	1 No
2mg/ml 1d vs. 1mg/ml 1d	0.299	0.0437	1 No
0.5mg/ml 4d vs. 1mg/ml 3d	0.299	0.0437	1 No
2mg/ml 1d vs. 2mg/ml 4d	0.149	0.0219	1 No
5mg/ml 1d vs. 2mg/ml 1d	0.149	0.0219	1 No
1mg/ml 4d vs. 2mg/ml 1d	0.149	0.0219	1 No
2mg/ml 4d vs. 1mg/ml 1d	0.149	0.0219	1 No
0.5mg/ml 2d vs. 0.5mg/ml 3d	0.149	0.0219	1 No
0.5mg/ml 1d vs. 1mg/ml 3d	0.149	0.0219	1 No
0.5mg/ml 4d vs. 0.5mg/ml 1d	0.149	0.0219	1 No
5mg/ml 1d vs. 1mg/ml 4d	3.55E-15	5.20E-16	1 No

Figure 2.4 eosin Y - p-AKT

One Way Analysis of Variance

Data source: Data 1 in eosin Y WB

Normality Test (Shapiro-Wilk) Passed (P = 0.794)

Equal Variance Test: Passed (P = 0.631)

Group Name	N	Missing	Mean	Std Dev	SEM
NA	3	0	1	0.0346	0.02
2.5ul/ml	3	0	0.915	0.194	0.112
5ul/ml	3	0	0.873	0.236	0.136
10ul/ml	3	0	0.836	0.1	0.058
25ul/ml	3	0	0.952	0.187	0.108

Source of Variation	DF	SS	MS	F	P
Between Groups	4	0.0496	0.0124	0.444	0.774
Residual	10	0.279	0.0279		
Total	14	0.329			

The differences in the mean values among the treatment groups are not great enough to exclude the possibility that the difference is due to random sampling variability; there is not a statistically significant difference (P = 0.774).

Power of performed test with alpha = 0.050: 0.050

The power of the performed test (0.050) is below the desired power of 0.800.

Less than desired power indicates you are less likely to detect a difference when one actually exists. Negative results should be interpreted cautiously.

Figure 2.4 eosin Y- AKT1

Normality Test (Shapiro-Wilk) Passed (P = 0.472)

Equal Variance Test: Passed (P = 0.708)

Group Name	N	Missing	Mean	Std Dev	SEM
NA	3	0	1	0.0354	0.0204
2.5ul/ml	3	0	1.014	0.0962	0.0555
5ul/ml	3	0	1.077	0.0439	0.0254
10ul/ml	3	0	1.029	0.0569	0.0329
25ul/ml	3	0	0.936	0.0658	0.038

Source of Variation	DF	SS	MS	F	P
Between Groups	4	0.0314	0.00785	1.963	0.176
Residual	10	0.04	0.004		

Total 14 0.0714

The differences in the mean values among the treatment groups are not great enough to exclude the possibility that the difference is due to random sampling variability; there is not a statistically significant difference ($P = 0.176$).

Power of performed test with $\alpha = 0.050$: 0.205

The power of the performed test (0.205) is below the desired power of 0.800. Less than desired power indicates you are less likely to detect a difference when one actually exists. Negative results should be interpreted cautiously.

Figure 2.5 Irgacure2959 - p-AKT

One Way Analysis of Variance

Data source: Data 1 in Irgacure 2959 WB

Normality Test (Shapiro-Wilk) Passed (P = 0.117)

Equal Variance Test: Passed (P = 0.423)

Group Name	N	Missing	Mean	Std Dev	SEM
NA	3	0	1	0.0254	0.0147
0mg/ml	3	0	1.01	0.0214	0.0123
1mg/ml	3	0	0.882	0.22	0.127
2mg/ml	3	0	0.843	0.381	0.22
5mg/ml	3	0	0.481	0.261	0.151
10mg/ml	3	0	0.0884	0.0716	0.0414

Source of Variation	DF	SS	MS	F	P
Between Groups	5	1.979	0.396	8.842	0.001
Residual	12	0.537	0.0448		
Total	17	2.516			

The differences in the mean values among the treatment groups are greater than would be expected by chance; there is a statistically significant difference (P = 0.001).

Power of performed test with alpha = 0.050: 0.985

All Pairwise Multiple Comparison Procedures (Holm-Sidak method):

Overall significance level = 0.05

Comparisons for factor:

Comparison	Diff of Me t	P	P<0.050
0mg/ml vs. 10mg/ml	0.921	5.333	0.003 Yes
NA vs. 10mg/ml	0.912	5.276	0.003 Yes
1mg/ml vs. 10mg/ml	0.793	4.591	0.008 Yes
2mg/ml vs. 10mg/ml	0.754	4.367	0.011 Yes
0mg/ml vs. 5mg/ml	0.529	3.063	0.103 No
NA vs. 5mg/ml	0.519	3.007	0.104 No
1mg/ml vs. 5mg/ml	0.401	2.322	0.299 No
5mg/ml vs. 10mg/ml	0.392	2.27	0.293 No
2mg/ml vs. 5mg/ml	0.362	2.097	0.341 No
0mg/ml vs. 2mg/ml	0.167	0.966	0.927 No
NA vs. 2mg/ml	0.157	0.91	0.909 No
0mg/ml vs. 1mg/ml	0.128	0.741	0.923 No
NA vs. 1mg/ml	0.118	0.685	0.88 No
1mg/ml vs. 2mg/ml	0.0388	0.225	0.97 No
0mg/ml vs. NA	0.00971	0.0562	0.956 No

Figure 2.5 Iragcure2959 - AKT1

Normality Test (Shapiro-Wilk) Passed (P = 0.104)

Equal Variance Test: Passed (P = 0.073)

Group Name	N	Missing	Mean	Std Dev	SEM
NA	3	0	1	0.0289	0.0167
0mg/ml	3	0	1.092	0.131	0.0757
1mg/ml	3	0	1.157	0.0318	0.0183
2mg/ml	3	0	1.178	0.149	0.0861
5mg/ml	3	0	1.084	0.0288	0.0166
10mg/ml	3	0	0.89	0.0418	0.0242

Source of Variation	DF	SS	MS	F	P
Between Groups	5	0.171	0.0342	4.684	0.013
Residual	12	0.0877	0.00731		
Total	17	0.259			

The differences in the mean values among the treatment groups are greater than would be expected by chance; there is a statistically significant difference (P = 0.013).

Power of performed test with alpha = 0.050: 0.765

All Pairwise Multiple Comparison Procedures (Holm-Sidak method):
Overall significance level = 0.05

Comparisons for factor:

Comparison	Diff of Me t	P	P<0.050
2mg/ml vs. 10mg/ml	0.288	4.121	0.021 Yes
1mg/ml vs. 10mg/ml	0.267	3.822	0.033 Yes
0mg/ml vs. 10mg/ml	0.202	2.895	0.161 No
5mg/ml vs. 10mg/ml	0.193	2.772	0.185 No
2mg/ml vs. NA	0.178	2.548	0.248 No
1mg/ml vs. NA	0.157	2.249	0.363 No
NA vs. 10mg/ml	0.11	1.573	0.747 No
2mg/ml vs. 5mg/ml	0.0942	1.35	0.836 No
0mg/ml vs. NA	0.0923	1.321	0.81 No
2mg/ml vs. 0mg/ml	0.0856	1.226	0.813 No
5mg/ml vs. NA	0.0836	1.198	0.769 No
1mg/ml vs. 5mg/ml	0.0734	1.051	0.779 No
1mg/ml vs. 0mg/ml	0.0648	0.928	0.752 No
2mg/ml vs. 1mg/ml	0.0208	0.299	0.947 No
0mg/ml vs. 5mg/ml	0.0086	0.123	0.904 No

Figure 2.6 DMPA - p-AKT

One Way Analysis of Variance

Data source: Data 1 in DMPA WB

Normality Test (Shapiro-Wilk) Passed (P = 0.349)

Equal Variance Test: Passed (P = 0.794)

Group Name	N	Missing	Mean	Std Dev	SEM
NA	3	0	1	0.0897	0.0518
0mg/ml	3	0	0.962	0.121	0.0697
0.5mg/ml	3	0	0.959	0.275	0.159
1mg/ml	3	0	0.539	0.134	0.0772
2mg/ml	3	0	0.271	0.0474	0.0273
5mg/ml	3	0	0.213	0.0753	0.0435

Source of Variation	DF	SS	MS	F	P
Between Groups	5	1.987	0.397	19.224	<0.001
Residual	12	0.248	0.0207		
Total	17	2.235			

The differences in the mean values among the treatment groups are greater than would be expected by chance; there is a statistically significant difference (P = <0.001).

Power of performed test with alpha = 0.050: 1.000

All Pairwise Multiple Comparison Procedures (Holm-Sidak method):

Overall significance level = 0.05

Comparisons for factor:

Comparison	Diff of Me t	P	P<0.050
NA vs. 5mg/ml	0.787	6.703 <0.001	Yes
0mg/ml vs. 5mg/ml	0.749	6.378 <0.001	Yes
0.5mg/ml vs. 5mg/ml	0.746	6.358 <0.001	Yes
NA vs. 2mg/ml	0.729	6.212 <0.001	Yes
0mg/ml vs. 2mg/ml	0.691	5.888 <0.001	Yes
0.5mg/ml vs. 2mg/ml	0.689	5.867 <0.001	Yes
NA vs. 1mg/ml	0.461	3.93 0.018	Yes
0mg/ml vs. 1mg/ml	0.423	3.605 0.029	Yes
0.5mg/ml vs. 1mg/ml	0.421	3.585 0.026	Yes
1mg/ml vs. 5mg/ml	0.326	2.773 0.097	No
1mg/ml vs. 2mg/ml	0.268	2.283 0.191	No
2mg/ml vs. 5mg/ml	0.0576	0.49 0.982	No
NA vs. 0.5mg/ml	0.0405	0.345 0.982	No
NA vs. 0mg/ml	0.0381	0.325 0.938	No
0mg/ml vs. 0.5mg/ml	0.00239	0.0203 0.984	No

Figure 2.6 DMPA - AKT1

Normality Test (Shapiro-Wilk) Passed (P = 0.256)

Equal Variance Test: Passed (P = 0.728)

Group Name	N	Missing	Mean	Std Dev	SEM
NA	3	0	1	0.0322	0.0186
0mg/ml	3	0	1.031	0.0703	0.0406
0.5mg/ml	3	0	1.125	0.14	0.0809
1mg/ml	3	0	1.168	0.0917	0.0529
2mg/ml	3	0	1.223	0.111	0.064
5mg/ml	3	0	1.131	0.211	0.122

Source of Variation	DF	SS	MS	F	P
Between Groups	5	0.106	0.0212	1.395	0.294
Residual	12	0.182	0.0152		
Total	17	0.288			

The differences in the mean values among the treatment groups are not great enough to exclude the possibility that the difference is due to random sampling variability; there is not a statistically significant difference (P = 0.294).

Power of performed test with alpha = 0.050: 0.115

The power of the performed test (0.115) is below the desired power of 0.800.

Less than desired power indicates you are less likely to detect a difference when one actually exists.

Negative results should be interpreted cautiously.

Figure 2.8 eosin Y - UV

One Way Analysis of Variance

Data source: Data 1 in eosin Y UV viability

Normality Test (Shapiro-Wilk) Passed (P = 0.424)

Equal Variance Test: Passed (P = 0.485)

Group Name	N	Missing	Mean	Std Dev	SEM
0d	3	0	99.649	12.734	7.352
NA 1d	3	0	143.86	19.702	11.375
2.5ul/ml 1d	3	0	92.982	2.191	1.265
5ul/ml 1d	3	0	69.474	14.24	8.221
10ul/ml 1d	3	0	60.702	11.643	6.722
NA 2d	3	0	187.719	16.787	9.692
2.5ul/ml 2d	3	0	67.719	5.986	3.456
5ul/ml 2d	3	0	63.86	7.468	4.312
10ul/ml 2d	3	0	49.474	5.57	3.216

Source of Variation	DF	SS	MS	F	P
Between Groups	8	49745.6	6218.2	43.12	<0.001
Residual	18	2595.753	144.208		
Total	26	52341.36			

The differences in the mean values among the treatment groups are greater than would be expected by chance; there is a statistically significant difference (P = <0.001).

Power of performed test with alpha = 0.050: 1.000

All Pairwise Multiple Comparison Procedures (Holm-Sidak method):

Overall significance level = 0.05

Comparisons for factor:

Comparison				
NA 2d vs. 10ul/ml 2d	138.246	14.099	<0.001	Yes
NA 2d vs. 10ul/ml 1d	127.018	12.954	<0.001	Yes
NA 2d vs. 5ul/ml 2d	123.86	12.632	<0.001	Yes
NA 2d vs. 2.5ul/ml 2d	120	12.239	<0.001	Yes
NA 2d vs. 5ul/ml 1d	118.246	12.06	<0.001	Yes
NA 2d vs. 2.5ul/ml 1d	94.737	9.662	<0.001	Yes
NA 1d vs. 10ul/ml 2d	94.386	9.626	<0.001	Yes
NA 2d vs. 0d	88.07	8.982	<0.001	Yes
NA 1d vs. 10ul/ml 1d	83.158	8.481	<0.001	Yes
NA 1d vs. 5ul/ml 2d	80	8.159	<0.001	Yes
NA 1d vs. 2.5ul/ml 2d	76.14	7.765	<0.001	Yes
NA 1d vs. 5ul/ml 1d	74.386	7.586	<0.001	Yes

NA 1d vs. 2.5ul/ml 1d	50.877	5.189	0.001	Yes
0d vs. 10ul/ml 2d	50.175	5.117	0.002	Yes
NA 1d vs. 0d	44.211	4.509	0.006	Yes
NA 2d vs. NA 1d	43.86	4.473	0.006	Yes
2.5ul/ml 1d vs. 10ul/ml 2d	43.509	4.437	0.006	Yes
0d vs. 10ul/ml 1d	38.947	3.972	0.017	Yes
0d vs. 5ul/ml 2d	35.789	3.65	0.032	Yes
2.5ul/ml 1d vs. 10ul/ml 1d	32.281	3.292	0.067	No
0d vs. 2.5ul/ml 2d	31.93	3.256	0.068	No
0d vs. 5ul/ml 1d	30.175	3.078	0.093	No
2.5ul/ml 1d vs. 5ul/ml 2d	29.123	2.97	0.109	No
2.5ul/ml 1d vs. 2.5ul/ml 2d	25.263	2.577	0.221	No
2.5ul/ml 1d vs. 5ul/ml 1d	23.509	2.398	0.285	No
5ul/ml 1d vs. 10ul/ml 2d	20	2.04	0.472	No
2.5ul/ml 2d vs. 10ul/ml 2d	18.246	1.861	0.562	No
5ul/ml 2d vs. 10ul/ml 2d	14.386	1.467	0.791	No
10ul/ml 1d vs. 10ul/ml 2d	11.228	1.145	0.917	No
5ul/ml 1d vs. 10ul/ml 1d	8.772	0.895	0.966	No
2.5ul/ml 2d vs. 10ul/ml 1d	7.018	0.716	0.981	No
0d vs. 2.5ul/ml 1d	6.667	0.68	0.97	No
5ul/ml 1d vs. 5ul/ml 2d	5.614	0.573	0.967	No
2.5ul/ml 2d vs. 5ul/ml 2d	3.86	0.394	0.973	No
5ul/ml 2d vs. 10ul/ml 1d	3.158	0.322	0.938	No
5ul/ml 1d vs. 2.5ul/ml 2d	1.754	0.179	0.86	No

Figure 2.9 Irgacure 2959 - UV

One Way Analysis of Variance

Data source: Data 1 in Irgacure 2959 UV viability

Normality Test (Shapiro-Wilk) Passed (P = 0.708)

Equal Variance Test: Passed (P = 0.345)

Group Name	N	Missing	Mean	Std Dev	SEM
0d	3	0	100	11.628	6.713
NA 1d	3	0	144.186	20.44	11.801
1mg/ml 1d	3	0	78.682	16.622	9.596
2mg/ml 1d	3	0	65.504	20.318	11.731
5mg/ml 1d	3	0	3.101	2.421	1.398
NA 2d	3	0	207.364	18.544	10.706
1mg/ml 2d	3	0	70.155	14.724	8.501
2mg/ml 2d	3	0	23.256	3.076	1.776
5mg/ml 2d	3	0	2.326	2.326	1.343

Source of Variation	DF	SS	MS	F	P
Between Groups	8	108435.6	13554.45	66.899	<0.001
Residual	18	3647.016	202.612		
Total	26	112082.6			

The differences in the mean values among the treatment groups are greater than would be expected by chance; there is a statistically significant difference (P = <0.001).

Power of performed test with alpha = 0.050: 1.000

All Pairwise Multiple Comparison Procedures (Holm-Sidak method):

Overall significance level = 0.05

Comparisons for factor:

Comparison	Diff of Me t	P	P<0.050
NA 2d vs. 5mg/ml 2d	205.039	17.642 <0.001	Yes
NA 2d vs. 5mg/ml 1d	204.264	17.575 <0.001	Yes
NA 2d vs. 2mg/ml 2d	184.109	15.841 <0.001	Yes
NA 2d vs. 2mg/ml 1d	141.86	12.206 <0.001	Yes
NA 1d vs. 5mg/ml 2d	141.86	12.206 <0.001	Yes
NA 1d vs. 5mg/ml 1d	141.085	12.139 <0.001	Yes
NA 2d vs. 1mg/ml 2d	137.209	11.806 <0.001	Yes
NA 2d vs. 1mg/ml 1d	128.682	11.072 <0.001	Yes
NA 1d vs. 2mg/ml 2d	120.93	10.405 <0.001	Yes
NA 2d vs. 0d	107.364	9.238 <0.001	Yes
0d vs. 5mg/ml 2d	97.674	8.404 <0.001	Yes
0d vs. 5mg/ml 1d	96.899	8.337 <0.001	Yes

NA 1d vs. 2mg/ml 1d	78.682	6.77	<0.001	Yes
0d vs. 2mg/ml 2d	76.744	6.603	<0.001	Yes
1mg/ml 1d vs. 5mg/ml 2d	76.357	6.57	<0.001	Yes
1mg/ml 1d vs. 5mg/ml 1d	75.581	6.503	<0.001	Yes
NA 1d vs. 1mg/ml 2d	74.031	6.37	<0.001	Yes
1mg/ml 2d vs. 5mg/ml 2d	67.829	5.836	<0.001	Yes
1mg/ml 2d vs. 5mg/ml 1d	67.054	5.77	<0.001	Yes
NA 1d vs. 1mg/ml 1d	65.504	5.636	<0.001	Yes
NA 2d vs. NA 1d	63.178	5.436	<0.001	Yes
2mg/ml 1d vs. 5mg/ml 2d	63.178	5.436	<0.001	Yes
2mg/ml 1d vs. 5mg/ml 1d	62.403	5.369	<0.001	Yes
1mg/ml 1d vs. 2mg/ml 2d	55.426	4.769	0.002	Yes
1mg/ml 2d vs. 2mg/ml 2d	46.899	4.035	0.009	Yes
NA 1d vs. 0d	44.186	3.802	0.014	Yes
2mg/ml 1d vs. 2mg/ml 2d	42.248	3.635	0.019	Yes
0d vs. 2mg/ml 1d	34.496	2.968	0.072	No
0d vs. 1mg/ml 2d	29.845	2.568	0.145	No
0d vs. 1mg/ml 1d	21.318	1.834	0.456	No
2mg/ml 2d vs. 5mg/ml 2d	20.93	1.801	0.426	No
2mg/ml 2d vs. 5mg/ml 1d	20.155	1.734	0.409	No
1mg/ml 1d vs. 2mg/ml 1d	13.178	1.134	0.719	No
1mg/ml 1d vs. 1mg/ml 2d	8.527	0.734	0.853	No
1mg/ml 2d vs. 2mg/ml 1d	4.651	0.4	0.906	No
5mg/ml 1d vs. 5mg/ml 2d	7.75E-01	6.67E-02	0.948	No

Figure 2.10 DMPA - UV

One Way Analysis of Variance

Data source: Data 1 in DMPA UV viability

Normality Test (Shapiro-Wilk) Failed (P < 0.050)

Equal Variance Test: Passed (P = 0.291)

Group Name	N	Missing	Mean	Std Dev	SEM
0d	3	0	100	11.628	6.713
NA 1d	3	0	144.186	20.44	11.801
1mg/ml 1d	3	0	9.69	2.421	1.398
2mg/ml 1d	3	0	9.69	3.357	1.938
5mg/ml 1d	3	0	11.628	5.068	2.926
NA 2d	3	0	207.364	18.544	10.706
1mg/ml 2d	3	0	5.814	0	0
2mg/ml 2d	3	0	8.14	2.014	1.163
5mg/ml 2d	3	0	7.364	4.699	2.713

Source of Variation	DF	SS	MS	F	P
Between Groups	8	138170.3	17271.29	160.94	<0.001
Residual	18	1931.675	107.315		
Total	26	140102			

The differences in the mean values among the treatment groups are greater than would be expected by chance; there is a statistically significant difference (P = <0.001).

Power of performed test with alpha = 0.050: 1.000

All Pairwise Multiple Comparison Procedures (Holm-Sidak method):

Overall significance level = 0.05

Comparisons for factor:

Comparison	Diff of Me t	P	P<0.050
NA 2d vs. 1mg/ml 2d	201.55	23.829 <0.001	Yes
NA 2d vs. 5mg/ml 2d	200	23.645 <0.001	Yes
NA 2d vs. 2mg/ml 2d	199.225	23.554 <0.001	Yes
NA 2d vs. 1mg/ml 1d	197.674	23.37 <0.001	Yes
NA 2d vs. 2mg/ml 1d	197.674	23.37 <0.001	Yes
NA 2d vs. 5mg/ml 1d	195.736	23.141 <0.001	Yes
NA 1d vs. 1mg/ml 2d	138.372	16.359 <0.001	Yes
NA 1d vs. 5mg/ml 2d	136.822	16.176 <0.001	Yes
NA 1d vs. 2mg/ml 2d	136.047	16.084 <0.001	Yes
NA 1d vs. 2mg/ml 1d	134.496	15.901 <0.001	Yes
NA 1d vs. 1mg/ml 1d	134.496	15.901 <0.001	Yes
NA 1d vs. 5mg/ml 1d	132.558	15.672 <0.001	Yes

NA 2d vs. 0d	107.364	12.693	<0.001	Yes
0d vs. 1mg/ml 2d	94.186	11.135	<0.001	Yes
0d vs. 5mg/ml 2d	92.636	10.952	<0.001	Yes
0d vs. 2mg/ml 2d	91.86	10.86	<0.001	Yes
0d vs. 2mg/ml 1d	90.31	10.677	<0.001	Yes
0d vs. 1mg/ml 1d	90.31	10.677	<0.001	Yes
0d vs. 5mg/ml 1d	88.372	10.448	<0.001	Yes
NA 2d vs. NA 1d	63.178	7.469	<0.001	Yes
NA 1d vs. 0d	44.186	5.224	<0.001	Yes
5mg/ml 1d vs. 1mg/ml 2d	5.814	0.687		1 No
5mg/ml 1d vs. 5mg/ml 2d	4.264	0.504		1 No
1mg/ml 1d vs. 1mg/ml 2d	3.876	0.458		1 No
2mg/ml 1d vs. 1mg/ml 2d	3.876	0.458		1 No
5mg/ml 1d vs. 2mg/ml 2d	3.488	0.412		1 No
1mg/ml 1d vs. 5mg/ml 2d	2.326	0.275		1 No
2mg/ml 1d vs. 5mg/ml 2d	2.326	0.275		1 No
2mg/ml 2d vs. 1mg/ml 2d	2.326	0.275		1 No
5mg/ml 1d vs. 1mg/ml 1d	1.938	0.229		1 No
5mg/ml 1d vs. 2mg/ml 1d	1.938	0.229		1 No
1mg/ml 1d vs. 2mg/ml 2d	1.55	0.183		1 No
2mg/ml 1d vs. 2mg/ml 2d	1.55	0.183		1 No
5mg/ml 2d vs. 1mg/ml 2d	1.55	0.183	0.997	No
2mg/ml 2d vs. 5mg/ml 2d	0.775	0.0916	0.995	No
1mg/ml 1d vs. 2mg/ml 1d	7.11E-15	8.40E-16		1 No

Figure 2.11 UV- p-AKT

One Way Analysis of Variance

Data source: Data 1 in UV photo WB

Normality Test (Shapiro-Wilk) Passed (P = 0.213)

Equal Variance Test: Passed (P = 0.902)

Group Name	N	Missing	Mean	Std Dev	SEM
NA	3	0	1	0.124	0.0718
DMPA 2mg/ml	3	0	0.572	0.0776	0.0448
DMPA 5mg/ml	3	0	0.521	0.0763	0.0441
eosin Y 10ul/ml	3	0	0.622	0.0811	0.0468
eosin Y 25ul/ml	3	0	0.271	0.061	0.0352
I2959 2mg/ml	3	0	0.423	0.0602	0.0347
I2959 5mg/ml	3	0	0.197	0.0586	0.0339

Source of Variation	DF	SS	MS	F	P
Between Groups	6	1.256	0.209	32.823	<0.001
Residual	14	0.0893	0.00638		
Total	20	1.346			

The differences in the mean values among the treatment groups are greater than would be expected by chance; there is a statistically significant difference (P = <0.001).

Power of performed test with alpha = 0.050: 1.000

All Pairwise Multiple Comparison Procedures (Holm-Sidak method):

Overall significance level = 0.05

Comparisons for factor:

Comparison	Diff of Me t	P	P<0.050
NA vs. I2959 5mg/ml	0.803	12.307 <0.001	Yes
NA vs. eosin Y 25ul/ml	0.729	11.178 <0.001	Yes
NA vs. I2959 2mg/ml	0.577	8.847 <0.001	Yes
NA vs. DMPA 5mg/ml	0.479	7.352 <0.001	Yes
NA vs. DMPA 2mg/ml	0.428	6.563 <0.001	Yes
eosin Y 10ul vs. I2959 5mg/ml	0.425	6.511 <0.001	Yes
NA vs. eosin Y 10ul/ml	0.378	5.796 <0.001	Yes
DMPA 2mg/ml vs. I2959 5mg/ml	0.375	5.744 <0.001	Yes
eosin Y 10ul vs. eosin Y 25ul	0.351	5.381 0.001	Yes
DMPA 5mg/ml vs. I2959 5mg/ml	0.323	4.955 0.003	Yes
DMPA 2mg/ml vs. eosin Y 25ul	0.301	4.614 0.004	Yes
DMPA 5mg/ml vs. eosin Y 25ul	0.249	3.826 0.018	Yes
I2959 2mg/ml vs. I2959 5mg/ml	0.226	3.461 0.034	Yes
eosin Y 10ul vs. I2959 2mg/ml	0.199	3.05 0.067	No

I2959 2mg/ml vs. eosin Y 25ul	0.152	2.331	0.222	No
DMPA 2mg/ml vs. I2959 2mg/ml	0.149	2.283	0.21	No
eosin Y 10ul vs. DMPA 5mg/ml	0.101	1.556	0.535	No
DMPA 5mg/ml vs. I2959 2mg/ml	0.0975	1.495	0.495	No
eosin Y 25ul vs. I2959 5mg/ml	0.0737	1.13	0.623	No
DMPA 2mg/ml vs. DMPA 5mg/n	0.0514	0.789	0.69	No
eosin Y 10ul vs. DMPA 2mg/ml	0.05	0.767	0.456	No

Figure 2.11 UV- AKT1

Normality Test (Shapiro-Wilk) Passed (P = 0.783)

Equal Variance Test: Passed (P = 0.424)

Group Name	N	Missing	Mean	Std Dev	SEM
NA	3	0	1	0.0659	0.0381
DMPA 2mg/ml	3	0	1.192	0.0955	0.0551
DMPA 5mg/ml	3	0	1.212	0.248	0.143
eosin Y 10ul/ml	3	0	1.208	0.129	0.0742
eosin Y 25ul/ml	3	0	1.307	0.133	0.0768
I2959 2mg/ml	3	0	1.168	0.167	0.0962
I2959 5mg/ml	3	0	1.349	0.206	0.119

Source of Variation	DF	SS	MS	F	P
Between Groups	6	0.225	0.0374	1.459	0.262
Residual	14	0.359	0.0256		
Total	20	0.584			

The differences in the mean values among the treatment groups are not great enough to exclude the possibility that the difference is due to random sampling variability; there is not a statistically significant difference (P = 0.262).

Power of performed test with alpha = 0.050: 0.138

The power of the performed test (0.138) is below the desired power of 0.800.

Less than desired power indicates you are less likely to detect a difference when one actually exists. Negative results should be interpreted cautiously.

Figure 2.12 viability

One Way Analysis of Variance

Data source: Data 1 in UV time eosin Y viability

Normality Test (Shapiro-Wilk) Passed (P = 0.471)

Equal Variance Test: Passed (P = 0.591)

Group Name	N	Missing	Mean	Std Dev	SEM
NA	3	0	0.179	0.0119	0.00689
eosin Y	3	0	0.0983	0.00777	0.00448
0h UV eosin Y	3	0	0.0537	0.00503	0.00291
6h UV eosin Y	3	0	0.00833	0.00306	0.00176
24h UV eosin Y	3	0	0.00933	0.00321	0.00186
48h UV eosin Y	3	0	0.009	0.00265	0.00153

Source of Variation	DF	SS	MS	F	P
Between Groups	5	0.0708	0.0142	333.427	<0.001
Residual	12	0.000509	4.24E-05		
Total	17	0.0713			

The differences in the mean values among the treatment groups are greater than would be expected by chance; there is a statistically significant difference (P = <0.001).

Power of performed test with alpha = 0.050: 1.000

All Pairwise Multiple Comparison Procedures (Holm-Sidak method):

Overall significance level = 0.05

Comparisons for factor:

Comparison	Diff of Me t	P	P<0.050
NA vs. 6h UV eosin Y	0.171	32.146 <0.001	Yes
NA vs. 48h UV eosin Y	0.17	32.021 <0.001	Yes
NA vs. 24h UV eosin Y	0.17	31.958 <0.001	Yes
NA vs. 0h UV eosin Y	0.126	23.624 <0.001	Yes
eosin Y vs. 6h UV eosin Y	0.09	16.919 <0.001	Yes
eosin Y vs. 48h UV eosin Y	0.0893	16.794 <0.001	Yes
eosin Y vs. 24h UV eosin Y	0.089	16.731 <0.001	Yes
NA vs. eosin Y	0.081	15.227 <0.001	Yes
0h UV eosin vs. 6h UV eosin	0.0453	8.522 <0.001	Yes
0h UV eosin vs. 48h UV eosin	0.0447	8.397 <0.001	Yes
eosin Y vs. 0h UV eosin Y	0.0447	8.397 <0.001	Yes
0h UV eosin vs. 24h UV eosin	0.0443	8.334 <0.001	Yes
24h UV eosin vs. 6h UV eosin	0.001	0.188 0.997	No
48h UV eosin vs. 6h UV eosin	0.000667	0.125 0.99	No
24h UV eosin vs. 48h UV eosin	0.000333	0.0627 0.951	No

Figure 2.13 UV - p-AKT

One Way Analysis of Variance

Data source: Data 1 in UV time eosin Y WB

Normality Test (Shapiro-Wilk) Failed (P < 0.050)

Equal Variance Test: Passed (P = 0.186)

Group Name	N	Missing	Mean	Std Dev	SEM
NA	3	0	1	0.0964	0.0556
eoain Y	3	0	1.043	0.115	0.0662
eosin Y UV 0h	3	0	0.0594	0.00737	0.00425
eosin Y UV 6h	3	0	0.0401	0.00549	0.00317
eosin Y UV 24h	3	0	0.015	0.00153	0.000882
eosin Y UV 48h	3	0	0.0351	0.0122	0.00704

Source of Variation	DF	SS	MS	F	P
Between Groups	5	3.88	0.776	205.414	<0.001
Residual	12	0.0453	0.00378		
Total	17	3.925			

The differences in the mean values among the treatment groups are greater than would be expected by chance; there is a statistically significant difference (P = <0.001).

Power of performed test with alpha = 0.050: 1.000

All Pairwise Multiple Comparison Procedures (Holm-Sidak method):

Overall significance level = 0.05

Comparisons for factor:

Comparison	Diff of Me t	P	P<0.050
eoain Y vs. eosin Y UV 24h	1.028	20.485 <0.001	Yes
eoain Y vs. eosin Y UV 48h	1.008	20.085 <0.001	Yes
eoain Y vs. eosin Y UV 6h	1.003	19.986 <0.001	Yes
NA vs. eosin Y UV 24h	0.985	19.628 <0.001	Yes
eoain Y vs. eosin Y UV 0h	0.984	19.6 <0.001	Yes
NA vs. eosin Y UV 48h	0.965	19.228 <0.001	Yes
NA vs. eosin Y UV 6h	0.96	19.129 <0.001	Yes
NA vs. eosin Y UV 0h	0.941	18.744 <0.001	Yes
eosin Y UV 0 vs. eosin Y UV 2	0.0444	0.885	0.97 No
eoain Y vs. NA	0.043	0.857	0.957 No
eosin Y UV 6 vs. eosin Y UV 2	0.0251	0.5	0.993 No
eosin Y UV 0 vs. eosin Y UV 4	0.0243	0.485	0.983 No
eosin Y UV 4 vs. eosin Y UV 2	0.0201	0.4	0.972 No
eosin Y UV 0 vs. eosin Y UV 6	0.0193	0.385	0.914 No
eosin Y UV 6 vs. eosin Y UV 4	0.00501	0.0998	0.922 No

Figure 2.13 UV - AKT1

Normality Test (Shapiro-Wilk) Passed (P = 0.268)

Equal Variance Test: Passed (P = 0.857)

Group Name	N	Missing	Mean	Std Dev	SEM
NA	3	0	1	0.0397	0.0229
eoain Y	3	0	1.116	0.0706	0.0407
eosin Y UV 0h	3	0	1.321	0.122	0.0704
eosin Y UV 6h	3	0	1.399	0.145	0.0837
eosin Y UV 24h	3	0	1.59	0.0696	0.0402
eosin Y UV 48h	3	0	1.504	0.0727	0.042

Source of Variation	DF	SS	MS	F	P
Between Groups	5	0.772	0.154	17.62	<0.001
Residual	12	0.105	0.00876		
Total	17	0.877			

The differences in the mean values among the treatment groups are greater than would be expected by chance; there is a statistically significant difference (P = <0.001).

Power of performed test with alpha = 0.050: 1.000

All Pairwise Multiple Comparison Procedures (Holm-Sidak method):
Overall significance level = 0.05

Comparisons for factor:

Comparison	Diff of Me t	P	P<0.050
eosin Y UV 24h vs. NA	0.59	7.725 <0.001	Yes
eosin Y UV 48h vs. NA	0.504	6.595 <0.001	Yes
eosin Y UV 24h vs. eoain Y	0.475	6.211 <0.001	Yes
eosin Y UV 6h vs. NA	0.399	5.216 0.003	Yes
eosin Y UV 48h vs. eoain Y	0.388	5.082 0.003	Yes
eosin Y UV 0h vs. NA	0.321	4.195 0.012	Yes
eosin Y UV 6h vs. eoain Y	0.283	3.702 0.027	Yes
eosin Y UV 2 vs. eosin Y UV 0	0.27	3.53 0.033	Yes
eosin Y UV 0h vs. eoain Y	0.205	2.681 0.132	No
eosin Y UV 2 vs. eosin Y UV 6	0.192	2.509 0.154	No
eosin Y UV 4 vs. eosin Y UV 0	0.183	2.4 0.157	No
eoain Y vs. NA	0.116	1.514 0.493	No
eosin Y UV 4 vs. eosin Y UV 6	0.105	1.379 0.474	No
eosin Y UV 2 vs. eosin Y UV 4	0.0863	1.129 0.483	No
eosin Y UV 6 vs. eosin Y UV 0	0.078	1.021 0.327	No

Figure 3.2

One Way Analysis of Variance

Data source: Data 1 in Notebook1

Normality Test (Shapiro-Wilk) Failed (P < 0.050)

Equal Variance Test: Failed (P < 0.050)

Group Name	N	Missing	Mean	Std Dev	SEM
NA	4	0	100	3.136	1.568
PEG17.4	4	0	95.716	4.984	2.492
PEG87	4	0	83.197	3.546	1.773
PEG174	4	0	70.769	2.238	1.119
PEG696	4	0	35.156	9.383	4.691
PEG1739	4	0	8.231	0.467	0.233
PEG-DA17.4	4	0	70.358	1.605	0.803
PEG-DA87	4	0	18.78	0.589	0.295
PEG-DA174	4	0	7.979	0.61	0.305
PEG-DA696	4	0	8.214	0.759	0.38
PEG-DA1739	4	0	7.946	0.355	0.178

Source of Variation	DF	SS	MS	F	P
Between Groups	10	58338.12	5833.812	444.062	<0.001
Residual	33	433.533	13.137		
Total	43	58771.65			

The differences in the mean values among the treatment groups are greater than would be expected by chance; there is a statistically significant difference (P = <0.001).

Power of performed test with alpha = 0.050: 1.000

All Pairwise Multiple Comparison Procedures (Holm-Sidak method):

Overall significance level = 0.05

Comparisons for factor:

Comparison	Diff of Me t	P	P<0.050
NA vs. PEG-DA1739	92.054	35.917 <0.001	Yes
NA vs. PEG-DA174	92.021	35.905 <0.001	Yes
NA vs. PEG-DA696	91.786	35.813 <0.001	Yes
NA vs. PEG1739	91.769	35.806 <0.001	Yes
PEG17.4 vs. PEG-DA1739	87.769	34.245 <0.001	Yes
PEG17.4 vs. PEG-DA174	87.737	34.233 <0.001	Yes
PEG17.4 vs. PEG-DA696	87.501	34.141 <0.001	Yes
PEG17.4 vs. PEG1739	87.485	34.135 <0.001	Yes
NA vs. PEG-DA87	81.22	31.69 <0.001	Yes
PEG17.4 vs. PEG-DA87	76.935	30.018 <0.001	Yes

PEG87 vs. PEG-DA1739	75.25	29.361	<0.001	Yes
PEG87 vs. PEG-DA174	75.218	29.348	<0.001	Yes
PEG87 vs. PEG-DA696	74.982	29.256	<0.001	Yes
PEG87 vs. PEG1739	74.966	29.25	<0.001	Yes
NA vs. PEG696	64.844	25.3	<0.001	Yes
PEG87 vs. PEG-DA87	64.417	25.134	<0.001	Yes
PEG174 vs. PEG-DA1739	62.822	24.512	<0.001	Yes
PEG174 vs. PEG-DA174	62.79	24.499	<0.001	Yes
PEG174 vs. PEG-DA696	62.554	24.407	<0.001	Yes
PEG174 vs. PEG1739	62.538	24.401	<0.001	Yes
PEG-DA17.4 vs. PEG-DA1739	62.412	24.352	<0.001	Yes
PEG-DA17.4 vs. PEG-DA174	62.38	24.339	<0.001	Yes
PEG-DA17.4 vs. PEG-DA696	62.144	24.247	<0.001	Yes
PEG-DA17.4 vs. PEG1739	62.128	24.241	<0.001	Yes
PEG17.4 vs. PEG696	60.559	23.629	<0.001	Yes
PEG174 vs. PEG-DA87	51.989	20.285	<0.001	Yes
PEG-DA17.4 vs. PEG-DA87	51.578	20.125	<0.001	Yes
PEG87 vs. PEG696	48.04	18.744	<0.001	Yes
PEG174 vs. PEG696	35.612	13.895	<0.001	Yes
PEG-DA17.4 vs. PEG696	35.202	13.735	<0.001	Yes
NA vs. PEG-DA17.4	29.642	11.565	<0.001	Yes
NA vs. PEG174	29.231	11.405	<0.001	Yes
PEG696 vs. PEG-DA1739	27.21	10.617	<0.001	Yes
PEG696 vs. PEG-DA174	27.178	10.604	<0.001	Yes
PEG696 vs. PEG-DA696	26.942	10.512	<0.001	Yes
PEG696 vs. PEG1739	26.926	10.506	<0.001	Yes
PEG17.4 vs. PEG-DA17.4	25.357	9.894	<0.001	Yes
PEG17.4 vs. PEG174	24.947	9.734	<0.001	Yes
NA vs. PEG87	16.803	6.556	<0.001	Yes
PEG696 vs. PEG-DA87	16.376	6.39	<0.001	Yes
PEG87 vs. PEG-DA17.4	12.838	5.009	<0.001	Yes
PEG17.4 vs. PEG87	12.519	4.885	<0.001	Yes
PEG87 vs. PEG174	12.428	4.849	<0.001	Yes
PEG-DA87 vs. PEG-DA1739	10.834	4.227	0.002	Yes
PEG-DA87 vs. PEG-DA174	10.801	4.214	0.002	Yes
PEG-DA87 vs. PEG-DA696	10.566	4.123	0.002	Yes
PEG-DA87 vs. PEG1739	10.55	4.116	0.002	Yes
NA vs. PEG17.4	4.284	1.672	0.585	No
PEG174 vs. PEG-DA17.4	0.41	0.16	1	No
PEG1739 vs. PEG-DA1739	0.284	0.111	1	No
PEG-DA696 vs. PEG-DA1739	0.268	0.105	1	No
PEG1739 vs. PEG-DA174	0.252	0.0983	1	No
PEG-DA696 vs. PEG-DA174	0.236	0.0919	1	No
PEG-DA174 vs. PEG-DA1739	0.0323	0.0126	1	No
PEG1739 vs. PEG-DA696	0.0163	0.00635	0.995	No

Figure 3.3

One Way Analysis of Variance

Data source: Data 1 in Notebook1

Normality Test (Shapiro-Wilk) Failed (P < 0.050)

Equal Variance Test: Failed (P < 0.050)

Group Name	N	Missing	Mean	Std Dev	SEM
NA	4	0	99.725	6.073	3.037
GF/0PEGDA+5eY	4	0	112.4	1.146	0.573
GF/1PEGDA+5eY	4	0	106.95	3.648	1.824
GF/2PEGDA+5eY	4	0	17.336	1.563	0.781
GF/5PEGDA+5eY	4	0	2.95	0.265	0.132
GF/10PEGDA+5eY	4	0	3.325	0.222	0.111
GF/20PEGDA+5eY	4	0	3.95	0.3	0.15

Source of Variation	DF	SS	MS	F	P
Between Groups	6	68751.17	11458.53	1481.032	<0.001
Residual	21	162.474	7.737		
Total	27	68913.65			

The differences in the mean values among the treatment groups are greater than would be expected by chance; there is a statistically significant difference (P = <0.001).

Power of performed test with alpha = 0.050: 1.000

All Pairwise Multiple Comparison Procedures (Holm-Sidak method):

Overall significance level = 0.05

Comparisons for factor:

Comparison	Diff of Me t	P	P<0.050
GF/0PEGDA+5e vs. GF/5PEGDA+5	109.45	55.648 <0.001	Yes
GF/0PEGDA+5e vs. GF/10PEGDA+	109.075	55.457 <0.001	Yes
GF/0PEGDA+5e vs. GF/20PEGDA+	108.45	55.139 <0.001	Yes
GF/1PEGDA+5e vs. GF/5PEGDA+5	104	52.877 <0.001	Yes
GF/1PEGDA+5e vs. GF/10PEGDA+	103.625	52.686 <0.001	Yes
GF/1PEGDA+5e vs. GF/20PEGDA+	103	52.368 <0.001	Yes
NA vs. GF/5PEGDA+5eY	96.775	49.204 <0.001	Yes
NA vs. GF/10PEGDA+5eY	96.4	49.013 <0.001	Yes
NA vs. GF/20PEGDA+5eY	95.775	48.695 <0.001	Yes
GF/0PEGDA+5e vs. GF/2PEGDA+5	95.064	48.333 <0.001	Yes
GF/1PEGDA+5e vs. GF/2PEGDA+5	89.614	45.562 <0.001	Yes
NA vs. GF/2PEGDA+5eY	82.389	41.889 <0.001	Yes
GF/2PEGDA+5e vs. GF/5PEGDA+5	14.386	7.315 <0.001	Yes
GF/2PEGDA+5e vs. GF/10PEGDA+	14.011	7.124 <0.001	Yes

GF/2PEGDA+5e vs. GF/20PEGDA+	13.386	6.806	<0.001	Yes
GF/0PEGDA+5eY vs. NA	12.675	6.444	<0.001	Yes
GF/1PEGDA+5eY vs. NA	7.225	3.673	0.007	Yes
GF/0PEGDA+5e vs. GF/1PEGDA+5	5.45	2.771	0.045	Yes
GF/20PEGDA+5 vs. GF/5PEGDA+5	1	0.508	0.944	No
GF/20PEGDA+5 vs. GF/10PEGDA+	0.625	0.318	0.939	No
GF/10PEGDA+5 vs. GF/5PEGDA+5	0.375	0.191	0.851	No

Figure 3.4

One Way Analysis of Variance

Data source: Data 1 in Notebook1

Normality Test (Shapiro-Wilk) Failed (P < 0.050)

Equal Variance Test: Failed (P < 0.050)

Group Name	N	Missing	Mean	Std Dev	SEM
0min	5	0	100	0	0
GF-15min	5	0	0.15	0.077	0.0345
GF/0eY-15min	5	0	0.124	0.063	0.0282
GF/2eY-15min	5	0	49.38	5.372	2.402
GF/5eY-15min	5	0	75.497	2.322	1.038
GF/10eY-15min	5	0	77.562	0.421	0.188
GF/2eY-30min	5	0	29.828	12.544	5.61
GF/5eY-30min	5	0	65.323	6.071	2.715
GF/10eY-30min	5	0	77.97	1.246	0.557
GF/2eY-60min	5	0	1.688	2.433	1.088
GF/5eY-60min	5	0	45.016	9.581	4.285
GF/10eY-60min	5	0	75.544	3.682	1.647
GF/2eY-120min	5	0	0	0	0
GF/5eY-120min	5	0	23.846	11.855	5.302
GF/10eY-120min	5	0	70.657	2.783	1.245

Source of Variation	DF	SS	MS	F	P
Between Groups	14	83545.78	5967.556	182.775	<0.001
Residual	60	1958.988	32.65		
Total	74	85504.77			

The differences in the mean values among the treatment groups are greater than would be expected by chance; there is a statistically significant difference (P = <0.001).

Power of performed test with alpha = 0.050: 1.000

All Pairwise Multiple Comparison Procedures (Holm-Sidak method):

Overall significance level = 0.05

Comparisons for factor:

Comparison	Diff of Me t	P	P<0.050
0min vs. GF/2eY-120min	100	27.671 <0.001	Yes
0min vs. GF/0eY-15min	99.876	27.637 <0.001	Yes
0min vs. GF-15min	99.85	27.63 <0.001	Yes
0min vs. GF/2eY-60min	98.312	27.204 <0.001	Yes
GF/10eY-30mi vs. GF/2eY-120mi	77.97	21.575 <0.001	Yes
GF/10eY-30min vs. GF/0eY-15min	77.846	21.541 <0.001	Yes

GF/10eY-30min vs. GF-15min	77.82	21.534	<0.001	Yes
GF/10eY-15mi vs. GF/2eY-120mi	77.562	21.462	<0.001	Yes
GF/10eY-15min vs. GF/0eY-15min	77.438	21.428	<0.001	Yes
GF/10eY-15min vs. GF-15min	77.412	21.421	<0.001	Yes
GF/10eY-30min vs. GF/2eY-60min	76.282	21.108	<0.001	Yes
0min vs. GF/5eY-120min	76.154	21.073	<0.001	Yes
GF/10eY-15min vs. GF/2eY-60min	75.874	20.995	<0.001	Yes
GF/10eY-60mi vs. GF/2eY-120mi	75.544	20.904	<0.001	Yes
GF/5eY-15min vs. GF/2eY-120min	75.497	20.891	<0.001	Yes
GF/10eY-60min vs. GF/0eY-15min	75.42	20.87	<0.001	Yes
GF/10eY-60min vs. GF-15min	75.394	20.863	<0.001	Yes
GF/5eY-15min vs. GF/0eY-15min	75.373	20.857	<0.001	Yes
GF/5eY-15min vs. GF-15min	75.347	20.85	<0.001	Yes
GF/10eY-60min vs. GF/2eY-60min	73.856	20.437	<0.001	Yes
GF/5eY-15min vs. GF/2eY-60min	73.809	20.424	<0.001	Yes
GF/10eY-120m vs. GF/2eY-120mi	70.657	19.552	<0.001	Yes
GF/10eY-120m vs. GF/0eY-15min	70.533	19.517	<0.001	Yes
GF/10eY-120min vs. GF-15min	70.507	19.51	<0.001	Yes
0min vs. GF/2eY-30min	70.172	19.417	<0.001	Yes
GF/10eY-120m vs. GF/2eY-60min	68.969	19.085	<0.001	Yes
GF/5eY-30min vs. GF/2eY-120min	65.323	18.076	<0.001	Yes
GF/5eY-30min vs. GF/0eY-15min	65.199	18.042	<0.001	Yes
GF/5eY-30min vs. GF-15min	65.174	18.034	<0.001	Yes
GF/5eY-30min vs. GF/2eY-60min	63.636	17.609	<0.001	Yes
0min vs. GF/5eY-60min	54.984	15.215	<0.001	Yes
GF/10eY-30mi vs. GF/5eY-120mi	54.123	14.977	<0.001	Yes
GF/10eY-15mi vs. GF/5eY-120mi	53.716	14.864	<0.001	Yes
GF/10eY-60mi vs. GF/5eY-120mi	51.698	14.305	<0.001	Yes
GF/5eY-15min vs. GF/5eY-120min	51.65	14.292	<0.001	Yes
0min vs. GF/2eY-15min	50.62	14.007	<0.001	Yes
GF/2eY-15min vs. GF/2eY-120min	49.38	13.664	<0.001	Yes
GF/2eY-15min vs. GF/0eY-15min	49.256	13.63	<0.001	Yes
GF/2eY-15min vs. GF-15min	49.231	13.623	<0.001	Yes
GF/10eY-30min vs. GF/2eY-30min	48.141	13.321	<0.001	Yes
GF/10eY-15min vs. GF/2eY-30min	47.733	13.208	<0.001	Yes
GF/2eY-15min vs. GF/2eY-60min	47.693	13.197	<0.001	Yes
GF/10eY-120m vs. GF/5eY-120mi	46.81	12.953	<0.001	Yes
GF/10eY-60min vs. GF/2eY-30min	45.716	12.65	<0.001	Yes
GF/5eY-15min vs. GF/2eY-30min	45.668	12.637	<0.001	Yes
GF/5eY-60min vs. GF/2eY-120min	45.016	12.456	<0.001	Yes
GF/5eY-60min vs. GF/0eY-15min	44.892	12.422	<0.001	Yes
GF/5eY-60min vs. GF-15min	44.866	12.415	<0.001	Yes
GF/5eY-60min vs. GF/2eY-60min	43.328	11.989	<0.001	Yes
GF/5eY-30min vs. GF/5eY-120min	41.477	11.477	<0.001	Yes
GF/10eY-120m vs. GF/2eY-30min	40.828	11.298	<0.001	Yes
GF/5eY-30min vs. GF/2eY-30min	35.495	9.822	<0.001	Yes
0min vs. GF/5eY-30min	34.677	9.595	<0.001	Yes
GF/10eY-30min vs. GF/5eY-60min	32.954	9.119	<0.001	Yes
GF/10eY-15min vs. GF/5eY-60min	32.546	9.006	<0.001	Yes

GF/10eY-60min vs. GF/5eY-60min	30.528	8.448	<0.001	Yes
GF/5eY-15min vs. GF/5eY-60min	30.481	8.435	<0.001	Yes
GF/2eY-30min vs. GF/2eY-120min	29.828	8.254	<0.001	Yes
GF/2eY-30min vs. GF/0eY-15min	29.704	8.22	<0.001	Yes
GF/2eY-30min vs. GF-15min	29.679	8.213	<0.001	Yes
0min vs. GF/10eY-120min	29.343	8.12	<0.001	Yes
GF/10eY-30min vs. GF/2eY-15min	28.589	7.911	<0.001	Yes
GF/10eY-15min vs. GF/2eY-15min	28.182	7.798	<0.001	Yes
GF/2eY-30min vs. GF/2eY-60min	28.141	7.787	<0.001	Yes
GF/10eY-60min vs. GF/2eY-15min	26.164	7.24	<0.001	Yes
GF/5eY-15min vs. GF/2eY-15min	26.116	7.227	<0.001	Yes
GF/10eY-120m vs. GF/5eY-60min	25.641	7.095	<0.001	Yes
GF/2eY-15min vs. GF/5eY-120min	25.534	7.066	<0.001	Yes
0min vs. GF/5eY-15min	24.503	6.78	<0.001	Yes
0min vs. GF/10eY-60min	24.456	6.767	<0.001	Yes
GF/5eY-120mi vs. GF/2eY-120mi	23.846	6.599	<0.001	Yes
GF/5eY-120min vs. GF/0eY-15min	23.722	6.564	<0.001	Yes
GF/5eY-120min vs. GF-15min	23.697	6.557	<0.001	Yes
0min vs. GF/10eY-15min	22.438	6.209	<0.001	Yes
GF/5eY-120min vs. GF/2eY-60min	22.159	6.132	<0.001	Yes
0min vs. GF/10eY-30min	22.03	6.096	<0.001	Yes
GF/10eY-120m vs. GF/2eY-15min	21.276	5.887	<0.001	Yes
GF/5eY-60min vs. GF/5eY-120min	21.169	5.858	<0.001	Yes
GF/5eY-30min vs. GF/5eY-60min	20.308	5.619	<0.001	Yes
GF/2eY-15min vs. GF/2eY-30min	19.552	5.41	<0.001	Yes
GF/5eY-30min vs. GF/2eY-15min	15.943	4.412	0.001	Yes
GF/5eY-60min vs. GF/2eY-30min	15.187	4.202	0.002	Yes
GF/10eY-30min vs. GF/5eY-30min	12.646	3.499	0.02	Yes
GF/10eY-15min vs. GF/5eY-30min	12.239	3.387	0.027	Yes
GF/10eY-60min vs. GF/5eY-30min	10.221	2.828	0.125	No
GF/5eY-15min vs. GF/5eY-30min	10.173	2.815	0.124	No
GF/10eY-30mi vs. GF/10eY-120m	7.313	2.024	0.603	No
GF/10eY-15mi vs. GF/10eY-120m	6.905	1.911	0.677	No
GF/2eY-30min vs. GF/5eY-120min	5.982	1.655	0.843	No
GF/10eY-120m vs. GF/5eY-30min	5.333	1.476	0.919	No
GF/10eY-60mi vs. GF/10eY-120m	4.887	1.352	0.95	No
GF/5eY-15min vs. GF/10eY-120m	4.84	1.339	0.943	No
GF/2eY-15min vs. GF/5eY-60min	4.365	1.208	0.968	No
GF/10eY-30min vs. GF/5eY-15min	2.473	0.684	1	No
GF/10eY-30mi vs. GF/10eY-60mi	2.425	0.671	1	No
GF/10eY-15min vs. GF/5eY-15min	2.065	0.571	1	No
GF/10eY-15mi vs. GF/10eY-60mi	2.018	0.558	1	No
GF/2eY-60min vs. GF/2eY-120min	1.688	0.467	1	No
GF/2eY-60min vs. GF/0eY-15min	1.564	0.433	1	No
GF/2eY-60min vs. GF-15min	1.538	0.426	0.999	No
GF/10eY-30mi vs. GF/10eY-15mi	0.408	0.113	1	No
GF-15min vs. GF/2eY-120min	0.15	0.0414	1	No
GF/0eY-15min vs. GF/2eY-120min	0.124	0.0343	1	No
GF/10eY-60min vs. GF/5eY-15min	0.0474	0.0131	1	No

GF-15min vs. GF/0eY-15min

0.0257

0.0071

0.994 No

Figure 3.5

One Way Analysis of Variance

Data source: Data 1 in Notebook1

Thickness (inch)

Normality Test (Shapiro-Wilk) Passed (P = 0.138)

Equal Variance Test: Failed (P < 0.050)

Group Name	N	Missing	Mean	Std Dev	SEM
GF	18	0	0.0177	0.00372	0.000877
sIPN GF	12	0	0.0145	0.00166	0.000479

Source of Variation	DF	SS	MS	F	P
Between Groups	1	7.03E-05	7.03E-05	7.409	0.011
Residual	28	0.000266	9.49E-06		
Total	29	0.000336			

The differences in the mean values among the treatment groups are greater than would be expected by chance; there is a statistically significant difference (P = 0.011).

Power of performed test with alpha = 0.050: 0.691

All Pairwise Multiple Comparison Procedures (Holm-Sidak method):

Overall significance level = 0.05

Comparisons for factor:

Comparison	Diff of Me t	P	P<0.050
GF vs. sIPN GF	0.00312	2.722	0.011 Yes

Peak Load (N)

Normality Test (Shapiro-Wilk) Passed (P = 0.954)

Equal Variance Test: Passed (P = 0.936)

Group Name	N	Missing	Mean	Std Dev	SEM
GF	18	0	2.414	1.23	0.29
sIPN GF	12	0	15.74	1.428	0.412

Source of Variation	DF	SS	MS	F	P
Between Groups	1	1278.752	1278.752	743.72	<0.001
Residual	28	48.143	1.719		
Total	29	1326.896			

The differences in the mean values among the treatment groups are greater than would be expected by chance; there is a statistically significant difference ($P = <0.001$).

Power of performed test with $\alpha = 0.050$: 1.000

All Pairwise Multiple Comparison Procedures (Holm-Sidak method):
Overall significance level = 0.05

Comparisons for factor:

Comparison	Diff of Me t	P	P<0.050
sIPN GF vs. GF	13.327	27.271 <0.001	Yes

Peak Stress (Mpa)

Normality Test (Shapiro-Wilk) Passed (P = 0.094)

Equal Variance Test: Passed (P = 0.729)

Group Name	N	Missing	Mean	Std Dev	SEM
GF	18	0	2.037	1.095	0.258
sIPN GF	12	0	16.067	1.474	0.425

Source of Variation	DF	SS	MS	F	P
Between Groups	1	1417.271	1417.271	896.475	<0.001
Residual	28	44.266	1.581		
Total	29	1461.538			

The differences in the mean values among the treatment groups are greater than would be expected by chance; there is a statistically significant difference ($P = <0.001$).

Power of performed test with $\alpha = 0.050$: 1.000

All Pairwise Multiple Comparison Procedures (Holm-Sidak method):
Overall significance level = 0.05

Comparisons for factor:

Comparison	Diff of Me t	P	P<0.050
sIPN GF vs. GF	14.03	29.941 <0.001	Yes

Modulus (Mpa)

Normality Test (Shapiro-Wilk) Passed (P = 0.073)

Equal Variance Test: Passed (P = 0.443)

Group Name	N	Missing	Mean	Std Dev	SEM
GF	18	0	135.485	53.042	12.502
sIPN GF	12	0	676.871	74.447	21.491

Source of Variation	DF	SS	MS	F	P
Between Groups	1	2110312	2110312	543.128	<0.001
Residual	28	108793.4	3885.477		
Total	29	2219105			

The differences in the mean values among the treatment groups are greater than would be expected by chance; there is a statistically significant difference (P = <0.001).

Power of performed test with alpha = 0.050: 1.000

All Pairwise Multiple Comparison Procedures (Holm-Sidak method):
Overall significance level = 0.05

Comparisons for factor:

Comparison	Diff of Me t	P	P<0.050
sIPN GF vs. GF	541.386	23.305 <0.001	Yes

Strain At Break (mm/mm)

Normality Test (Shapiro-Wilk) Passed (P = 0.833)

Equal Variance Test: Passed (P = 0.491)

Group Name	N	Missing	Mean	Std Dev	SEM
GF	18	0	0.0208	0.00772	0.00182
sIPN GF	12	0	0.0497	0.00925	0.00267

Source of Variation	DF	SS	MS	F	P
Between Groups	1	0.00602	0.00602	86.326	<0.001
Residual	28	0.00195	6.97E-05		
Total	29	0.00797			

The differences in the mean values among the treatment groups are greater than would be expected by chance; there is a statistically significant difference (P = <0.001).

Power of performed test with alpha = 0.050: 1.000

All Pairwise Multiple Comparison Procedures (Holm-Sidak method):
Overall significance level = 0.05

Comparisons for factor:

Comparison	Diff of Me t	P	P<0.050
sIPN GF vs. GF	0.0289	9.291 <0.001	Yes

Energy To Break (N*mm)

Normality Test (Shapiro-Wilk) Failed (P < 0.050)

Equal Variance Test: Failed (P < 0.050)

Group Name	N	Missing	Mean	Std Dev	SEM
GF	18	0	0.227	0.17	0.04
sIPN GF	12	0	3.884	1.179	0.34

Source of Variation	DF	SS	MS	F	P
Between Groups	1	96.258	96.258	170.807	<0.001
Residual	28	15.779	0.564		
Total	29	112.037			

The differences in the mean values among the treatment groups are greater than would be expected by chance; there is a statistically significant difference (P = <0.001).

Power of performed test with alpha = 0.050: 1.000

All Pairwise Multiple Comparison Procedures (Holm-Sidak method):

Overall significance level = 0.05

Comparisons for factor:

Comparison	Diff of Me t	P	P<0.050
sIPN GF vs. GF	3.656	13.069 <0.001	Yes

Figure 3.7

One Way Analysis of Variance

Data source: Data 1 in Notebook1

Normality Test (Shapiro-Wilk) Failed (P < 0.050)

Equal Variance Test: Passed (P = 0.473)

Group Name	N	Missing	Mean	Std Dev	SEM
GF	60	0	3.154	1.244	0.161
sIPN GF	60	0	4.868	1.522	0.197

Source of Variation	DF	SS	MS	F	P
Between Groups	1	88.121	88.121	45.594	<0.001
Residual	118	228.061	1.933		
Total	119	316.182			

The differences in the mean values among the treatment groups are greater than would be expected by chance; there is a statistically significant difference (P = <0.001).

Power of performed test with alpha = 0.050: 1.000

All Pairwise Multiple Comparison Procedures (Holm-Sidak method):
Overall significance level = 0.05

Comparisons for factor:

Comparison	Diff of Me t	P	P<0.050
sIPN GF vs. GF	1.714	6.752 <0.001	Yes

Figure 3.9

One Way Analysis of Variance

Data source: Data 1 in Notebook1

Normality Test (Shapiro-Wilk) Passed (P = 0.592)

Equal Variance Test: Passed (P = 0.417)

Group Name	N	Missing	Mean	Std Dev	SEM
sIPN GIF 15min	3	0	44.792	1.96	1.132
sIPN GIF 30min	3	0	48.371	1.974	1.14
sIPN GIF 60min	3	0	53.276	1.889	1.09
sIPN GIF 90min	3	0	56.532	2.657	1.534
sIPN GIF 120min	3	0	58.556	4.108	2.372
sIPN GIF 240min	3	0	64.451	3.007	1.736
GIF 15min	3	0	56.304	0.827	0.478
GIF 30min	3	0	65.122	0.652	0.376

Source of Variation	DF	SS	MS	F	P
Between Groups	7	1058.221	151.174	26.642	<0.001
Residual	16	90.79	5.674		
Total	23	1149.011			

The differences in the mean values among the treatment groups are greater than would be expected by chance; there is a statistically significant difference (P = <0.001).

Power of performed test with alpha = 0.050: 1.000

All Pairwise Multiple Comparison Procedures (Holm-Sidak method):
Overall significance level = 0.05

Comparisons for factor:

Comparison	Diff of Me t	P	P<0.050
GIF 30min vs. sIPN GIF 15min	20.33	10.453 <0.001	Yes
sIPN GIF 240 vs. sIPN GIF 15m	19.659	10.108 <0.001	Yes
GIF 30min vs. sIPN GIF 30min	16.751	8.612 <0.001	Yes
sIPN GIF 240 vs. sIPN GIF 30m	16.08	8.268 <0.001	Yes
sIPN GIF 120 vs. sIPN GIF 15m	13.764	7.077 <0.001	Yes
GIF 30min vs. sIPN GIF 60min	11.846	6.09 <0.001	Yes
sIPN GIF 90m vs. sIPN GIF 15m	11.74	6.036 <0.001	Yes
GIF 15min vs. sIPN GIF 15min	11.512	5.919 <0.001	Yes
sIPN GIF 240 vs. sIPN GIF 60m	11.175	5.746 <0.001	Yes
sIPN GIF 120 vs. sIPN GIF 30m	10.185	5.237 0.002	Yes
GIF 30min vs. GIF 15min	8.818	4.534 0.006	Yes
GIF 30min vs. sIPN GIF 90min	8.59	4.416 0.007	Yes
sIPN GIF 60m vs. sIPN GIF 15m	8.484	4.362 0.008	Yes

sIPN GIF 90m vs. sIPN GIF 30m	8.161	4.196	0.01	Yes
sIPN GIF 240min vs. GIF 15min	8.147	4.189	0.01	Yes
GIF 15min vs. sIPN GIF 30min	7.933	4.079	0.011	Yes
sIPN GIF 240 vs. sIPN GIF 90m	7.919	4.071	0.011	Yes
GIF 30min vs. sIPN GIF 120min	6.566	3.376	0.042	Yes
sIPN GIF 240 vs. sIPN GIF 120	5.895	3.031	0.077	No
sIPN GIF 120 vs. sIPN GIF 60m	5.28	2.715	0.13	No
sIPN GIF 60m vs. sIPN GIF 30m	4.905	2.522	0.167	No
sIPN GIF 30m vs. sIPN GIF 15m	3.579	1.84	0.46	No
sIPN GIF 90m vs. sIPN GIF 60m	3.256	1.674	0.515	No
GIF 15min vs. sIPN GIF 60min	3.028	1.557	0.527	No
sIPN GIF 120min vs. GIF 15min	2.252	1.158	0.707	No
sIPN GIF 120 vs. sIPN GIF 90m	2.024	1.04	0.677	No
GIF 30min vs. sIPN GIF 240min	0.671	0.345	0.93	No
sIPN GIF 90min vs. GIF 15min	0.228	0.117	0.908	No

Figure 3.11

One Way Analysis of Variance

Data source: Data 1 in Notebook1

p-AKT

Normality Test (Shapiro-Wilk) Passed (P = 0.143)

Equal Variance Test: Failed (P < 0.050)

Group Name	N	Missing	Mean	Std Dev	SEM
NA	4	0	1	0	0
Insulin	4	0	6.207	0.128	0.0641
GF	4	0	1.855	0.687	0.343
sIPN GF	4	0	1.512	0.647	0.323
GIF	4	0	6.326	0.443	0.222

Source of Variation	DF	SS	MS	F	P
Between Groups	4	112.608	28.152	127.609	<0.001
Residual	15	3.309	0.221		
Total	19	115.917			

The differences in the mean values among the treatment groups are greater than would be expected by chance; there is a statistically significant difference (P = <0.001).

Power of performed test with alpha = 0.050: 1.000

All Pairwise Multiple Comparison Procedures (Holm-Sidak method):

Overall significance level = 0.05

Comparisons for factor:

Comparison	Diff of Me t	P	P<0.050
GIF vs. NA	5.326	16.037 <0.001	Yes
Insulin vs. NA	5.207	15.678 <0.001	Yes
GIF vs. sIPN GF	4.815	14.496 <0.001	Yes
Insulin vs. sIPN GF	4.695	14.137 <0.001	Yes
GIF vs. GF	4.471	13.462 <0.001	Yes
Insulin vs. GF	4.352	13.102 <0.001	Yes
GF vs. NA	0.855	2.576 0.082	No
sIPN GF vs. NA	0.512	1.541 0.373	No
GF vs. sIPN GF	0.344	1.035 0.534	No
GIF vs. Insulin	0.119	0.359 0.724	No

AKT1

Normality Test (Shapiro-Wilk) Passed (P = 0.489)

Equal Variance Test: Passed (P = 0.155)

Group Name	N	Missing	Mean	Std Dev	SEM
NA	4	0	1	0	0
Insulin	4	0	0.889	0.126	0.063
GF	4	0	0.967	0.143	0.0716
sIPN GF	4	0	1.04	0.112	0.0561
GIF	4	0	0.924	0.175	0.0874

Source of Variation	DF	SS	MS	F	P
Between Groups	4	0.0576	0.0144	0.905	0.486
Residual	15	0.239	0.0159		
Total	19	0.296			

The differences in the mean values among the treatment groups are not great enough to exclude the possibility that the difference is due to random sampling variability; there is not a statistically significant difference (P = 0.486).

Power of performed test with alpha = 0.050: 0.050

The power of the performed test (0.050) is below the desired power of 0.800.

Less than desired power indicates you are less likely to detect a difference when one actually exists. Negative results should be interpreted cautiously.

Figure 3.12

One Way Analysis of Variance

Data source: Data 1 in Notebook1

p-AKT

Normality Test (Shapiro-Wilk) Failed (P < 0.050)

Equal Variance Test: Passed (P = 1.000)

Group Name	N	Missing	Mean	Std Dev	SEM
NA	3	0	1	0	0
GIF 30min	3	0	6.052	0.275	0.159
sIPN GIF 15min	3	0	3.218	0.659	0.38
sIPN GIF 30min	3	0	3.712	0.967	0.559
sIPN GIF 60min	3	0	4.386	0.757	0.437
sIPN GIF 120min	3	0	5.838	0.668	0.386

Source of Variation	DF	SS	MS	F	P
Between Groups	5	52.264	10.453	25.442	<0.001
Residual	12	4.93	0.411		
Total	17	57.194			

The differences in the mean values among the treatment groups are greater than would be expected by chance; there is a statistically significant difference (P = <0.001).

Power of performed test with alpha = 0.050: 1.000

All Pairwise Multiple Comparison Procedures (Holm-Sidak method):
Overall significance level = 0.05

Comparisons for factor:

Comparison	Diff of Me t	P	P<0.050
GIF 30min vs. NA	5.052	9.653 <0.001	Yes
sIPN GIF 120min vs. NA	4.838	9.243 <0.001	Yes
sIPN GIF 60min vs. NA	3.386	6.469 <0.001	Yes
GIF 30min vs. sIPN GIF 15min	2.833	5.414 0.002	Yes
sIPN GIF 30min vs. NA	2.712	5.183 0.003	Yes
sIPN GIF 120 vs. sIPN GIF 15m	2.619	5.004 0.003	Yes
GIF 30min vs. sIPN GIF 30min	2.339	4.47 0.007	Yes
sIPN GIF 15min vs. NA	2.218	4.239 0.009	Yes
sIPN GIF 120 vs. sIPN GIF 30m	2.125	4.061 0.011	Yes
GIF 30min vs. sIPN GIF 60min	1.666	3.184 0.046	Yes
sIPN GIF 120 vs. sIPN GIF 60m	1.452	2.775 0.081	No
sIPN GIF 60m vs. sIPN GIF 15m	1.167	2.23 0.17	No
sIPN GIF 60m vs. sIPN GIF 30m	0.673	1.286 0.53	No

sIPN GIF 30m vs. sIPN GIF 15m	0.494	0.944	0.595 No
GIF 30min vs. sIPN GIF 120min	0.214	0.409	0.69 No

AKT1

Normality Test (Shapiro-Wilk) Passed (P = 0.168)

Equal Variance Test: Passed (P = 0.064)

Group Name	N	Missing	Mean	Std Dev	SEM
NA	3	0	1	0	0
GIF 30min	3	0	0.928	0.0657	0.038
sIPN GIF 15min	3	0	1.104	0.109	0.0629
sIPN GIF 30min	3	0	1.156	0.0959	0.0554
sIPN GIF 60min	3	0	1.075	0.144	0.0834
sIPN GIF 120min	3	0	1.033	0.268	0.155

Source of Variation	DF	SS	MS	F	P
Between Groups	5	0.0976	0.0195	0.99	0.463
Residual	12	0.236	0.0197		
Total	17	0.334			

The differences in the mean values among the treatment groups are not great enough to exclude the possibility that the difference is due to random sampling variability; there is not a statistically significant difference (P = 0.463).

Power of performed test with alpha = 0.050: 0.050

The power of the performed test (0.050) is below the desired power of 0.800. Less than desired power indicates you are less likely to detect a difference when one actually exists. Negative results should be interpreted cautiously.

Figure 3.14

One Way Analysis of Variance

Data source: Data 1 in Notebook1

Normality Test (Shapiro-Wilk) Passed (P = 0.070)

Equal Variance Test: Failed (P < 0.050)

Group Name	N	Missing	Mean	Std Dev	SEM
0 min	8	0	100	0	0
15 min	8	0	74.875	2.961	1.047
30 min	8	0	54.625	15.716	5.556
60 min	8	0	39.938	12.339	4.362
120 min	8	0	35.438	17.514	6.192
240 min	8	0	8.813	6.948	2.457

Source of Variation	DF	SS	MS	F	P
Between Groups	5	40949.3	8189.859	64.401	<0.001
Residual	42	5341.156	127.17		
Total	47	46290.45			

The differences in the mean values among the treatment groups are greater than would be expected by chance; there is a statistically significant difference (P = <0.001).

Power of performed test with alpha = 0.050: 1.000

All Pairwise Multiple Comparison Procedures (Holm-Sidak method):

Overall significance level = 0.05

Comparisons for factor:

Comparison	Diff of Me t	P	P<0.050
0 min vs. 240 min	91.188	16.172 <0.001	Yes
15 min vs. 240 min	66.063	11.716 <0.001	Yes
0 min vs. 120 min	64.563	11.45 <0.001	Yes
0 min vs. 60 min	60.063	10.652 <0.001	Yes
30 min vs. 240 min	45.813	8.125 <0.001	Yes
0 min vs. 30 min	45.375	8.047 <0.001	Yes
15 min vs. 120 min	39.438	6.994 <0.001	Yes
15 min vs. 60 min	34.938	6.196 <0.001	Yes
60 min vs. 240 min	31.125	5.52 <0.001	Yes
120 min vs. 240 min	26.625	4.722 <0.001	Yes
0 min vs. 15 min	25.125	4.456 <0.001	Yes
15 min vs. 30 min	20.25	3.591 0.003	Yes
30 min vs. 120 min	19.188	3.403 0.004	Yes
30 min vs. 60 min	14.688	2.605 0.025	Yes
60 min vs. 120 min	4.5	0.798 0.429	No

Figure 3.16

One Way Analysis of Variance

Data source: Data 1 in Notebook1

Normality Test (Shapiro-Wilk) Passed (P = 0.326)

Equal Variance Test: Passed (P = 0.393)

Group Name	N	Missing	Mean	Std Dev	SEM
sIPN GIF 15min	3	0	0.666	0.0144	0.00829
sIPN GIF 30min	3	0	0.712	0.0066	0.00381
sIPN GIF 60min	3	0	0.868	0.037	0.0213
sIPN GIF 120min	3	0	1.612	0.0551	0.0318
sIPN GIF 240min	3	0	1.798	0.0419	0.0242
Insulin 15min	3	0	0.666	0.0611	0.0353
Insulin 30min	3	0	0.75	0.00287	0.00166
Insulin 60min	3	0	0.879	0.0349	0.0202
Insulin 120min	3	0	1.507	0.0811	0.0468
Insulin 240min	3	0	1.563	0.0743	0.0429

Source of Variation	DF	SS	MS	F	P
Between Groups	9	5.646	0.627	267.426	<0.001
Residual	20	0.0469	0.00235		
Total	29	5.692			

The differences in the mean values among the treatment groups are greater than would be expected by chance; there is a statistically significant difference (P = <0.001).

Power of performed test with alpha = 0.050: 1.000

All Pairwise Multiple Comparison Procedures (Holm-Sidak method):

Overall significance level = 0.05

Comparisons for factor:

Comparison	Diff of Me t	P	P<0.050
sIPN GIF 240 vs. sIPN GIF 15m	1.132	28.624 <0.001	Yes
sIPN GIF 240 vs. Insulin 15mi	1.132	28.624 <0.001	Yes
sIPN GIF 240 vs. sIPN GIF 30m	1.086	27.471 <0.001	Yes
sIPN GIF 240 vs. Insulin 30mi	1.049	26.52 <0.001	Yes
sIPN GIF 120 vs. sIPN GIF 15m	0.945	23.907 <0.001	Yes
sIPN GIF 120 vs. Insulin 15mi	0.945	23.907 <0.001	Yes
sIPN GIF 240 vs. sIPN GIF 60m	0.93	23.514 <0.001	Yes
sIPN GIF 240 vs. Insulin 60mi	0.919	23.245 <0.001	Yes
sIPN GIF 120 vs. sIPN GIF 30m	0.9	22.754 <0.001	Yes
Insulin 240m vs. sIPN GIF 15m	0.897	22.684 <0.001	Yes
Insulin 240m vs. Insulin 15mi	0.897	22.684 <0.001	Yes

sIPN GIF 120 vs. Insulin 30mi	0.862	21.804	<0.001	Yes
Insulin 240m vs. sIPN GIF 30m	0.851	21.531	<0.001	Yes
Insulin 120m vs. sIPN GIF 15m	0.841	21.262	<0.001	Yes
Insulin 120m vs. Insulin 15mi	0.841	21.262	<0.001	Yes
Insulin 240m vs. Insulin 30mi	0.814	20.581	<0.001	Yes
Insulin 120m vs. sIPN GIF 30m	0.795	20.109	<0.001	Yes
Insulin 120m vs. Insulin 30mi	0.758	19.159	<0.001	Yes
sIPN GIF 120 vs. sIPN GIF 60m	0.743	18.797	<0.001	Yes
sIPN GIF 120 vs. Insulin 60mi	0.733	18.528	<0.001	Yes
Insulin 240m vs. sIPN GIF 60m	0.695	17.575	<0.001	Yes
Insulin 240m vs. Insulin 60mi	0.684	17.305	<0.001	Yes
Insulin 120m vs. sIPN GIF 60m	0.639	16.152	<0.001	Yes
Insulin 120m vs. Insulin 60mi	0.628	15.883	<0.001	Yes
sIPN GIF 240 vs. Insulin 120m	0.291	7.362	<0.001	Yes
sIPN GIF 240 vs. Insulin 240m	0.235	5.94	<0.001	Yes
Insulin 60mi vs. sIPN GIF 15m	0.213	5.379	<0.001	Yes
Insulin 60mi vs. Insulin 15mi	0.213	5.379	<0.001	Yes
sIPN GIF 60m vs. sIPN GIF 15m	0.202	5.11	<0.001	Yes
sIPN GIF 60m vs. Insulin 15mi	0.202	5.11	<0.001	Yes
sIPN GIF 240 vs. sIPN GIF 120	0.187	4.717	0.002	Yes
Insulin 60mi vs. sIPN GIF 30m	0.167	4.226	0.006	Yes
sIPN GIF 60m vs. sIPN GIF 30m	0.156	3.957	0.01	Yes
Insulin 60mi vs. Insulin 30mi	0.13	3.275	0.044	Yes
sIPN GIF 60m vs. Insulin 30mi	0.119	3.006	0.074	No
sIPN GIF 120 vs. Insulin 120m	0.105	2.645	0.145	No
Insulin 30mi vs. sIPN GIF 15m	0.0832	2.103	0.359	No
Insulin 30mi vs. Insulin 15mi	0.0832	2.103	0.327	No
Insulin 240m vs. Insulin 120m	0.0562	1.422	0.729	No
sIPN GIF 120 vs. Insulin 240m	0.0484	1.223	0.801	No
sIPN GIF 30m vs. sIPN GIF 15m	0.0456	1.153	0.782	No
sIPN GIF 30m vs. Insulin 15mi	0.0456	1.153	0.704	No
Insulin 30mi vs. sIPN GIF 30m	0.0376	0.95	0.73	No
Insulin 60mi vs. sIPN GIF 60m	0.0106	0.269	0.956	No
Insulin 15mi vs. sIPN GIF 15m	3.33E-16	8.42E-15	1	No